

Universidade de Brasília

Instituto de Química



Luis Alonso Espinoza Velasquez

Reological and thermodynamical properties of mixtures
containing [BMIM][Cl] and glycerol.

Brasilia/DF

2018

Luis Alonso Espinoza Velasquez.

Reological and thermodynamical properties of mixtures containing [BMIM][Cl] and glycerol.

Dissertação apresentada a universidade de Brasília como parte das exigências do programa de Pós-Graduação em Tecnologias Químicas e Biológicas para obtenção do título de "Mestre"

Orientadora

Prof^a Dr^a Simone Monteiro e Silva

Brasília/DF

2018

FOLHA DE APROVAÇÃO

Comunicamos a aprovação da Defesa de Dissertação do (a) aluno (a) **Luis Alonso Espinoza Velasquez**, matrícula nº **16/0098351**, intitulada ***“Reological and thermodynamical properties of mixtures containing [BMIM][Cl] and glycerol”***, apresentada no (a) sala PADCT do Instituto de Química (IQ) da Universidade de Brasília (UnB) em 27 de fevereiro de 2018.

Prof.^a Dra. Simone Monteiro e Silva
Presidente de Banca (IQ/UnB)

Prof. Dr. José Joaquín Linares León
Membro Titular (IQ/UnB)

Prof. Dr. Leonardo Giordano Paterno
Membro Titular (IQ/UnB)

Prof. Dr. Davi Alessandro Cardoso Ferreira
Membro Suplente (IQ/UnB)

Em 27 de fevereiro de 2018.

Resumo

De acordo com as nossas pesquisas, no momento não há dados suficientes sobre as propriedades reológicas e termodinâmicas das misturas de cloreto de 1-butil-3-metilimidazolio [bmim] [Cl] e glicerol em qualquer fração molar, nem a temperatura nenhuma. Ambos [bmim] [Cl] e glicerol são compostos muito interessantes. O primeiro é um líquido iônico relativamente econômico e fácil de sintetizar; e o segundo é um subproduto do processo de produção de biocombustíveis, de modo que conhecer esse tipo de dados pode nos ajudar a encontrar novos usos para eles. A densidade, a viscosidade e o índice de refração da mistura foram estudados em todo o intervalo de fração molar e a temperaturas variando de 333,15 K a 373,15 K. A mistura é não ideal, a viscosidade apresentou um mínimo em $X_{LI}=0,3$, essa diminuição poderia ser atribuída as ligações de hidrogênio, a mistura apresentou comportamento newtoniano, o volume de excesso molar apresentou um máximo na região de $X_{LI}=0,4$ e a variação da viscosidade apresentou um mínimo perto de $X_{LI}=0,6$ em todas as temperaturas. A partir desses dados experimentais estudamos o desvio da idealidade desta mistura, as propriedades de excesso, determinando também os parâmetros de ativação para entalpia, entropia e excesso de energia de ativação Molar de Gibbs. Também correlacionamos esses dados com equações encontradas na literatura para prever melhor os dados em pontos diferentes dos que estudamos. Por último, recomendamos o estudo das ligações e interações intermoleculares para entender melhor esta mistura e suas propriedades.

Palavras-chave:

Líquido Iônico, Glicerol, Densidade, Viscosidade, Índice de Refracção, Propriedades de Excesso, Energia de Ativação, Redlich-Kister, VFT, Ghatee et al.

Abstract

At this stage, there is no sufficient data about the rheological and thermodynamic properties of the mixtures of 1-Butyl-3-methylimidazolium chloride [bmim][Cl] and glycerol at any molar fraction nor temperature. Both [bmim][Cl] and glycerol are very interesting compounds, the first one is an relatively cheap and easy to synthetize ionic liquid and the second one is the byproduct of the biofuel production process, so knowing this kind of data could help us in finding new uses for them. Density, viscosity and refractive index of the mixture were studied at the entire molar fraction range and at temperatures ranging from 333.15 K to 373.15 K. The mixture was not ideal, the viscosity had a minimum in $X_{IL} = 0.3$, this decrease could be attributed to hydrogen bonds, the mixture presented Newtonian behavior, the molar excess volume presented a maximum in the region of $X_{IL} = 0.4$ and the variation of viscosity showed a minimum near $X_{IL} = 0.6$ at all temperatures. From this experimental data we studied the deviation from ideality and excess properties of this mixture, determined the activation parameters for enthalpy, entropy and Excess Molar Gibbs energy of activation. We also correlated this data to equations found in literature to better predict data at points different from those we studied. Last, we recommend the study of intermolecular bonds and interactions improve our understanding of this mixture and its properties.

Keywords:

Ionic Liquid, Glycerol, Density, Viscosity, Refractive Index, Excess Properties, Energy of Activation, Redlich-Kister, VFT, Ghatee et al.

Symbols list.

ρ ... Density

η ... Viscosity

MW ... Molar Weight

SSE ... Sum of Squares Due to Error

SST ... The total sum of squares

R^2 ... R-Square

Adjusted R^2 ... Adjusted R-Square

RMSE ... Root Mean Squared Error

X_i ... Molar fraction

IL... Ionic Liquid

RTIL... Room Temperature Ionic Liquid

M.P. ... Melting Point

R.I. ... Refractive Index

DES ... Deep Eutectic Solvent

DMSO ... Dimethyl sulfoxide

NEA ... N-ethylaniline

H ... Enthalpy

S ... Entropy

G ... Gibbs Energy

V^E ... Excess molar volumen

[bmim][Cl] ... 1-Butyl-3-methylimidazolium chloride

RPM ... Revolutions per minute

cP ... Centipoise

Re ... Reynolds Number

n ... Moles number

Figures list.

| | |
|---|----|
| Figure 1:Chemical structures of (a) N-octadecyl-N-octadecylimidazolium iodide (OoimI) and (b) Octadecyltriphenylphosphonium iodide (OtpHl) ionic liquids.[7]..... | 2 |
| Figure 2:1-Butyl-3-methylimidazolium chloride [Bmim][Cl] molecular structure. | 3 |
| Figure 3: Transesterification reaction of triacylglycerol [23] | 6 |
| Figure 4: Laminar and turbulent flow. Before hitting the cylinder, we have well defined layers typically associated to a laminar flow and after hitting it we can see how this layers mix with one another. Figure taken from (Young et al 2011) [34]. | 8 |
| Figure 5: Fluid between two plates..... | 9 |
| Figure 6: Inciding beam of light [37]. | 11 |
| Figure 7: Mixture´s enthalpy concentration diagram for aqueous sulfuric acid at 1 atm.[47]..... | 15 |
| Figure 8: Density values for the [bmim][Cl] and glycerol mixture at 60,70,80 and 90 °C at thewhole molar fraction composition range. | 23 |
| Figure 9: Viscosity behavior for the 0.7 molar fraction at 80 ⁰ C. (a) Shear Stress (D/cm ²) vs Shear rate (1/s) (b) Viscosity (cP) vs Shear rate (1/s)..... | 23 |
| Figure 10: Viscosity values for the [bmim][Cl] and glycerol mixture at 60,70,80 and 90 °C at thewhole molar fraction composition range. | 25 |
| Figure 11:Refractive index values for the [bmim][Cl] and glycerol mixture at 50,60,70 and 80 °C at the whole molar fraction composition range. | 26 |
| Figure 12: Excess molar volumes values for the [bmim][Cl] and glycerol mixture at 60,70,80 and 90 °C at thewhole molar fraction composition range. | 29 |
| Figure 13: Viscosity deviation values for the [bmim][Cl] and glycerol mixture at 60,70,80 and 90 °C at the whole molar fraction composition range. | 30 |
| Figure 14: Refractive index deviation values for the [bmim][Cl] and glycerol mixture at 60,70,80 and 90 °C at the whole molar fraction composition range. | 32 |
| Figure 15Enthalpy of activation and (ΔS^*) Activation Entropy for the [bmim][Cl] and glycerol mixture for the 50 ⁰ C to 80 °C at the whole molar fraction composition range | 33 |
| Figure 16;(ΔH^{E*}) Excess Enthalpy of activation and (ΔS^{E*}) Excess Entropy of Activation for the [bmim][Cl] and glycerol mixture for the 50 ⁰ C to 80 °C at the whole molar fraction composition range..... | 35 |

Figure 17: Molar Gibbs energy of activation (ΔG^*) and Excess Molar Gibbs energy of activation (ΔG^{E*}) for the [bmim][Cl] and glycerol mixture for the 50^oC to 80^oC at the whole molar fraction composition range. 37

Figure 18: (a) Experimental Values for the Excess Molar Volume V^E for 333.15K, the fitting to the Redlich-Kister equation is represented with the solid line. (b) Absolute Residual values plot for this fitting..... 42

Figure 19: (a) Experimental Values for the Viscosity's deviation $\Delta\eta$ for 333.15K, the fitting to the Redlich-Kister equation is represented with the solid line. (b) Absolute Residual values plot for this fitting..... 44

Equations List

| | |
|--|----|
| $\rho = mV$ Eq. 1..... | 7 |
| $\vartheta = VmMW = 1\rho MW$ Eq. 2 | 7 |
| $Z = PvRT$ Eq. 3..... | 7 |
| $v = \eta\rho$ Eq. 4 | 8 |
| $Re = \rho VD\mu$ Eq. 5 | 8 |
| $\tau_{xy} = -\mu dv_x dy$ Eq. 6..... | 9 |
| $n = cv$ Eq. 7: | 11 |
| $M = i = 1cx_i M_i$ Eq. 8..... | 13 |
| $\Delta M = Mm - (x_1 M_1 + x_2 M_2)$ Eq. 9 | 14 |
| $M_i = \partial(nM) \partial n_i P, T, n_j$ Eq. 10..... | 14 |
| $y = mx + b$ Eq. 11..... | 16 |
| $SSE = \sum_i = 1n(y_i - \hat{y}_i)^2$ Eq. 12 | 16 |
| $SST = \sum_i = 1n(y_i - \bar{y})^2$ Eq. 13..... | 16 |
| $R - square = 1 - SSE/SST$ Eq. 14 | 17 |
| $adjusted R - square = 1 - SSE(n - 1)/SST(v)$ Eq. 15..... | 17 |
| $RMSE = \sqrt{SSE/v}$ Eq. 16 | 17 |
| $\eta = hNve\Delta H * RTe - \Delta S * R$ Eq. 17 | 33 |
| $\ln V \eta h N = \Delta H * RT - \Delta S * R$ Eq. 18..... | 33 |
| $\Delta G^* = \Delta H^* - \Delta S^* T$ Eq. 19 | 35 |
| $\Delta G E^* = RT \ln \eta M \rho_2 \eta_2 M_2 \rho - x_1 \ln \eta_1 M_1 \rho_2 \eta_2 M_2 \rho_1$ Eq. 20 | 35 |
| $\eta = Ae^{BT - T_0}$ Eq. 21..... | 38 |
| $1/\eta \phi = a + bT$ Eq. 22 | 38 |
| $VmE = x_1 x_2 i = 0kAix_1 - x_2 i$ Eq. 23..... | 40 |
| <i>Absolute Residual value = V_{Experimental value} - V_{Redlich Kister}</i> Eq. 24... 40 | |
| <i>Absolute Residual value = η_{Experimental value} - η_{Redlich Kister}</i> Eq. 25.... 43 | |

Tables list

| | |
|---|----|
| Table 1: Most common properties of Ionic Liquids. Table obtained from (Keith E., 2007) [1]..... | 1 |
| Table 2: Physical and chemical properties of 1-Butyl-3-methylimidazolium chloride. Molar Weight, Melting Point, Thermal Decomposition, Density, Viscosity and Refractive Index. | 4 |
| Table 3: Glycerol Physicochemical Properties: Molar Weight, Melting Point, Boiling Point, Density, Viscosity and Refractive Index..... | 6 |
| Table 4: Viscosity values for hydrocarbons, hexane, heptane, octane, nonane and decane.[35] | 10 |
| Table 5: Influence of intermolecular forces in fluid's viscosity..... | 10 |
| Table 6: Densimeter characteristics..... | 19 |
| Table 7: Rheometer characteristics..... | 20 |
| Table 8: Refractometer characteristics. | 20 |
| Table 9: Density values for the [bmim][Cl] and glycerol mixture at 333.15,343.15,353.15 and 363.15°C at the whole molar fraction composition range. | 22 |
| Table 10: Viscosity values for the [bmim][Cl] and glycerol mixture at 60,70,80 and 90 °C at the whole molar fraction composition range | 24 |
| Table 11: Refractive index values for the [bmim][Cl] and glycerol mixture at 50,60,70 and 80 °C at the whole molar fraction composition range. | 27 |
| Table 12: (ΔH^*) Enthalpy of activation and (ΔS^*) Activation Entropy for the [bmim][Cl] and glycerol mixture for the 50°C to 80 °C at the whole molar fraction composition range. | 34 |
| Table 13: (ΔH^{E*}) Excess Enthalpy of activation and (ΔS^{E*}) Excess Entropy of Activation for the [bmim][Cl] and glycerol mixture for the 50°C to 80 °C at the whole molar fraction composition range..... | 35 |
| Table 14: Molar Gibbs energy of activation (ΔG^*) and Excess Molar Gibbs energy of activation (ΔG^{E*}) for the [bmim][Cl] and glycerol mixture for the 50°C to 80 °C at the whole molar fraction composition range. | 36 |
| Table 15: Fitted parameters and deviation values for the VFT equation for the [bmim][Cl] and glycerol mixture for the 50°C to 80 °C at the whole molar fraction composition range. | 39 |

Table 16: Fitted parameters and deviation values for the Ghatee et al. equation for the [bmim][Cl] and glycerol mixture for the 50⁰C to 80⁰C at the whole molar fraction composition range..... 41

Table 17: Fitted parameters and deviation values for the Redlich-Kister equation, correlating Molar Excess Volume VE dependence on molar fraction X_{i1} for the [bmim][Cl] and glycerol mixture for the 50⁰C to 80⁰C at the whole molar fraction composition range. 42

Table 18: Fitted parameters and deviation values for the Redlich-Kister equation, correlating Viscosity's deviation dependence on molar fraction X_{i1} for the [bmim][Cl] and glycerol mixture for the 50⁰C to 80⁰C at the whole molar fraction composition... 43

Index

| | |
|---|------|
| Resumo | iv |
| Symbols list. | vi |
| Figures list. | viii |
| Equations List..... | x |
| Tables list..... | xi |
| Index | xiii |
| Introduction | 1 |
| Ionic Liquids..... | 1 |
| [bmim][Cl]..... | 3 |
| Glycerol | 5 |
| Measured Properties. | 7 |
| Density..... | 7 |
| Viscosity. | 8 |
| Refractive Index | 11 |
| Enthalpy of activation (ΔH^*)..... | 12 |
| Entropy of activation (ΔS^*). | 12 |
| Gibbs free energy of activation (ΔG^*)..... | 12 |
| Properties of mixtures..... | 12 |
| Why this mixture of all the possible ones?..... | 13 |
| Ideal mixtures. | 13 |
| Deviation from ideality for properties of mixtures..... | 14 |
| Partial properties..... | 14 |
| Fitting Equations to experimental data..... | 15 |
| Objectives. | 18 |
| Specific Objectives. | 18 |
| Results and discussions. | 21 |

| | |
|--|----|
| Density measurements..... | 21 |
| Viscosity measurements..... | 23 |
| Refractive indexes measurements..... | 25 |
| Deviations from ideal behavior. Excess molar volume..... | 28 |
| Viscosity deviations..... | 29 |
| Refractive index deviations..... | 30 |
| Association activation parameters. Enthalpy of activation (ΔH^*), Gibbs Energy of activation (ΔG^*), Activation Entropy (ΔS^*) and change in heat capacity of activation (ΔC_p^*)..... | 33 |
| Fitting experimental data to literature reported equations..... | 38 |
| Correlating viscosity's dependence on temperature..... | 38 |
| Correlating Excess Molar Volume dependence with molar fraction..... | 40 |
| Conclusions..... | 45 |
| Recommendations..... | 46 |
| Apendix..... | 47 |
| Pure Glycerol..... | 47 |
| $X_{IL}=0.1$ | 51 |
| $X_{IL}=0.2$ | 55 |
| $X_{IL}=0.3$ | 59 |
| $X_{IL}=0.4$ | 63 |
| $X_{IL}=0.5$ | 67 |
| $X_{IL}=0.6$ | 71 |
| $X_{IL}=0.7$ | 75 |
| $X_{IL}=0.85$ | 79 |
| $X_{IL}=0.95$ | 83 |
| Pure [bmim][Cl]..... | 87 |
| References..... | 91 |

Introduction

Ionic Liquids

Ionic liquids are organic salts that remain liquid at relatively low temperatures: under 100 °C is commonly regarded as the threshold to be considered into this category, we can see other properties usually related with them in Table 1.

Table 1: Most common properties of Ionic Liquids. Table obtained from (Keith E., 2007) [1].

| | |
|-------------------------|--|
| A salt | Cation and or anion quite large |
| Freezing point | Preferably below 100°C |
| Liquid range | Often > 200°C |
| Thermal stability | Usually high |
| Viscosity | Normally < 100 cP, workable |
| Dielectric constant | Implied < 30 |
| Polarity | Moderate |
| Specific conductivity | Usually < 10 mScm ⁻¹ , “Good” |
| Molar conductivity | < 10 Scm ² mol ⁻¹ |
| Electrochemical window | > 2V, even 4.5 V, except for Brønsted acidic systems |
| Solvent and/or catalyst | Excellent for many organic reactions |
| Vapor pressure | Usually negligible |

There is a class of ionic liquids that remain liquid at room temperature, they are referred to as (RTIL) *Room Temperature Ionic Liquid*, there are now known IL's with melting point (M.P.) as low as -96°C . Ions contained in common salts differ from ions in IL's in the fact that they usually have stronger forces bounding them together, this is typically due to their cations and anions being smaller and usually having a highly concentrated charges, which in turn leads to usually high melting points [2][3].

Going deeper into the reasons for the ILs to remain in that state, we can find that they are more thermodynamically favorable; once again, the large size of their anions, their flexibility and asymmetrical structures will make it difficult for ionic liquids to pack efficiently into the solid state. ILs will tend to have lesser lattice enthalpies and entropy changes that supports melting[4].

Therefore, IL's although interacting through bounding forces similar to any other salt, have much lower M.P. due to their ions being larger. They distribute the molecule's charge in a bigger volume, they are also sometimes asymmetrical and possess their charges delocalized, as we can see in Figure 1, this makes it harder for these salts to form organized structures that would remain in solid states[5][6].

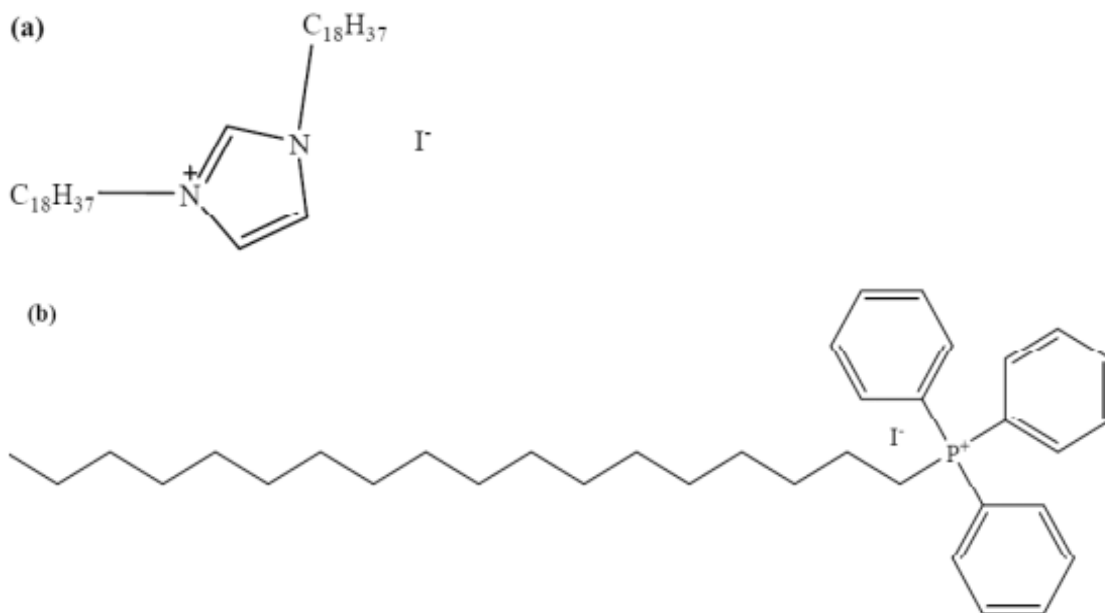


Figure 1: Chemical structures of (a) *N*-octadecyl-*N*-octadecylimidazolium iodide (OoimI) and (b) Octadecyltriphenylphosphonium iodide (OtpI) ionic liquids.[7]

There is an increasing interest in IL's, proof of this is the increasing number of articles being written about them but "Where does this excitement comes from? What is it about them that lures the attention?". Despite interactions amongst cations and anions in the

IL's being weaker than bonding forces in other salts, they still have negligible vapor pressures. One of the typical applications of ILs is to substitute the classic solvents, as for example low molecular weight hydrocarbons, which commonly have a loss to the environment through evaporative loss; the fact that ILs don't have this loss this characteristic would represent an environmental advantage. They have shown better selectivity on many solvating tasks, greater product yields in chemical reactions, and possible advantages on their reusing and recovering [8].

In addition to this the capability of modifying the cation or anion of our IL, classified as *Task Specific Ionic Liquids*, enabling various functionalities into traditional IL's, increasing its uses in many fields of chemistry, including organic synthesis and catalysis chemistry [9]

Ionic liquids are widely used in the polymer science; people successfully used them as solvents, plasticizer agent, coupling agent, compatibilizer, co-solvent in mixtures, and even as monomers in the creation of new polymers. All of these uses are a proof of the versatility of the IL's and the many advantages they possess [4][10][11].

[bmim][Cl]

1-Butyl-3-methylimidazolium chloride, [bmim][Cl] or [C4mim][Cl] described in Figure 2 is an ionic liquid with a medium size cation, having a delocalized positive charge, and chloride as the anion. This kind of dialkylimidazolium salts together with alkylpyridinium related compounds were amongst the first modern ionic salts to be found in the literature [1].

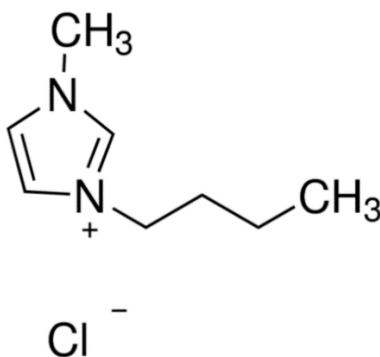


Figure 2: 1-Butyl-3-methylimidazolium chloride [Bmim][Cl] molecular structure.

We can synthesize it by nucleophilic substitution reaction of n-methylimidazolium and 1-chlorobutane, some of its pure properties are already present in the literature, some of its physical and chemical properties appear in Table 2, nonetheless to study its probable uses

in diverse applications there is still much work to do. We can find some rheological properties of its mixtures with other components as: water, cellulose, dimethylsulfoxide and others yet much research still needs to be done to fully understand its behavior.[12]

[bmim][Cl] is an ionic liquid relatively simply to synthesize, its previous reagents are somehow cheap, it is an interesting previous step before we get to other IL's but nonetheless data about its properties is not so abundant and to the best of our knowledge the properties found in this work are not reported in literature.

Table 2: Physical and chemical properties of 1-Butyl-3-methylimidazolium chloride. Molar Weight, Melting Point, Thermal Decomposition, Density, Viscosity and Refractive Index.

| Property | [bmim][Cl] |
|---------------------------------------|------------|
| MW (g/mol) | 174.67 |
| η @80°C (Pa s) [13] | 0.142 |
| ρ @25°C (g/cm ³)[14] | 1.0800 |
| ρ @75°C (g/cm ³)[15] | 1.0557 |
| R.I. @25°C [16] | 1.524 |
| Thermal decomposition (°C)[14] | 254 |
| Melting point (°C)[14] | 41 |

[bmim][Cl] has been used as reaction media to catalyze unsubstituted and alkoxy-carbonyl-substituted coumarins, allowing the presence of the NaOMe[17]. [bmim][Cl] in a mixture with glycerol has been specifically used as combined plasticizers of cassava starch-based films, obtaining highly amorphous structures that were more flexible had more thermal stability and lower production costs when using the ionic liquid alone[18].

The amount of sulfur compounds in the fuels we currently use has become an environmental concern, in part because of the acid rains and air pollution it produces, for this reason, efforts transformed into laws have been made globally to reduce these compounds. Hydrodesulfurization, a widely used technique for this purpose, does not do well at treating the dibenzothiophene and its derivative levels, using organic solvents for this task is also a common option. Nonetheless, concerns about their environmental risks as the ability to be recycled, and high volatility drives a search for other possibilities as ionic liquids might present.

The use of this particular ionic liquid [bmim][Cl], has been tested for the extractive deep-desulfurization of liquid fuels and it was found that it successfully treated dibenzothiophene and its derivatives. It could be regenerated with little loss in its activity, could be used as catalyst in other desulfurization processes and could present a more environmentally fit option[19].

Glycerol

Brazil has a significant role in the world's oil production stage, fats and biodiesel [20], centering in palm's and soy's cultivation. In 2016, Brazil's oilseeds production surpassed its own production in the preceding year, maintaining a many years growth tendency, coming from 84 million tons in 2012/2013 to 99 million tons in 2015/2016 and producing 106 million tons in 2015/2016 in January 2017 [21].

The oilseeds industry has an enormous potential to combine the food and biofuel industries, and with this process use biomass to cogenerate energy and obtain high value products. This process would be involved in the biorefinery scheme, which focuses in getting the most from agroindustrial feedstocks, adding value in processes very similar to oil refineries, having at the same time a lesser environmental impact and pointing to more sustainable systems. From this point on, we can visualize new technological and economical frontiers to the agroindustry and chemical process itself [22].

Glycerol is a significant byproduct in the biofuel production process from oilseeds. The transesterification reaction of triacylglycerol in the presence of NaOH, as seen in Figure 3 , KOH or a lipase, directly results in three ester molecules and a molecule of glycerol is set free from the initial compound.

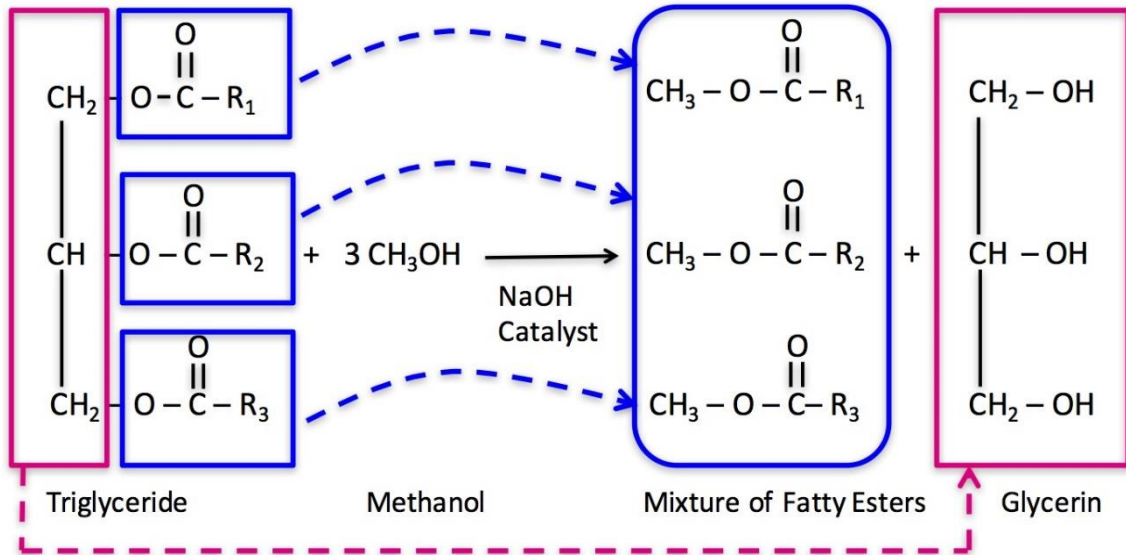


Figure 3: Transesterification reaction of triacylglycerol [23]

Glycerol is an undesirable component in biofuels, this in part to it being highly viscous as we can see in Table 3, which could make the fuel's viscosity higher making the use of it difficult in high-pressure injection [24]. This reaction produces 1 kg of glycerol for every 10 kg of biofuel, due to its great abundance and contaminated nature this raw glycerol has a low value cost. There are some efforts reported in the literature to develop conversion techniques to transform this raw glycerol into a high value one [25] and also into its purification [26].

Table 3: Glycerol Physicochemical Properties: Molar Weight, Melting Point, Boiling Point, Density, Viscosity and Refractive Index.

| Property | C ₃ H ₈ O ₃ |
|--|--|
| MW (g/mol) | 92.09 |
| Melting point (K)[27] | 291.33 |
| Boiling point (K)[27] | 561.00 |
| $\rho@25^{\circ}\text{C}(\text{g}/\text{cm}^3)$ [27] | 1.2570 |
| $\rho@75^{\circ}\text{C}(\text{g}/\text{cm}^3)$ [28] | 1.22287 |
| $\eta@60^{\circ}\text{C}(\text{Pa s})$ [29] | 81.3 |
| R.I. @25 ^o C [30] | 1.47301 |

Measured Properties.

There are many physical and chemical properties to describe a compound or substance; in particular, rheological properties are useful to many engineering design tasks, such as bomb, tanks and pipe design amongst others. On the other hand, the refractive index has applications as determining purity, concentrations of solutes in a solution; one of the most common applications is the brix Degree that measures the sugar concentration in a solution. [31]

Density.

Density is one of the most fundamental and widely used properties of substances; Eq.1 describes it as the ratio of this substance's mass "m" and its volume "V".

$$\rho = \frac{m}{V} \text{ Eq. 1}$$

Density is pressure and temperature dependent, it usually doesn't present great variations for solids and liquids but does so for gases, this property typically increases with pressure, as higher pressures will decrease a volume's substance. Temperature generally decreases density as it augments its volume. [32]

Another property closely related to density used in the field of thermodynamics is the molar volume defined in Eq.2 (ϑ), where "MW" stands for molecular weight. This property could have a heterogeneous value throughout its body or volume, be it for a difference of pressure, a gradient in concentration; mass or momentum so this possibility needs to be taken into account at any time.

$$\vartheta = \frac{v}{m} MW = \frac{1}{\rho} MW \text{ Eq. 2}$$

Molar volume is a fundamental property in many engineering applications; it is typically used in Eq.3, where Z , P , v , R , T correspond to compressibility factor, pressure, molar volume, universal gas constant and temperature, respectively. One common area where we can find it is air conditioning designing, measuring properties of refrigerant gases as R-410A, R-404A and R-507A, to better design equipment for expected pike loads[33].

$$Z = \frac{Pv}{RT} \text{ Eq. 3}$$

Density is used together with the absolute value of viscosity η to define the *kinematic viscosity* as Eq.4, both of them at the same temperature. In this work we will be typically mentioning absolute viscosity

$$v = \frac{\eta}{\rho} \text{ Eq. 4}$$

A common use for the density (ρ) value in fluid mechanics is the Reynolds Number (Re) as defined in Eq.5, where V represents the velocity of the fluid, D the diameter where it flows and μ its viscosity. At low Reynold numbers the fluid is considered laminar, meaning that it goes on in an orderly manner with no eddies or swirls, we could see it flowing in parallel layers that do not mix with one another. At high Reynold numbers the fluid is considered turbulent, a more chaotic regime where it undergoes irregular fluctuations, mixing and swirls. We can see this kind of flows exemplified in Figure 4.

$$Re = \frac{\rho VD}{\mu} \text{ Eq. 5}$$

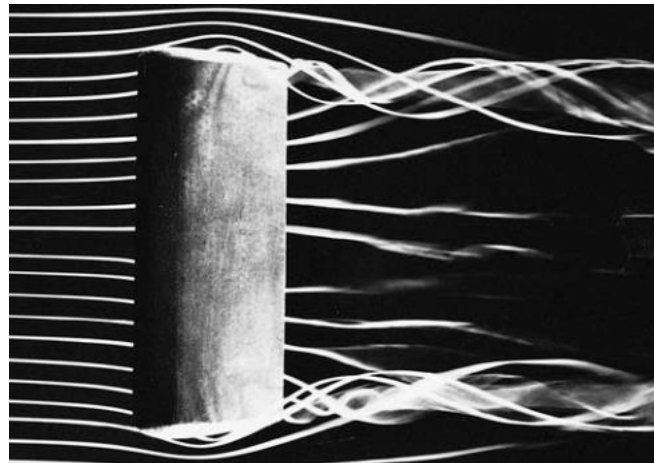


Figure 4: Laminar and turbulent flow. Before hitting the cylinder, we have well defined layers typically associated to a laminar flow and after hitting it we can see how layers mix with one another. Figure taken from (Young et al 2011) [34].

Viscosity.

Fluids, be them liquids or gases, will continually deform when a shear stress is applied to them, **viscosity** is the resistance these fluids oppose to be deformed. We routinely associate different values of viscosity to different daily life substances as water, honey or motor oil we notice not all of them will come down of their containers at the same speed, neither will they spread at the same rate on a loaf of bread, this differences are partly influenced to their viscosity.

In

Figure 5: Fluid between two plates.

Figure 5 we can see a typical description used to explain viscosity's mathematical value μ ; a fluid remains stationary between two plates and then the top one starts moving in the x -axis, producing a velocity gradient as a shear force is applied.

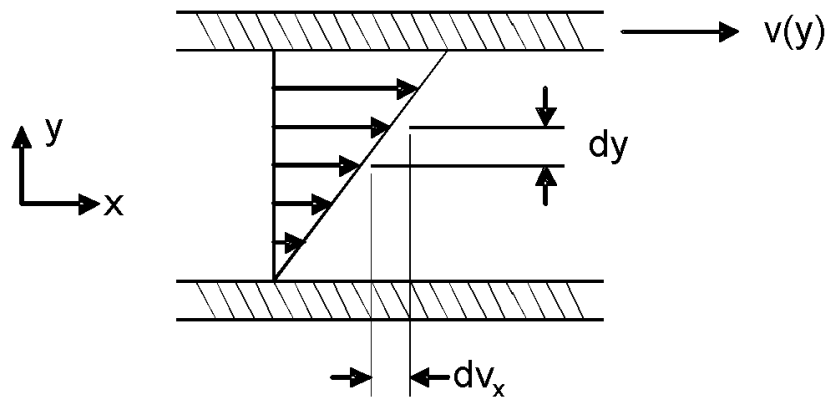


Figure 5: Fluid between two plates.

We then have Eq.6, the shear stress τ_{xy} in, represents the force applied on the fluid and goes in the x direction perpendicular to the y distance. Between the moving plate and the stationary one there will be a velocity gradient dv_x , with its maximum value on the area of contact with the moving plate and the minimum where the static plate remains, the ratio of it and the distance dy will be called the shear rate. Thus, viscosity will be considered as the internal frictions a fluid opposes to external forces.

$$\tau_{xy} = -\mu \frac{dv_x}{dy} \text{ Eq. 6}$$

This property sums up the resistance a fluid opposes to flow, the fluid's intermolecular forces will oppose its movement, typically as this force increases the difficulty of each molecule moving past each other also increases and thus viscosity rises. Usually higher molecular weights will create higher intermolecular forces and viscosity will also increase as we can see in Table 4 [2].

Table 4: Viscosity values for hydrocarbons, hexane, heptane, octane, nonane and decane.[35]

| Substance | Molar mass (g/mol) | Viscosity (kg/m.s) |
|-----------|--------------------|-----------------------|
| Hexane | 86.18 | 3.26×10^{-4} |
| Heptane | 100.21 | 4.09×10^{-4} |
| Octane | 114.23 | 5.42×10^{-4} |
| Nonane | 128.26 | 7.11×10^{-4} |
| Decane | 142.29 | 1.42×10^{-3} |

Not only molecular weight weighs in the intermolecular forces that shape viscosity's values, others as London dispersion forces and hydrogen bonds influence this property as we can see in Table 5.

Table 5: Influence of intermolecular forces in fluid's viscosity.

| Fluid | Viscosity (cP) | Type of IM attraction |
|--------------------|----------------|-----------------------|
| Water | 1.002 | H-bonding. |
| Tetrachloromethane | 0.969 | Halogen bonds. |
| Olive oil | 84 | London. |
| Oleic acid | 25 | London and H-bonding. |
| Glycerine | 1490 | H-bonding. |

For low-density gases viscosity increases as temperature rises but for most liquids, we see the opposing trend, their viscosity will decrease when the temperature increases. In the case of gases, their molecules are farther apart from one another and thus increasing their momentum through the rise of temperature will increase the chances of them finding one another.

In the case of liquids, their molecules are closer to each other and there will be cohesive forces between them. As in gases, the raise of temperature will increase the rate of interchanges between these molecules but this will also begin to disrupt the force that binds them together. In the end, this weakening of the cohesive forces will be the prevailing factor in most of the cases and viscosity will decrease [36].

Refractive Index

Whenever light hits a flat surface, it will interact with it in a way briefly described in Figure 6, part of this beam of light will be reflected away from it and the other part will go through it.

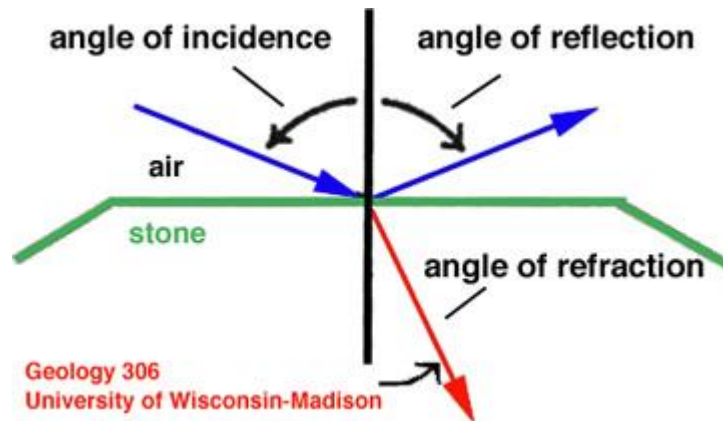


Figure 6: Inciding beam of light [37].

A very important characteristic of elements and compounds alike is the way they refract the inciding light that hits them, it is a reflex of the interactions between its molecules and its inherent chemical and physical structure. This property is measured as the Refractive Index and is calculated with help of the Eq.7.

$$n = \frac{c}{v} \text{ Eq. 7:}$$

In this equation c stands for the speed of light in vacuum and v as the speed of light in the material. Thus any material will have an absolute value greater than one as none will be faster than c , R.I. will be a dimensionless number as it is the ratio between two speeds [38].

This property is highly important in any application that involves the use of optic characteristics of any material. A Fresnel lens, for instance, was designed with the expectative of having a high R.I. as it will see uses in integrated optics, optical trapping, and fiber probes [39]. Another use of this property is to gems identification as the R.I. will depend on the number, size and arrangement of the atoms that compose the structure it will vary the speed at which light passes through them, allowing us to distinguish a stone from one another[37].

Other applications of the R.I. allow the estimation of thermodynamic and physical properties of pure hydrocarbons and petroleum fluids. Great accuracy in the prediction of

densities of heavier compounds with the use of equations of state using parameters coming from R.I. values, and also to determine the sulfur concentration in otherwise unknown solutions [40]. The refractive index can reflect the molecule electronic polarizability and provide useful information about the interaction forces in solution systems[41].

Enthalpy of activation (ΔH^*).

The Enthalpy of Activation sometimes referred, as Activation Energy (E_a) is the energy level or barrier that the molecules in a fluid must overcome before movement can occur due to shear stress[42][43].

Entropy of activation (ΔS^*).

In this studied system, this state property translates into the amount of microscopic states our fluid can have before and after being deformed by shear stresses, this could be considered in simpler terms as the degree of molecular disorder present in our system[42][44].

Gibbs free energy of activation (ΔG^*).

This energy determines the max amount of energy we could obtain from a fluid after applying a shear stress and deforming it. If its value its lower than zero the process will be spontaneous, if its greater than zero it will not be spontaneous and if it is equal to zero it will be in thermodynamic equilibrium [42][45].

Properties of mixtures.

Having appropriate data about the physical, chemical and thermodynamic properties of the compounds we are using is fundamental to engineering design, laboratory applications and industrial uses.

There are innumerable databases we can consult to find the values of the properties we are looking for but as we try to use new materials and chemical compounds our opportunities get narrower. If we go one step further and start combining these compounds to create mixtures to be analyzed, the possible combinations grow exponentially and thus gets statistically harder for us to find what we are looking for.

The existing data might have been found through experimental research, through computer simulation or a mixture of both. It would be desirable to have experimental information about any information we are considering, as we hope that with this approach,

we would have a smaller discrepancy and a more reliable data, but this takes time, effort and other kinds of investments that make it difficult to create such extensive databases.

We have the possibility of fitting and correlating experimental data through theoretical based equations, semi-empirical equations and diverse software that would allow us to make the most of the experimentally obtained data, this approach allow us to carefully interpolate or extrapolate different data points from the data we already have [35], [42].

The purely theoretical approach tries to estimate intermolecular and intramolecular forces in the existing mixtures, parting from data as size of the molecule, polarity, or in some cases the values of the pure properties [46].

Why this mixture of all the possible ones?

Since ionic liquids are a relatively new class of compounds, data about their properties is hard to find in the literature, to the best of our knowledge, the mixture studied in here is a new and there is no experimental, theoretical or simulated data about it.

[bmim][Cl] is a chemical compound relatively cheap and easy to synthesize, its interaction will share light on the ionic liquid interactions with glycerol, and this could be an useful comparison point to study interactions of ionic liquids with many organic molecules having hydrogen bonds or not which can extend to many applications involving them.

This study might bring new opportunities to the use of the glycerol as a by-product in the biofuels production, perhaps as new ways to extract it in liquid-liquid phases or to catalyze potential reactions.

Ideal mixtures.

The most simple and naive guess one can make to predict estimations of a mixture of components is to assume the resulting value will be a corresponding contribution of the pure properties according to their concentrations in said mixtures, we can see this expressed for a mixtures of c components in $M = \sum_{i=1}^c x_i M_i$ Eq. 8. Mixtures that obey this equation are called ideal mixtures.

$$M = \sum_{i=1}^c x_i M_i \quad \text{Eq. 8}$$

In Eq.8 M stands for the property we are analyzing and x_i for the molar fraction. As intermolecular forces usually change the behavior, of the properties' mixture, this guess is not frequently valid and we will then have a deviation from ideality. In Figure 7 we can see an example of this deviation, we can see in it the variation of the mixture's enthalpy

according to the change of concentration of sulfuric acid H_2SO_4 , and the temperature of the solution. If the mixtures had an ideal behavior, there would be a straight line between the 0 and 100 percentage for every temperature.

Deviation from ideality for properties of mixtures.

Once we have obtained a mixture's value for some property by it for ways of experimental procedures, theoretical or simulated means we will be interested in how much this value differs from the ideal behavior, there is an expression typically used in literature for binary mixtures, we can see it in Eq.9. In it M_m stands as the property's mixture value we determined and M_1 and M_2 stand for the pure components property's values.

$$\Delta M = M_m - (x_1M_1 + x_2M_2) \quad \text{Eq. 9}$$

Partial properties.

A partial property is the deviation from the ideal behavior occurred when we add a component i to a mixture, at constant temperature pressure, and j compositions, as we can see in Eq.10.

$$\overline{M}_i = \left[\frac{\partial(nM)}{\partial n_i} \right]_{P,T,n_j} \quad \text{Eq. 10.}$$

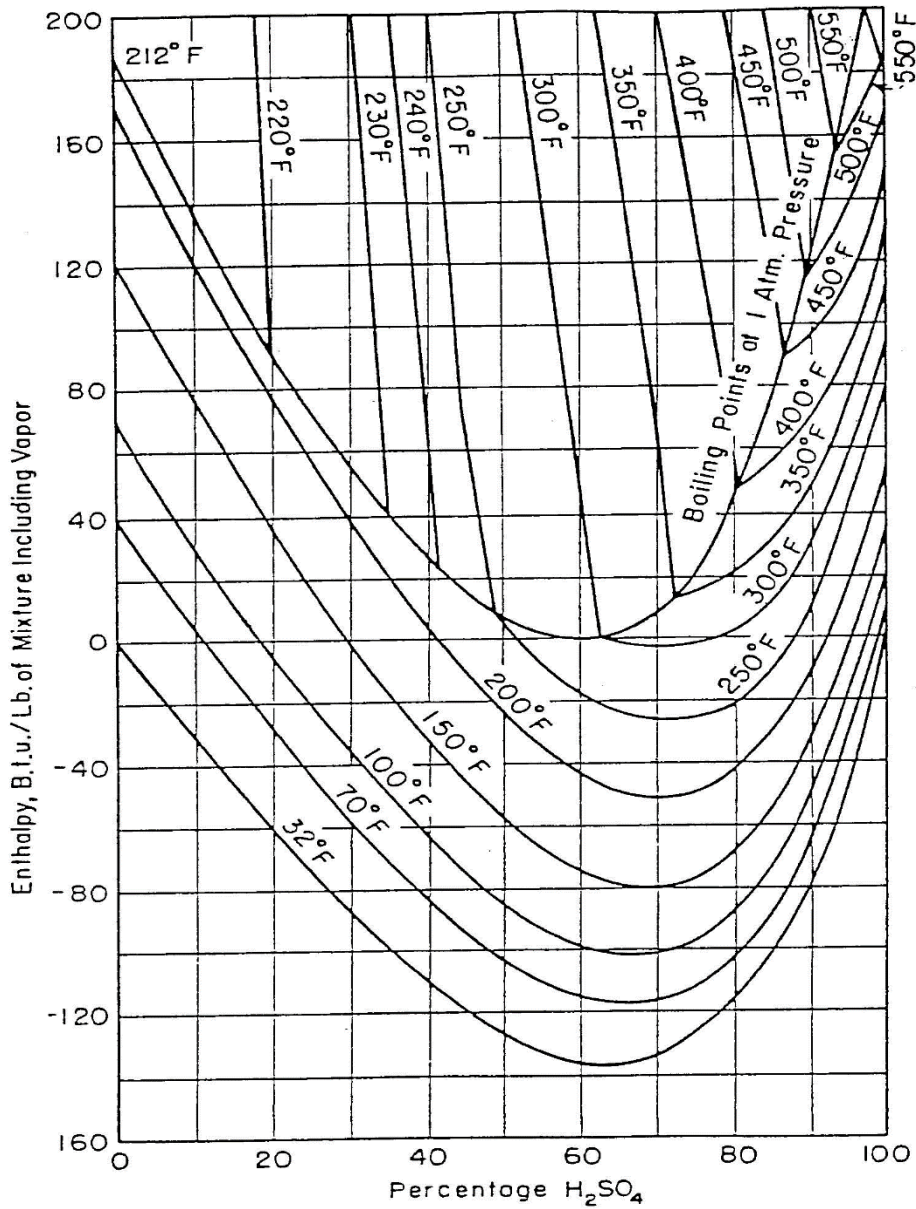


Figure 7: Mixture's enthalpy concentration diagram for aqueous sulfuric acid at 1 atm.[47]

Fitting Equations to experimental data.

It is of general interest in many fields of science to fit a curve to a given set of data points. This can be done to help us visually find patterns in the data we are analyzing, to aid us in the task of interpolating or extrapolating values for a property where no experimental data is available, to find relationships between independent and dependent variables among other reasons.

Unfortunately, there is no one true and definite way to determine the best fit to a particular set of data points, the data we are trying to fit might have errors itself and the curves we might propose will present other deviations of their own [48].

Linear regression is the most common curve fitting method, finding the values of m and b for Eq.11 defines a straight line that in many cases allows representing the dependency between variables. Nonetheless, it is not always straightforward to find the values of the properties we are looking for through this procedure and we will have to make algebraic maneuvers to find them [49].

$$y = mx + b \quad \text{Eq. 11}$$

Linear and non-linear fittings usually require iterative processes with computer aid processes, the Levenberg-Marquardt and the Trust region methods or algorithms are typically used in this kind of tasks [50]. Usually we give starting values (δ) to this kind of algorithms for them to evaluate the objective function, these starting points might influence in the convergence of the methods and the speed at which it gets to an answer [51]. Then it goes again with a value slightly different ($\delta+\epsilon$) until it reaches within a deviation value we previously established.

To evaluate how good the curve we have found fits our data points or to choose between different functions that might do this job we might simply do a visual evaluation or determine the goodness of the fitting trough statistical definitions as the ones shown below.

The *Sum of Squares Due to Error* (SSE) is the total discrepancy between the values obtained with the fitted curve and the original set of data points; it can be obtained using Eq.12. Values closer to 0 mean that our fit is better, the error is lower and that it could be used to determine values different from our original data.

$$SSE = \sum_{i=1}^n (y_i - \hat{y}_i)^2 \quad \text{Eq. 12}$$

The *total sum of squares* (SST), can be defined with Eq.13, where \bar{y} represents the mean of the fitted values.

$$SST = \sum_{i=1}^n (y_i - \bar{y})^2 \quad \text{Eq. 13}$$

The *R-Square*, is a measure of how well our curve fits to the data we are using, and can be seen in Eq.14, our curve will better correlate our data if this value is closer to one.

$$R - square = 1 - \frac{SSE}{SST} \text{ Eq. 14}$$

One of the problems with the R-Square parameter is that increasing the number of coefficients in our function will increase this value but will not necessarily be a better fit. For this reason, we also use the *Adjusted R-Square*, seen in Eq.15, n stands for the number of response values and v stands for the number of degrees of freedom.

$$adjusted R - square = 1 - \frac{SSE(n-1)}{SST(v)} \text{ Eq. 15}$$

Another parameter frequently used is the *Root Mean Squared Error* (RMSE) found in Eq.16, it is usually considered as the deviation of the predicted values from our function and the actual values from which the curve was originated[52].

$$RMSE = \sqrt{\frac{SSE}{v}} \text{ Eq. 16}$$

Objectives.

The goal of this work was to determine the rheological properties and refractive index of the mixture of Glycerol and 1-Butyl-3-methylimidazolium chloride. These properties were correlated with the equations currently reported in the literature and were used to determine subsequent thermodynamic properties.

Specific Objectives.

To measure the density of the mixture of glycerol and [bmim][Cl] at molar fractions ranging from 0 to 1 at temperatures from 333.15K to 363.15K

To measure the viscosity of the mixture of glycerol and [bmim][Cl] at molar fractions ranging from 0 to 1 at temperatures from 333.15K to 363.15K The experiments were carried at RPM speeds from 10 to 250.

To measure the Refractive index for the mixture of Glycerol and [bmim][Cl] at molar fractions ranging from 0 to 1 at temperatures from 323.15K to 353.15K

To estimate the deviations from ideality for the mixtures of Glycerol and [bmim][Cl] in the properties evaluated, the excess volume property, viscosity deviation and R.I. deviation were shown in this work.

To estimate the properties: enthalpy of activation (ΔH^*), free energy of activation (ΔG^*) and entropy of activation (ΔS^*) for these mixtures.

To fit experimental data to the most commonly used equations in the literature available. Correlations depending on temperature's variation as well as equations depending on concentration variations will be examined.

Materials and Methods

Mixture's preparation.

Glycerol was purchased from the *Sigma-Aldrich*®, 99.5% purity without further purification, [bmim][Cl] was synthesized by our laboratory team. The binary mixtures were prepared by mass from the mentioned substances using a *BIOPRECISA, Electronic Balance FA-2104N*® accurate to ± 0.1 mg. Conversion to molar fractions is based on the relative molar weights found in the literature. Each binary mixture was used after being mixed for ten minutes by magnetic agitation.

Density.

These measurements were done with a densimeter *Rudolph Research Analytical DDM 2910*®, this equipment is briefly described in Table 6.

Table 6: Densimeter characteristics.

| | |
|-----------------------|---|
| Measurement Range | Density: 0 a 3 g/cm ³ Temperature: 0 to 90 °C Pressure: 0 to 10 bars |
| Precision | Density: ± 0.0001 g/cm ³ Temperature: ± 0.01 °C |
| Minimum sample volume | 1 ml |
| Measurement method | Simple, Continuous. |

Viscosity.

These measurements were done with a rheometer *Brookfield LV*®, using a spindle SC-34, this equipment is briefly described in Table 7.

Table 7: Rheometer characteristics.

| | |
|-----------------------|---|
| Measurement Range | Viscosity : 1 to 10^6 cP Temperature: 20 to 250 °C |
| Precision | Density: $\pm 1\%$ cP Temperature: ± 0.1 °C |
| Minimum sample volume | 10ml |
| Measurement method | Continuous, multiple. |

Refractive Index.

These measurements were done with a refractometer *The electron Machine Corporation DSA E-SCAN®*, , this equipment is briefly described in Table 8.

Table 8: Refractometer characteristics.

| | |
|-----------------------|---|
| Measurement Range | Refractive Index: 1.329-1.539 R.I. Room temperature: 0 to 50 °C Sample temperature: 10 to 85 °C |
| Precision | Refractive Index: ± 0.000075 R.I. Temperature: ± 0.1 °C |
| Minimum sample volume | 0.5ml |
| Measurement method | Simple |

Results and discussions.

Density measurements.

We can see a brief summary of the density measurements that were taken in this work in Table 9, the molar fraction of the [bmim][Cl] was increased from 0 to 1 in order to have a better understanding of the whole composition range as typically done in the literature [53]. The temperature range was established to study the ionic liquid in its pure form at liquid state, as it is not liquid at room temperature when there is no moisture present, and to have comparison points available in the literature [13].

In Figure 8 we can see the values for the density ranging from 0 to 1 in molar fraction concentration, we can see a clear tendency between the pure values of both compounds and appreciate this tendency is nonlinear. The dependence of density against temperature in the whole range of temperatures and compositions is clear and is in accordance with the expected tendencies and available literature, its value diminishes with the rise of temperature. This is usually explained with the increment of volume at constant pressure, due to molecules having higher energies and moving farther apart one from another and thus as the mass remains constant, the value of density contracts [54].

Comparing the variation of the density against molar fraction with other works in literature we can see a similar tendency [55]. Properties of ideal mixtures are usually united with a straight line between the two pure components properties. In this case there is a clear deviation from ideality in the values of density we obtain yet the values fit between a maximum value of density for pure glycerol and a minimum for ionic liquid [56].

We found the value of pure glycerol in literature to be $\rho=1.22287 \text{ g/cm}^3$ at 75°C [28], comparing with our value at 70°C $\rho=1.22894 \text{ g/cm}^3$ we can agree it is an tolerable deviation. In the case of pure IL the literature's value is $\rho=1.0557 \text{ g/cm}^3$ [15] and our experimental value is $\rho=1.05937 \text{ g/cm}^3$ which is also a good approximation.

Table 9: Density values for the [bmim][Cl] and glycerol mixture at 333.15,343.15,353.15 and 363.15°C at the whole molar fraction composition range.

| X_{IL} | T(K) | | | |
|----------|---------|---------|---------|---------|
| | 333.15 | 343.15 | 353.15 | 363.15 |
| 0 | 1.23555 | 1.22894 | 1.22226 | 1.21548 |
| 0.1 | 1.19243 | 1.18591 | 1.17933 | 1.17272 |
| 0.2 | 1.16278 | 1.15640 | 1.15000 | 1.14358 |
| 0.3 | 1.13875 | 1.13253 | 1.12630 | 1.12008 |
| 0.4 | 1.12062 | 1.11455 | 1.10847 | 1.10250 |
| 0.5 | 1.10643 | 1.10050 | 1.09461 | 1.08874 |
| 0.6 | 1.09509 | 1.08927 | 1.08350 | 1.07780 |
| 0.7 | 1.08480 | 1.07907 | 1.07336 | 1.06770 |
| 0.85 | 1.07066 | 1.06499 | 1.05938 | 1.05382 |
| 0.95 | 1.06681 | 1.06123 | 1.05567 | 1.05020 |
| 1 | 1.06406 | 1.05937 | 1.05327 | 1.04727 |

$\rho(\text{g}/\text{cm}^3)$

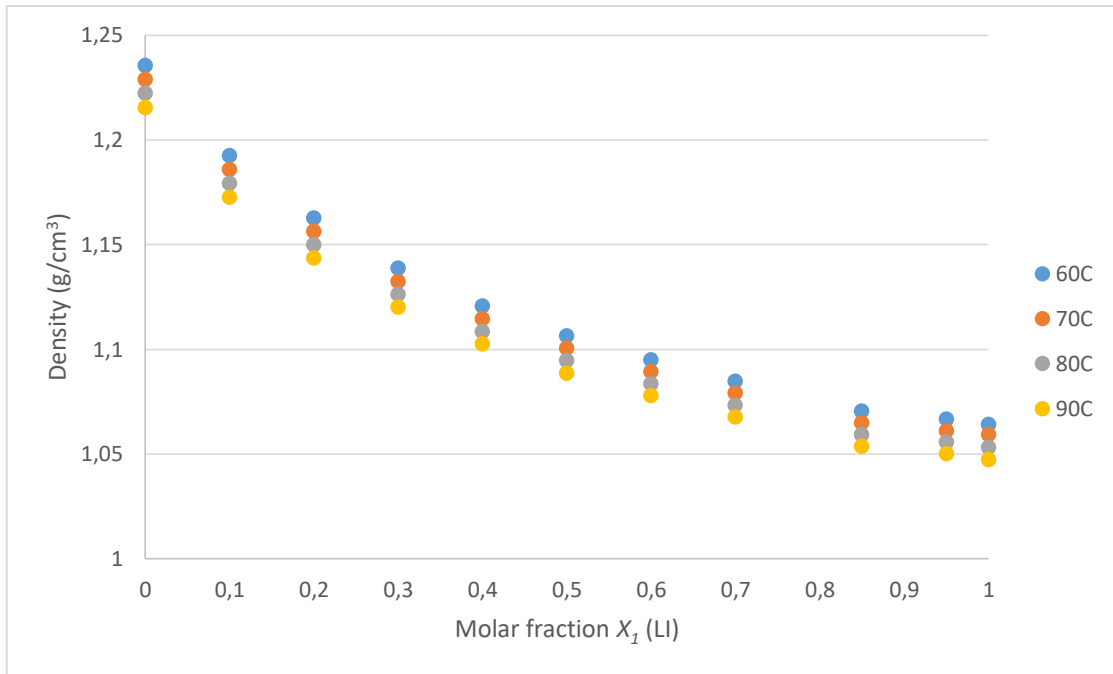


Figure 8: Density values for the [bmim][Cl] and glycerol mixture at 60,70,80 and 90 °C at the whole molar fraction composition range.

Viscosity measurements.

The viscosity measurements were done at different speeds and therefore different shear rates as we can see exemplified in Figure 9, both part a and part b point toward the mixture being a Newtonian fluid [57], the shear stress is linearly proportional to the shear rate and its viscosity's value its constant and independent from the shear rate. Being it a Newtonian fluid with a linear tendency we can use Eq.6 to obtain the viscosity's value for the mixture, R^2 value for this fitting is high, as we can see in the pointed figure, so we now have one more evidence to use this value.

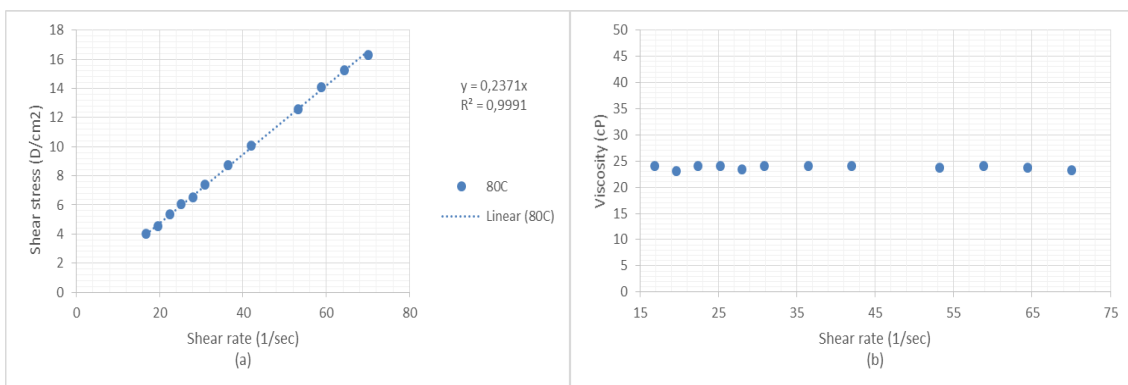


Figure 9: Viscosity behavior for the 0.7 molar fraction at 80 °C. (a) Shear Stress (D/cm^2) vs Shear rate (1/s) (b) Viscosity (cP) vs Shear rate (1/s).

Viscosity's values in in Table 10 were obtained following this procedure for the full range of concentrations, and temperatures. The lowest value of R^2 was 0.989, so we can say the assumption of the mixture being a Newtonian fluid holds well. All of the experimental data obtained in the viscosities measurements can be found in the appendix of this work.

Table 10: Viscosity values for the [bmim][Cl] and glycerol mixture at 60,70,80 and 90 °C at the whole molar fraction composition range

| T(°C) | X_{IL} | | | | | | | | | | | |
|-------|----------|-------|-------|-------|-------|-------|-------|-------|-------|-------|--------|--|
| | 0 | 0.1 | 0.2 | 0.3 | 0.4 | 0.5 | 0.6 | 0.7 | 0.85 | 0.95 | 1 | |
| 60 | 82.99 | 50.34 | 32.94 | 26.46 | 30.84 | 32.86 | 38.43 | 50.72 | 76.93 | 132.8 | 170.64 | |
| 70 | 50.58 | 31.81 | 22.84 | 18.93 | 21.94 | 23.16 | 26.95 | 33.08 | 49.70 | 76.20 | 99.98 | |
| 80 | 32.00 | 19.50 | 15.53 | 13.57 | 16.67 | 16.79 | 19.71 | 23.71 | 34.38 | 48.55 | 63.40 | |
| 90 | 23.00 | 14.82 | 12.21 | 11.57 | 13.93 | 13.17 | 14.89 | 17.8 | 24.9 | 33.32 | 43.17 | |

Consequently, in Figure 10 we have the viscosity's values for the whole temperature and concentration range, the influence of temperature is clear and falls into what is expected for this tendency, the rise of temperature causes a drop in the viscosity's values.

In the case of dependency of viscosity against molar fraction, the results are non-ideal, with values of the mixture's viscosity going lower than any of both of the pure component's viscosities. This and other cases can be found in the literature, due to varied and many complexes structures of the ionic liquids they sometimes work toward increasing the viscosity of the mixture and sometimes to reduce it [58]. For the particular case of [bmim][Cl] it has been suggested and used to lower viscosity of organic solvents [7], in this specific mixture with glycerol we observe a minimum value of viscosity around the 0.3 molar fraction for the whole range of temperatures studied, it then goes up toward the pure components viscosity as its respective concentration goes up.

Both 1-Butyl-3-methylimidazolium chloride and glycerol are commonly known for having high viscosity values, in medical and cosmetic applications this in advantage for the typically used glycerol but in many others this is an impeding factor as increases pumping efforts, including economical and technical expenses and difficult chemical transport[48].

In a somehow related field, the Deep Eutectic Solvent (DES) glyceline, formed by choline chloride and glycerol in 1:2 molar ratio also has a significantly lower viscosity value than

glycerol in its pure form, also around the $X_{IL}=0.3$ value. We know glycerol has a high viscosity value due to its intermolecular forces as for example their hydrogen bonds, ionic liquids also have typically high viscosities due to their usually large asymmetrical ions. It was found in literature that the presence of choline chloride interferes with the collective dynamics of glycerol and its hydrogen bonds so we can expect the components of our mixture interfering in the delicate intermolecular structures of one another [59].

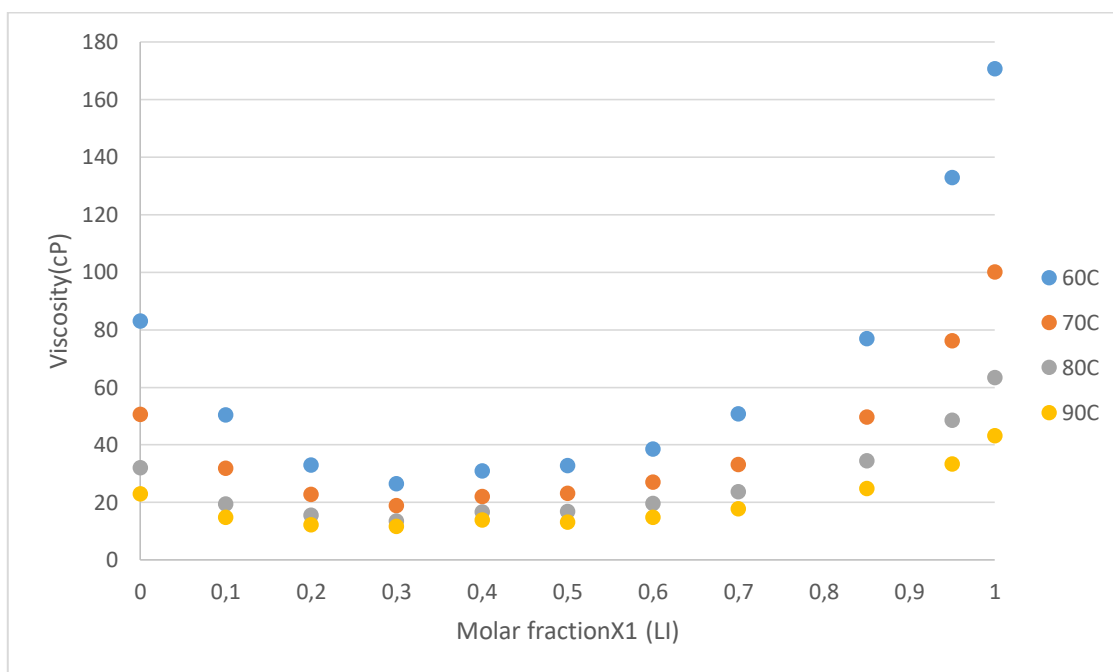


Figure 10: Viscosity values for the [bmim][Cl] and glycerol mixture at 60,70,80 and 90 °C at the whole molar fraction composition range.

Refractive indexes measurements.

The values for refractive indexes at 50, 60, 70 and 80 °C are in Table 11 and they appear in Figure 11. This shows that the value of the refractive index diminishes with the raise of temperature; this could be interpreted as a difficulty for the molecules to refract light as they increase their internal energy. The experimental data also agrees with what is found on literature, the values for the entire composition range increase with the addition of ionic liquid between the R.I. for the pure compounds of the binary system almost linearly [60] [41] [61].

In Figure 11 we can see that the values of R.I. follow an almost straight line between the pure properties values. As [bmim][Cl] has a higher R.I. considering Eq.9 it is expected

that the mixture's value will increase, we can conclude from the values obtained that the interactions of the components of this mixture do not influence its R.I.

This indicates that the mixture is close to being ideal and there could be small deviations from ideality, this is opposed to what we find in some cases where there is a clear and positive deviation from ideality [61]. This could also be seen as an indicator that the concentration of the mixtures were properly prepared and there were no great contaminations in the experimental procedures.

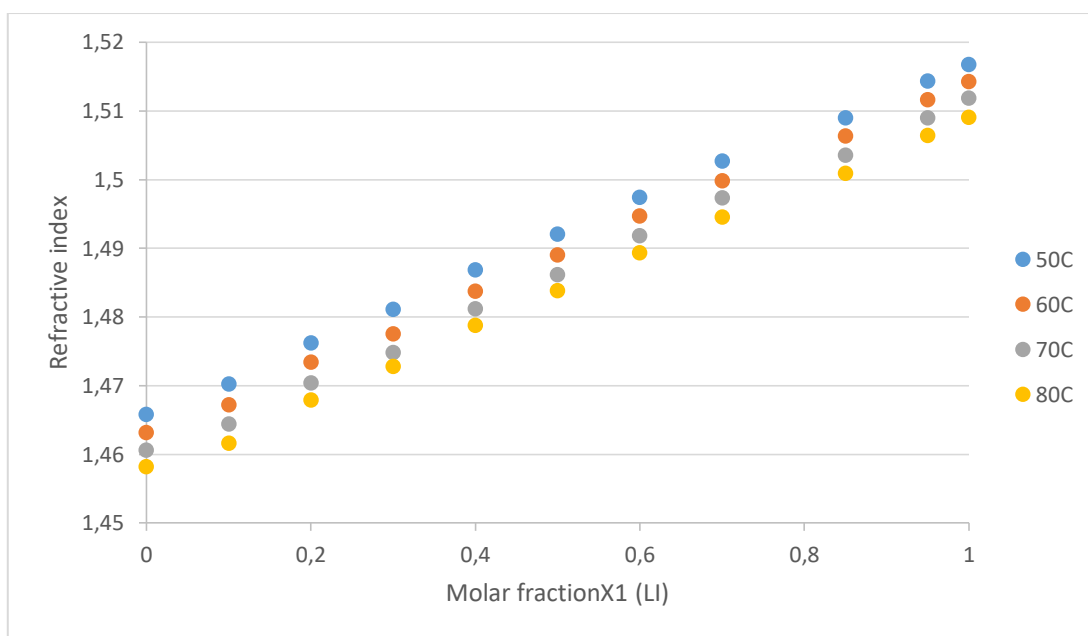


Figure 11: Refractive index values for the [bmim][Cl] and glycerol mixture at 50, 60, 70 and 80 °C at the whole molar fraction composition range.

Table 11: Refractive index values for the [bmim][Cl] and glycerol mixture at 50,60,70 and 80 °C at the whole molar fraction composition range.

| X_1 | T(°C) | | | |
|----------|---------|---------|----------|----------|
| | 50 | 60 | 70 | 80 |
| 0 | 1.46574 | 1.46312 | 1.46059 | 1.45813 |
| 0.1 | 1.47020 | 1.46715 | 1.46433 | 1.46153 |
| 0.2 | 1.47615 | 1.47338 | 1.47034 | 1.46783 |
| 0.3 | 1.48103 | 1.47751 | 1.47477 | 1.47279 |
| 0.4 | 1.48681 | 1.48369 | 1.48116 | 1.478718 |
| I.R. 0.5 | 1.49202 | 1.48895 | 1.486075 | 1.48378 |
| 0.6 | 1.49735 | 1.49462 | 1.49182 | 1.48927 |
| 0.7 | 1.50266 | 1.49976 | 1.49732 | 1.4945 |
| 0.85 | 1.50896 | 1.50631 | 1.50351 | 1.50085 |
| 0.95 | 1.51432 | 1.51158 | 1.50895 | 1.50638 |
| 1 | 1.51671 | 1.51422 | 1.51184 | 1.50906 |

Deviations from ideal behavior. Excess molar volume.

Better than presenting the deviation for the values of density, we will use the much more common excess molar volume, the values were calculated with Eq.9, in Figure 12 we can see the curves for the whole range of compositions and temperatures studied in this work. It is hard to see the influence or tendency of the temperature in the values of excess molar volume for this studied system, nonetheless in the range of $X_{IL}(0.3-1)$ we can see the excess molar volume is higher for 70 °C, and then we have the 80°C value and last the 90°C.

It is interesting to see that the highest value for the molar excess volume, which means the highest deviation from ideality, occurs in $X_{IL}=0.4$ near the area where viscosity also deviates the most from ideality, with a shoulder at 0.8.

In the reported literature we see diverse orientations about excess molar volumes for the IL [bmim][Cl], in mixtures with organic solvents with presence of some hydroxyl groups and other functional groups we usually have negative values for this property. In the mixture of [bmim][Cl] with Dimethyl sulfoxide (DMSO) the Excess molar volume turned out to be positive, in the mixture of this IL with acetonitrile, ethanol and acetone the values were negative [16] [62]. We can see that both the three-dimensional structure, size and kind of bonds it offers to have with the mixture affect this property.

There is a very interesting case for the ionic liquids family where this value goes both sides of the axis, it starts with negative values and passing the molar fraction 0.4 this values changes its tendency to positive values, this happens with a mixture of the ionic liquid and N,N-Dimethylformamide [63]

The highest values of the Excess molar volume for the entire composition are found near the same area that we find the lowest values for viscosities, this agrees with the literature in a sense that molecules that are somehow farther apart will find it easier to move past another in other words they will find less resistance to flow.

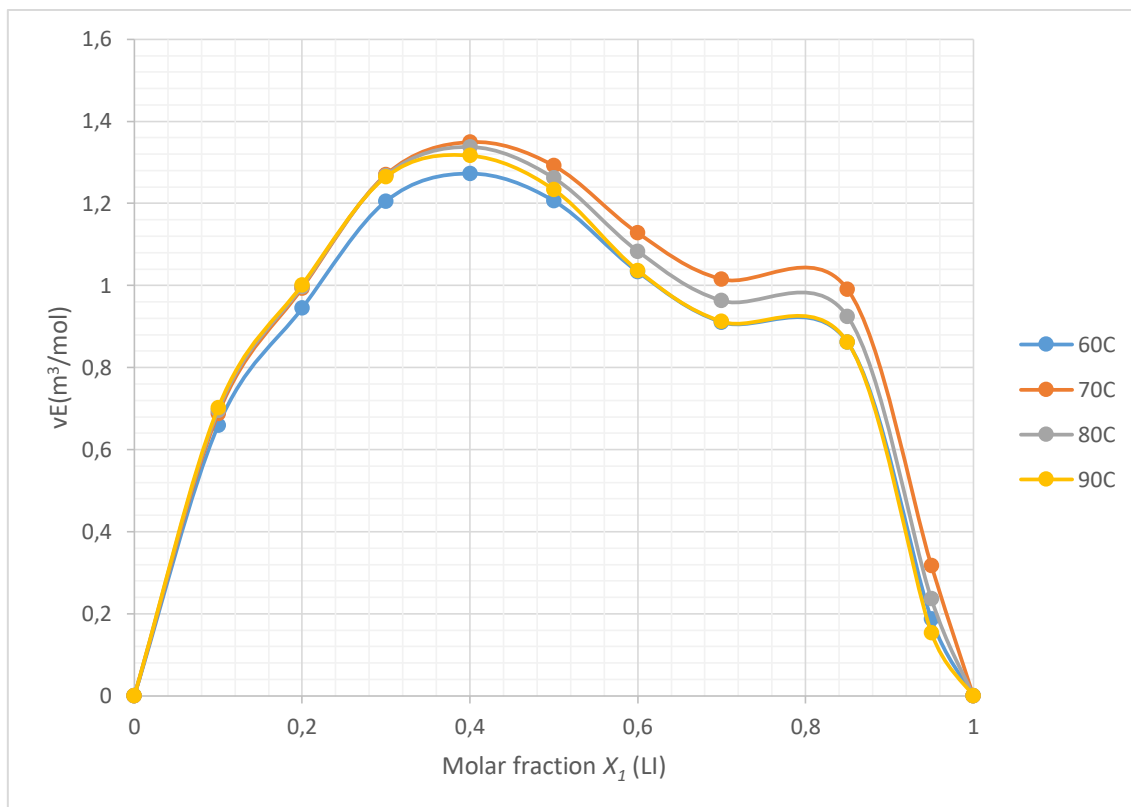


Figure 12: Excess molar volumes values for the [bmim][Cl] and glycerol mixture at 60,70,80 and 90 °C at the whole molar fraction composition range.

Viscosity deviations.

Deviation values for viscosity $\Delta\eta$ appear in Figure 13, the values were calculated with Eq.9, as we can see the influence of temperature in this property is clear, the deviation from ideality is greater at lower temperatures than at higher ones.

This trend can be seen in other mixtures of ionic liquids as for example, 8-hydrogen-1,8-diazabicyclo[5,4,0]-undec-7-enium imidazolid ([HDBU]IM) and 8-butyl-1,8-diazabicyclo[5,4,0]-undec-7-enium imidazolid ([BDBU]IM) both of them in mixtures with water [64].

From the concentration point of view, we can see that the values that deviate more from ideality are around $X_{LI}=0.6$, although the lowest values for the viscosity property are found around the 0.3 molar fraction, this behavior repeats itself in all the studied temperatures. The fact that the deviation is negative occurs also in the mixture of the same ionic liquid with N-methyl-2-pyrrolidone [65] also in a mixture that contains a ionic liquid that shares the same cation 1-butyl-3-methylimidazolium bis(trifluoromethylsulfonyl)imide, [bmim][NTf2] with ethanol [66]. However we can

also find positive deviations for the viscosity property in mixtures of other ionic liquids as [HDBU]IM and [BDBU]IM with water [64]. To explain these kinds of deviations, be them positive or negative, we are going to need to take an step further and analyze the molecular structures our mixtures are forming, what kind of bonds are appearing and which of them predominate.

This diversity of possibilities is what makes IL's relevant and interesting; with the right tailoring of cations and anions, we could have the modifications we need in the properties we want. In the particular case of [bmim][Cl] and glycerol they are known for having high viscosities values that might reduce their capability to be used in industrial applications, knowing this mixture lowers their viscosity might be useful in future industries. Ionic liquids typically have strong interactions between its ions and glycerol establishes hydrogen bond between its own molecules, as we can see in the diminishing values of viscosity these delicate interactions are disturbed as the other component begins to appear in the mixture.

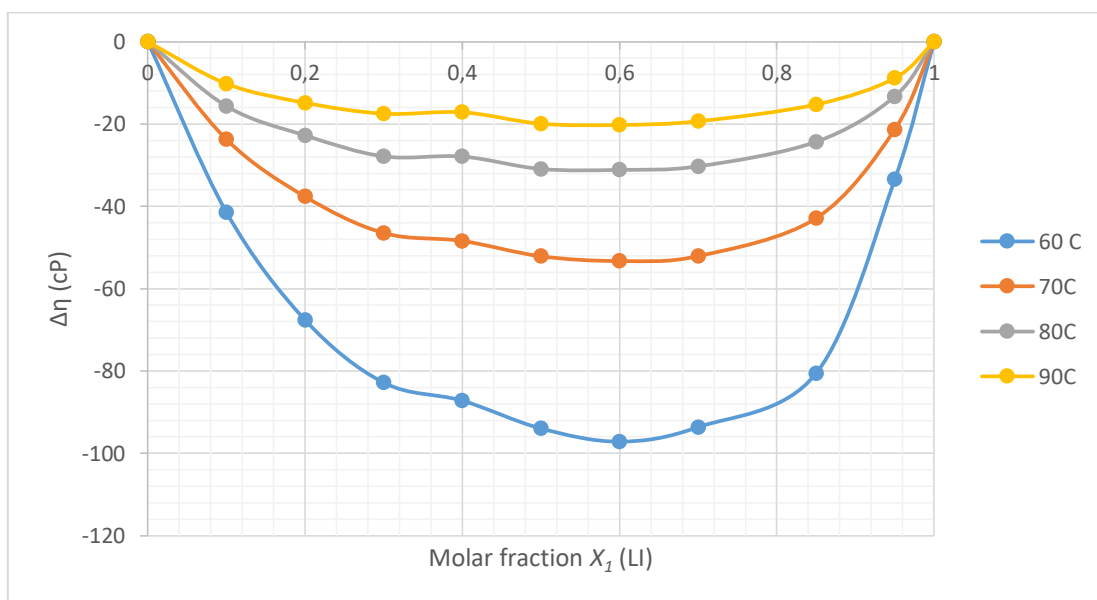


Figure 13: Viscosity deviation values for the [bmim][Cl] and glycerol mixture at 60,70,80 and 90 °C at the whole molar fraction composition range.

Refractive index deviations.

The values of the deviation of the refractive index are plotted in Figure 14, the values were calculated with Eq.9, it is difficult to observe a clear trend in between the established temperatures of the experiment, to some degree we could say that these values are higher

for lower temperatures than at higher ones. Comparing this tendency with the available literature, we find that for the mixture of 2-hydroxyethyl trimethyl ammonium L-lactate ($[(\text{C}_2\text{H}_4\text{OH})(\text{CH}_3)_3\text{N}]\text{-[Lactate]}$) with water, the deviation for R.I. is always positive and its value is higher at lower temperatures than at higher ones [67]. For the mixture of 1-(1-methylpiperidinium-1-yl)hexane-(1-pyridinium)bi[bis(trifluoromethanesulfonyl)imide] ($[\text{MPiC}_6\text{Py}][\text{NTf}_2]_2$) with acetonitrile the influence of temperature had an opposite effect, generating higher values of deviation for higher temperatures [68]

The development of deviation for the R.I. throughout the whole range composition follows more or less the same characteristic pattern for all temperatures, it has positive and negative values and inflection points near the same molar fraction values. Most values found in literature for ionic liquids point to positive values of deviation, although there are reported cases of negative deviations in the R.I. as for example N-ethylaniline (NEA) with phenetole [69], mixtures of [bmim]I, an ionic liquid that shares cation with ours, with 1-butanol shows this positive deviation tendency [70]. Another effort that works with binary mixtures of the IL 1,1,3,3-tetramethylguanidine imidazolide ([TMG]IM) with water, methanol, ethanol, 1-propanol and 1-butanol also shows this trend [71].

When we see how small the deviation values for this property are, we might think this are related with experimental errors, be them associated with the equipment or the techniques used in the laboratory. Nonetheless we do see this kind of magnitude in some of the literature we have reported for this deviation, we have to take into account that as this errors get smaller we could speak of our mixture having an ideal behavior regarding the R.I. property.

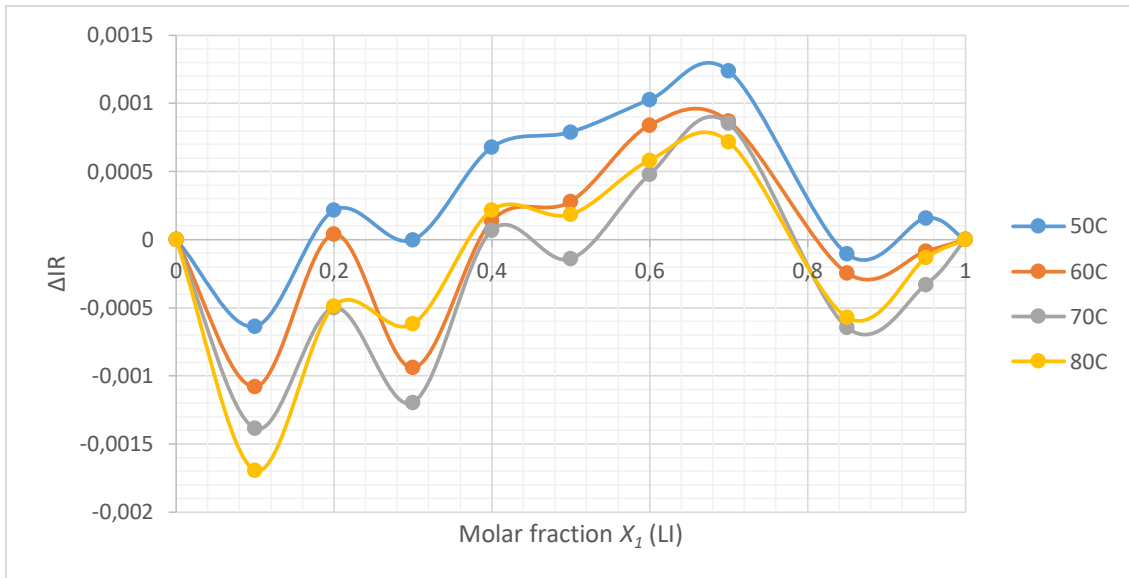


Figure 14: Refractive index deviation values for the [bmim][Cl] and glycerol mixture at 60,70,80 and 90 °C at the whole molar fraction composition range.

Association activation parameters. Enthalpy of activation (ΔH^), Gibbs Energy of activation (ΔG^*), Activation Entropy (ΔS^*) and change in heat capacity of activation (ΔC_p^*).*

To determine the association activation parameters we use the Arrhenius form of viscosity (η) relation shown in Eq.17, in it we have, (ΔH^*) Enthalpy of activation, (ΔS^*) Activation Entropy, (h) Planck's constant, (N) Avogadro's number, (V) molar volume of the mixture at the same temperature. We use a little bit of algebra to get $\ln\left(\frac{v\eta}{hN}\right) = \frac{\Delta H^*}{RT} - \frac{\Delta S^*}{R}$ Eq. 18Eq.18, plotting $\ln\left(\frac{v\eta}{hN}\right)$ against $1/T$ and using the linear regression method with the experimental data available we obtain the slope $\frac{\Delta H^*}{R}$ and the intercept $-\frac{\Delta S^*}{R}$, the values obtained using this method for (ΔH^*) Enthalpy of activation and (ΔS^*) Activation Entropy are shown in Table 12 and plotted in Figure 15.

$$\eta = \left(\frac{hN}{V}\right) e^{\Delta H^*/RT} e^{-\Delta S^*/R} \quad \text{Eq. 17}$$

$$\ln\left(\frac{v\eta}{hN}\right) = \frac{\Delta H^*}{RT} - \frac{\Delta S^*}{R} \quad \text{Eq. 18}$$

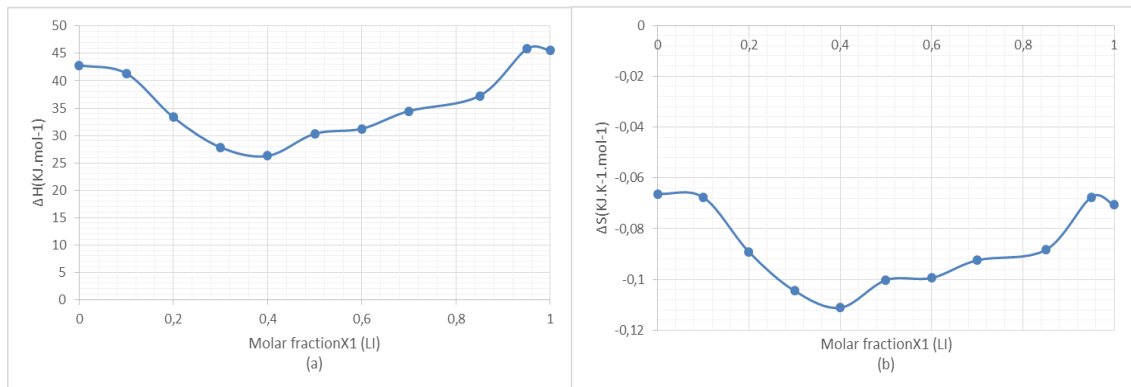


Figure 15 Enthalpy of activation and (ΔS^*) Activation Entropy for the [bmim][Cl] and glycerol mixture for the 50 °C to 80 °C at the whole molar fraction composition range

Table 12: (ΔH^*) Enthalpy of activation and (ΔS^*) Activation Entropy for the [bmim][Cl] and glycerol mixture for the 50 °C to 80 °C at the whole molar fraction composition range.

| X_{IL} | 0 | 0.1 | 0.2 | 0.3 | 0.4 | 0.5 | 0.6 | 0.7 | 0.85 | 0.95 | 1 |
|---|--------|--------|--------|--------|--------|--------|--------|--------|--------|--------|--------|
| ΔH (KJ.mol ⁻¹) | 42.854 | 41.350 | 33.326 | 27.844 | 26.280 | 30.333 | 31.253 | 34.480 | 37.263 | 45.814 | 45.584 |
| ΔS (KJ.K ⁻¹ mol ⁻¹) | -0.066 | -0.068 | -0.089 | -0.104 | -0.111 | -0.100 | -0.099 | -0.092 | -0.088 | -0.068 | -0.071 |

As we can see in Figure 16 (a) the Enthalpy of activation (ΔH^*) also referred as Energy of activation in the literature decreases with the increment of the molar fraction to a minimum close to the 0.4 value, and then goes up almost steadily to pure ionic liquid. The lowering of the values of (ΔH^*) can be seen as a gain in mobility for the molecules in the mixture. The increment of the foreign molecules in the pure liquids diminishes the hindrance of movement of ions and molecules of glycerol, which makes it easier to produce vacant sites in the solvent matrix, until the minimum near $X_{IL}=0.4$ [72][73].

The values of entropy (ΔS^*) shown in Figure 16 (b) are all negative and decreasing to $X_{IL}=0.4$, and then it goes up to any of the pure liquids form. This dropping value of the entropy of activation can be seen as the appearance of intermolecular forces between the IL and glycerol that reduces disorder in this process. We can also interpret this as a molecular rearrangement in our mixture that diminishes the possible microscopic configurations and as we already see with the values of enthalpy of activation makes it easier to flow [72].

In Table 13, we can find the values for the excess enthalpy of activation (ΔH^{E*}) and excess entropy of activation (ΔS^{E*}), they are also plotted in Figure 16. Both properties are negative which can be interpreted as our mixtures needing a lower energy to move to an activated state, and having a more ordered state than the ideal mixture would need, and again they have a minimum value near the $X_{IL}=0.4$.

Table 13: (ΔH^{E*}) Excess Enthalpy of activation and (ΔS^{E*}) Excess Entropy of Activation for the [bmim][Cl] and glycerol mixture for the 50 °C to 80 °C at the whole molar fraction composition range.

| X_{IL} | 0 | 0.1 | 0.2 | 0.3 | 0.4 | 0.5 | 0.6 | 0.7 | 0.85 | 0.95 | 1 |
|-------------------------------|---|--------|--------|--------|--------|--------|--------|--------|--------|--------|---|
| ΔH^{E*} (kJ/mol) | 0 | 1.7771 | 10.074 | 15.829 | 17.666 | 13.886 | 13.239 | 10.284 | 7.9115 | 0.3660 | 0 |
| ΔS^{E*} (kJ/K.mol) | 0 | 0.0009 | 0.0220 | 0.0368 | 0.0430 | 0.0317 | 0.0305 | 0.0231 | 0.0183 | 0.0028 | 0 |

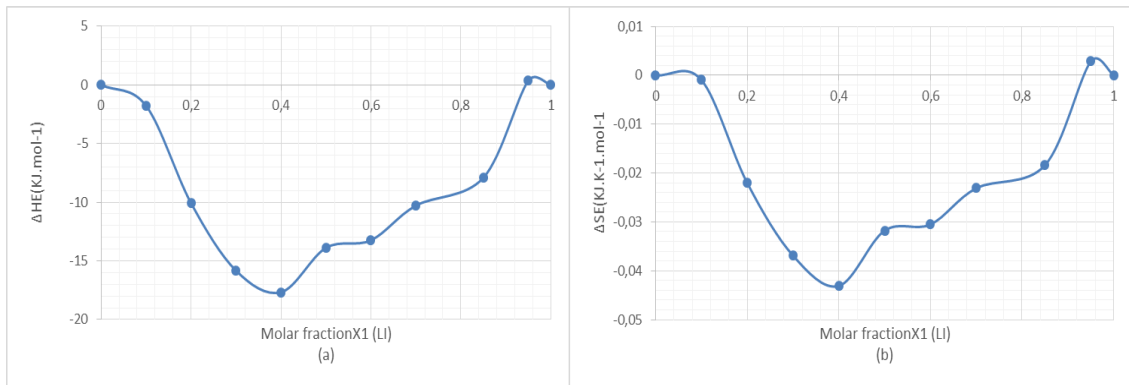


Figure 16; (ΔH^{E*}) Excess Enthalpy of activation and (ΔS^{E*}) Excess Entropy of Activation for the [bmim][Cl] and glycerol mixture for the 50 °C to 80 °C at the whole molar fraction composition range.

The values related to Molar Gibbs energy of activation (ΔG^*) were obtained using the thermodynamic fundamental equation, seen in Eq.19 and Excess Molar Gibbs energy of activation (ΔG^{E*}) using Eq.20 are presented in Table 14 and are plotted in Figure 17 [74].

$$\Delta G^* = \Delta H^* - \Delta S^*T \quad \text{Eq. 19}$$

$$\Delta G^{E*} = RT \left[\ln \frac{\eta^M \rho_2}{\eta_2 M_2 \rho} - x_1 \ln \frac{\eta_1 M_1 \rho_2}{\eta_2 M_2 \rho_1} \right] \quad \text{Eq. 20}$$

Table 14: Molar Gibbs energy of activation (ΔG^*) and Excess Molar Gibbs energy of activation (ΔG^{E*}) for the [bmim][Cl] and glycerol mixture for the 50 °C to 80 °C at the whole molar fraction composition range.

| X_{IL} | $\Delta G^{E*}(\text{KJ.mol}^{-1})$ | | | | $\Delta G^*(\text{KJ.mol}^{-1})$ | | | |
|----------|-------------------------------------|--------|--------|--------|----------------------------------|--------|--------|--------|
| | 363.15 | 353.15 | 343.15 | 333.15 | 363.15 | 353.15 | 343.15 | 333.15 |
| | T (K) | | | | T (K) | | | |
| 0 | 0.000 | 0.000 | 0.000 | 0.000 | 66.92 | 66.26 | 65.59 | 64.93 |
| 0.1 | -1.388 | -1.530 | -1.396 | -1.467 | 65.92 | 65.24 | 64.57 | 63.89 |
| 0.2 | -2.087 | -2.324 | -2.463 | -2.771 | 65.70 | 64.81 | 63.92 | 63.03 |
| 0.3 | -2.394 | -2.877 | -3.149 | -3.536 | 65.78 | 64.73 | 63.69 | 62.64 |
| 0.4 | -2.008 | -2.458 | -2.907 | -3.296 | 66.62 | 65.51 | 64.40 | 63.29 |
| 0.5 | -2.374 | -2.644 | -2.954 | -3.326 | 66.73 | 65.72 | 64.72 | 63.72 |
| 0.6 | -2.220 | -2.400 | -2.740 | -3.116 | 67.34 | 66.35 | 65.36 | 64.36 |
| 0.7 | -1.910 | -2.095 | -2.386 | -2.583 | 68.04 | 67.11 | 66.19 | 65.27 |
| 0.85 | -1.260 | -1.381 | -1.590 | -1.800 | 69.35 | 68.47 | 67.58 | 66.70 |
| 0.95 | -0.648 | -0.644 | -0.638 | -0.559 | 70.35 | 69.67 | 69.00 | 68.32 |
| 1 | 0.000 | 0.000 | 0.000 | 0.000 | 71.23 | 70.52 | 69.82 | 69.11 |

The influence of temperature in Molar Gibbs energy of activation (ΔG^*) and Excess Molar Gibbs energy of activation (ΔG^{E*}) is clear, they both rise as the temperatures increase. As the ionic liquid increases (ΔG^*) diminishes to a minimum near the 0.3 value, then it goes up steadily to the pure glycerol form, these values are always positive. The (ΔG^{E*}) property goes to a minimum near the $X_{IL}=0.3$ as well, which goes into accord with the minimum value found for the viscosity of this mixture in the same molar fraction. Then it goes up only slightly to the $X_{IL}=0.4$, falls again for the $X_{IL}=0.5$ value to then go up steadily, this behavior marks the region with an unstable behavior [75] [76], these values always negative and therefore lower than what we would ideally expect.

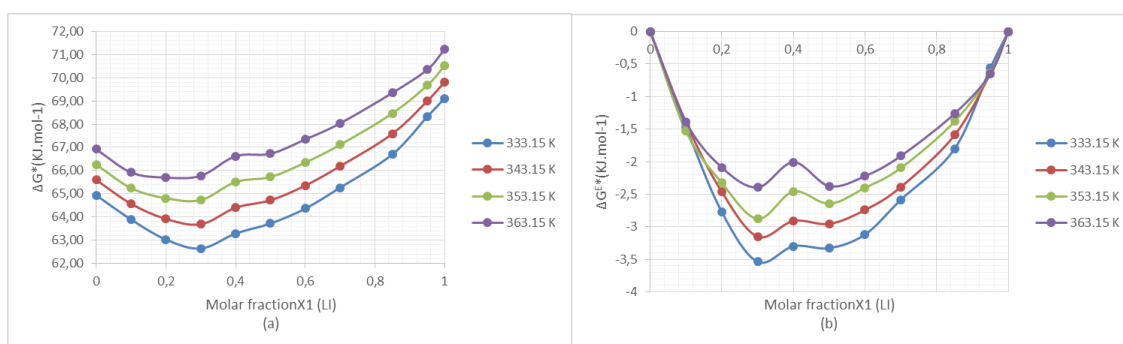


Figure 17: Molar Gibbs energy of activation (ΔG^*) and Excess Molar Gibbs energy of activation (ΔG^{E*}) for the [bmim][Cl] and glycerol mixture for the 50 °C to 80 °C at the whole molar fraction composition range.

Fitting experimental data to literature reported equations.

Correlating viscosity's dependence on temperature.

One of the most widely used equations to correlate the viscosity of a fluid, as a function of temperature is the Vogel-Fulcher-Tammann (VFT) equation; it is shown in Eq.21 and the values obtained for this work can be seen in Table 15 [77] [78].

$$\eta = Ae^{\left(\frac{B}{T-T_0}\right)} \quad \text{Eq. 21}$$

As we can see in the values of deviation the VFT equation fits well to the values experimentally found, obtaining good values of deviation having R^2 as low as 0.9964 and as high as rounded up 1. This point toward the possibility of using the fitted parameters for this equation to predict values of viscosity different from the molar fraction we examined in this work.

Other efforts have been made to correlate the function of viscosity on temperature; Ghatee et al. equation is one of them and is expressed as Eq.22, in this form, the relation $1/\eta$ has an almost linear tendency with respect to the temperature variable. The value typically used for (ϕ) in $\left(\frac{1}{\eta}\right)^\phi = a + bT$ Eq. 22Eq.22, a fitting parameter that varies according to the type of fluid we are analyzing, is 0.3 in the case of ionic liquids, obtaining good results with molecules involving imidazolium-, pyrrolidinium-, quaternary ammonium-, and nicotinium [79] [80]

$$\left(\frac{1}{\eta}\right)^\phi = a + bT \quad \text{Eq. 22}$$

We can see the data fitted using the Ghatee et al. equation in Table 16, we have a good accuracy for this fit shown with a low values of the sum of squares due to error (SSE), proposing it as a good option to predict values for viscosity.

These two equations are commonly found in the literature to fit the dependence of viscosity on temperature, decisions about choosing one or another will depend on factors as easiness of calculation methods and analyzing goodness of fit parameters for both equations.

Table 15: Fitted parameters and deviation values for the VFT equation for the [bmim][Cl] and glycerol mixture for the 50 °C to 80 °C at the whole molar fraction composition range.

| XI | Fitting Values | | | | Goodness of fit | | | |
|------|----------------|----------|-------|---------|--------------------|----------------|----------|--|
| | A | B | To | RMSE | AD. R ² | R ² | SSE | |
| 0 | 710.9 | 0.1618 | 219.2 | 0.8296 | 0.9989 | 0.9996 | 0.7967 | |
| 0.1 | 915.8 | 0.05202 | 200 | 1.346 | 0.9928 | 0.9976 | 1.813 | |
| 0.2 | 842.4 | 0.009251 | 189.8 | 0.7003 | 0.9942 | 0.9981 | 0.4904 | |
| 0.3 | 206.5 | 1.4777 | 261.6 | 0.6869 | 0.9893 | 0.9964 | 0.4718 | |
| 0.4 | 136 | 2.94 | 275.3 | 0.2537 | 0.9988 | 0.9996 | 0.06435 | |
| 0.5 | 526.3 | 0.3612 | 216.5 | 0.2621 | 0.9991 | 0.9997 | 0.06871 | |
| 0.6 | 890.2 | 0.1166 | 179.6 | 0.0144 | 1 | 1 | 0.000207 | |
| 0.7 | 305.8 | 1.107 | 253.2 | 0.1501 | 0.9999 | 1 | 0.02252 | |
| 0.85 | 617.3 | 0.3436 | 219.1 | 0.07824 | 1 | 1 | 0.006121 | |
| 0.95 | 473.3 | 0.5932 | 245.7 | 0.05059 | 1 | 1 | 0.002559 | |
| 1 | 703.4 | 0.2807 | 223.4 | 0.1622 | 1 | 1 | 0.0263 | |

Correlating Excess Molar Volume dependence with molar fraction.

The calculated values for the Excess Molar Volume V_m^E was fitted the Redlich-Kister Equation, this expansion series is widely used in the literature studied for this work, it is expressed in $V_m^E = x_1 x_2 \sum_{i=0}^k A^i (x_1 - x_2)^i$ Eq. 23 Eq.23, this equation is typically used to fit many physical and chemical quantities, deviations of properties and excess values [74] [81]. In this work, we have chosen four as the value for k as further development of this mathematical series does not add greater accuracy for the fitting, and we used Matlab® to do the calculations necessary, Nonlinear Least Squares method and the Trust Region algorithm [82].

$$V_m^E = x_1 x_2 \sum_{i=0}^k A^i (x_1 - x_2)^i \quad \text{Eq. 23}$$

In Table 17 we can see the fitted parameters for the Redlich-Kister and the deviation values for it, 0.9729 can be considered as a R^2 value somehow low for this type of fitting, other values as SSE go as low as 0.04254. In Figure 18 part (a) we can graphically see the quality of this fitting together with residual plots for it in part (b), the residual values are absolute and were calculated with Eq.24, we found a greater deviation in $X_{IL}=0.85$ and $X_{IL}=0.95$.

$$\text{Absolute Residual value} = V_{\text{Experimental value}} - V_{\text{Redlich Kister}} \quad \text{Eq. 24}$$

Table 16: Fitted parameters and deviation values for the Ghatee et al. equation for the [bmim][Cl] and glycerol mixture for the 50 °C to 80 °C at the whole molar fraction composition range.

| X_{il} | Fitted Values | | | Goodness of fit | | |
|----------|---------------|---------|-------------------------|-----------------|-------------------------|----------|
| | A(P2) | B(P1) | SSE | R ² | ADJUSTED R ² | RMSE |
| 0 | 0.3294 | 0.05417 | 1.47x10 ⁻⁵ | 0.9983 | 0.9975 | 0.002707 |
| 0.1 | 0.3796 | 0.06202 | 7.57 x10 ⁻⁵ | 0.9931 | 0.9896 | 0.006152 |
| 0.2 | 0.4132 | 0.05327 | 4.05 x10 ⁻⁵ | 0.9953 | 0.9929 | 0.0045 |
| 0.3 | 0.4313 | 0.04644 | 0.000105 | 0.9841 | 0.9761 | 0.007235 |
| 0.4 | 0.4093 | 0.04167 | 5.53 x10 ⁻⁵ | 9895 | 0.9842 | 0.00526 |
| 0.5 | 0.4077 | 0.04797 | 1.32 x10 ⁻⁵ | 0.9981 | 0.9971 | 0.002566 |
| 0.6 | 0.3901 | 0.04737 | 7.283 x10 ⁻⁷ | 0.9999 | 0.9998 | 0.000604 |
| 0.7 | 0.3666 | 0.04876 | 1.416 x10 ⁻⁵ | 0.998 | 0.997 | 0.002661 |
| 0.85 | 0.3272 | 0.04706 | 2.125 x10 ⁻⁶ | 0.9997 | 0.9995 | 0.001031 |
| 0.95 | 0.2911 | 0.05103 | 5.14 x10 ⁻⁶ | 0.9993 | 0.999 | 0.001603 |
| 1 | 0.2691 | 0.04704 | 1.10 x10 ⁻⁶ | 0.9998 | 0.9998 | 0.00074 |

Table 17: Fitted parameters and deviation values for the Redlich-Kister equation, correlating Molar Excess Volume V^E dependence on molar fraction X_i for the [bmim][Cl] and glycerol mixture for the 50 °C to 80 °C at the whole molar fraction composition range.

| T (K) | 333.15 | 343.15 | 353.15 | 363.15 |
|-------------------------|---------|---------|---------|---------|
| A0 | 4.67 | 5.034 | 4.901 | 4.754 |
| A1 | -1.759 | -1.745 | -1.918 | -2.058 |
| A2 | 3.442 | 3.213 | 3.577 | 4.051 |
| A3 | 2.304 | 3.517 | 2.844 | 2.146 |
| A4 | -0.9568 | 1.003 | -0.3655 | -1.868 |
| Goodness of fit | | | | |
| SSE | 0.0555 | 0.04254 | 0.05385 | 0.06715 |
| R ² | 0.9758 | 0.9831 | 0.9784 | 0.9729 |
| ADJUSTED R ² | 0.9597 | 0.9718 | 0.964 | 0.9549 |
| RMSE | 0.09614 | 0.0842 | 0.09474 | 0.1058 |

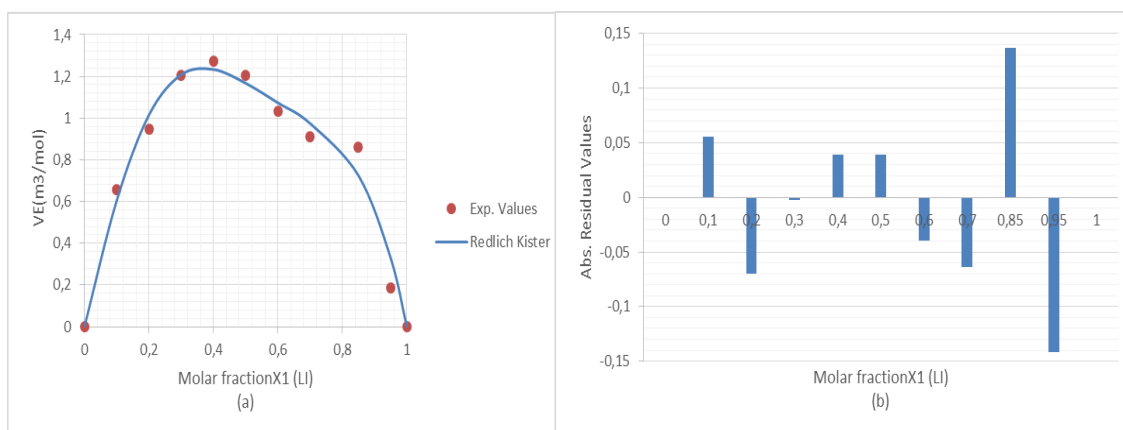


Figure 18: (a) Experimental Values for the Excess Molar Volume V^E for 333.15K, the fitting to the Redlich-Kister equation is represented with the solid line. (b) Absolute Residual values plot for this fitting.

Correlating Viscosity's deviation dependence with molar fraction.

Using $V_m^E = x_1x_2 \sum_{i=0}^k A^i(x_1 - x_2)^i$ Eq. 23Eq.23, the Redlich-Kister Equation to calculate the fitting parameters for the dependence of viscosity on the molar fraction of the ionic liquid we obtain the values seen in Table 18 [83]. The value of R^2 are fairly high, the lowest of them being 0.9970 for the temperature of 353.15 K, so we could the equation fits well viscosity's deviation;

Seeing the SSE value for the 333.15K we might be worried that the fitting is not so good yet values for other parameters at the same temperature show the correlation represents well the experimental data in general, including other temperatures [62].

Table 18: Fitted parameters and deviation values for the Redlich-Kister equation, correlating Viscosity's deviation dependence on molar fraction X_{il} for the [bmim][Cl] and glycerol mixture for the 50 °C to 80 °C at the whole molar fraction composition.

| T (K) | 333.15 | 343.15 | 353.15 | 363.15 |
|-----------------|--------|--------|--------|--------|
| A0 | -370.9 | -207.2 | -122.2 | -78.11 |
| A1 | -68.49 | -29.16 | -16.03 | -14.39 |
| A2 | -348.4 | -153.8 | -70 | -36.38 |
| A3 | -106.6 | -70.76 | -24.07 | -3.853 |
| A4 | 62.93 | -46.54 | -81.82 | -70.75 |
| Goodness of fit | | | | |
| SSE | 26.53 | 3.243 | 4.079 | 3.653 |
| R2 | 0.9981 | 0.9992 | 0.9970 | 0.9933 |
| ADJUSTED R2 | 0.9968 | 0.9987 | 0.995 | 0.9889 |
| RMSE | 2.103 | 0.7352 | 0.8246 | 0.7803 |

After visually evaluating the fitting equation used to correlate the experimental data in Figure 19 part a, we can say it is reasonable accurate. We can see in the residual plots in part b of the same figure that near the $X_{IL}=0.85$, values we can find a greater deviation from the fitting presented, these residual values were calculated with Eq.25.

$$\text{Absolute Residual value} = \eta_{\text{Experimental value}} - \eta_{\text{Redlich Kister}} \quad \text{Eq. 25}$$

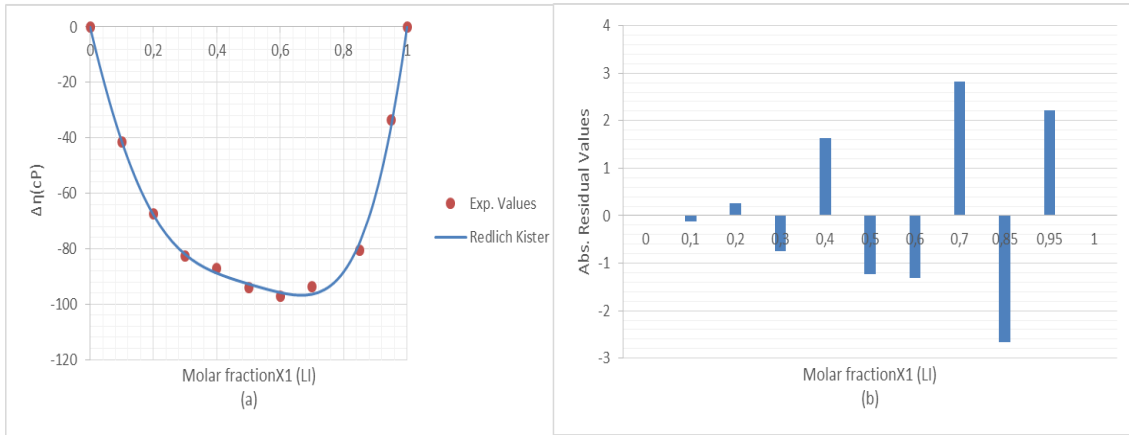


Figure 19: (a) Experimental Values for the Viscosity's deviation $\Delta\eta$ for 333.15K, the fitting to the Redlich-Kister equation is represented with the solid line. (b) Absolute Residual values plot for this fitting.

Conclusions

We found the values for the density of the mixtures at the entire molar fraction range and temperatures ranging from 333.15 K to 373.15 K. These values presented a negative deviation from ideality. The dependence of density with temperature followed what was theoretically expected, as the temperature raised the density values diminished.

We found the values for the viscosity of the mixtures at the entire molar fraction range and temperatures ranging from 333.15 K to 373.15 K. Viscosity values continually decreased with the rise of temperature as was expected. We found a deviation from ideality for the behavior of the mixture's viscosity with the increasing X_{IL} up to a minimum around the 0.3 value and then it went up to the pure IL's value. We need more studies to comprehend the viscosity's lowering values nonetheless there are some hints that point toward the heavy influence of hydrogen bonds.

We found the values for the mixtures Refractive Indexes at the entire molar fraction range and temperatures ranging from 333.15 K to 373.15 K. These values followed an almost straight line from the pure values of both of the components; we could interpret this as having a mixture an almost ideal behavior specifically for this behavior.

We found a positive deviation for the molar excess volume of the mixture in the entire range of composition, with a maximum near the $X_{IL}=0.4$. The deviations for the viscosity values were found to be negative with a minimum near the $X_{IL}=0.6$ value, this deviation persistently decreased as the temperatures raised. It was hard to find a pattern for the deviations of refractive index but for every temperature, nonetheless the variation of the R.I. for every temperature had inflection points at similar molar fractions.

We found the parameters for the Vogel-Fulcher-Tammann (VFT) and Ghatee et al. equations for the correlation viscosity and its dependency on temperature. We also correlated the dependence of the excess molar value and deviation of viscosity on the molar fraction, the goodness of fit for every case was fairly accurate.

Recommendations

We recommend for future works the periodical dehydration of [bmim][Cl] as the presence of even small amounts of water heavily influences in its properties.

We propose studies of the mixtures of glycerol with other organic compounds with none, one or two hydroxyl groups.

We suggest other experiments using the glycerol compound together with other ionic liquids related with [bmim][Cl] for example: [bmim][BF₄], [bmim][NTf₂], [BZMIM][Cl], [BCNIm][Cl], etc.

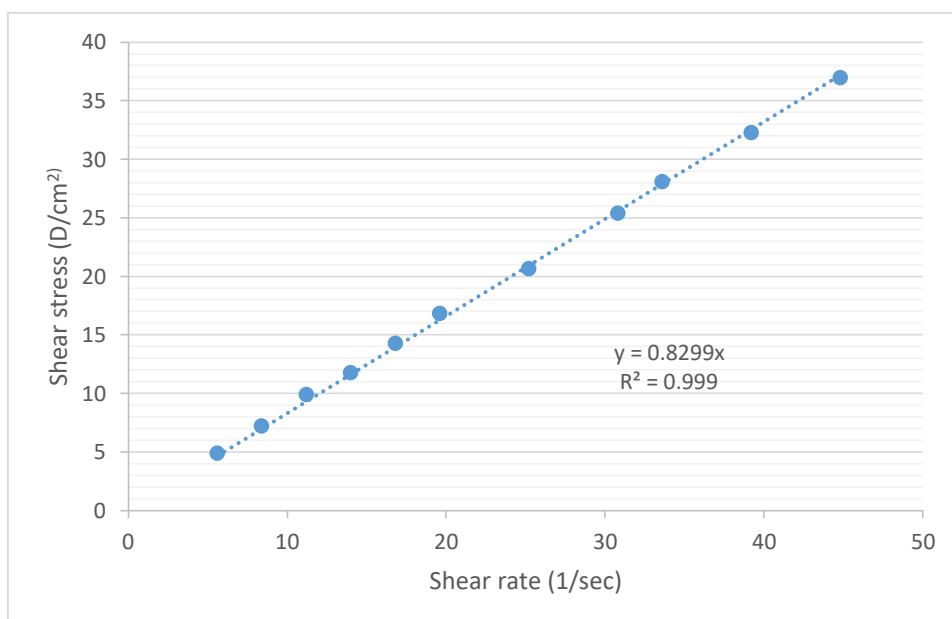
We found several deviations from ideality for the mixture of [bmim][Cl] and glycerol this points to further investigate the reasons of this discrepancies, it would be interesting to make findings about the structural network of this mixture, the kinds and magnitude of the intermolecular forces present in the mixture.

Make other experiments varying pressure values to effectively correlate this data to equations of state.

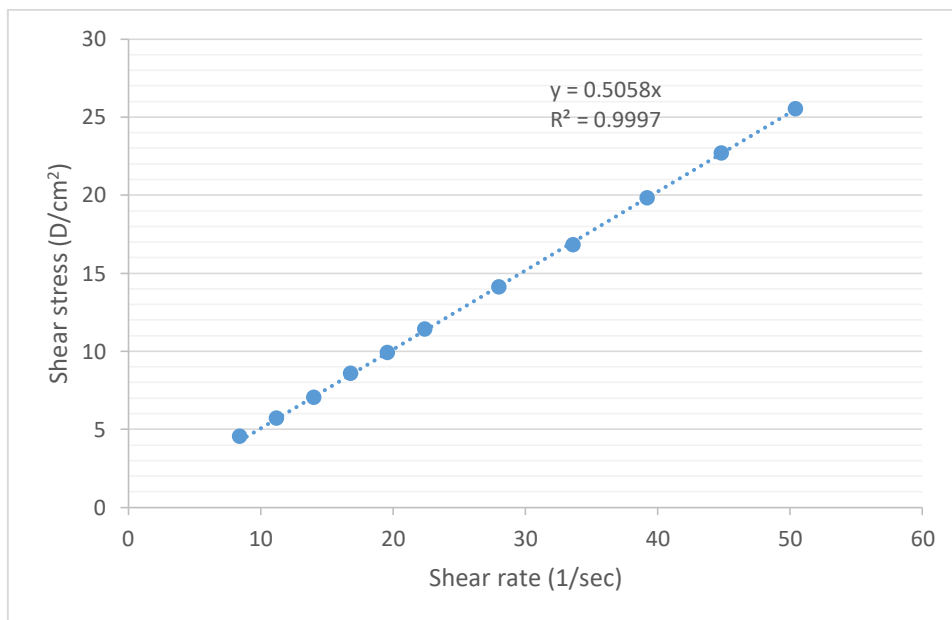
Apendix

Pure Glycerol

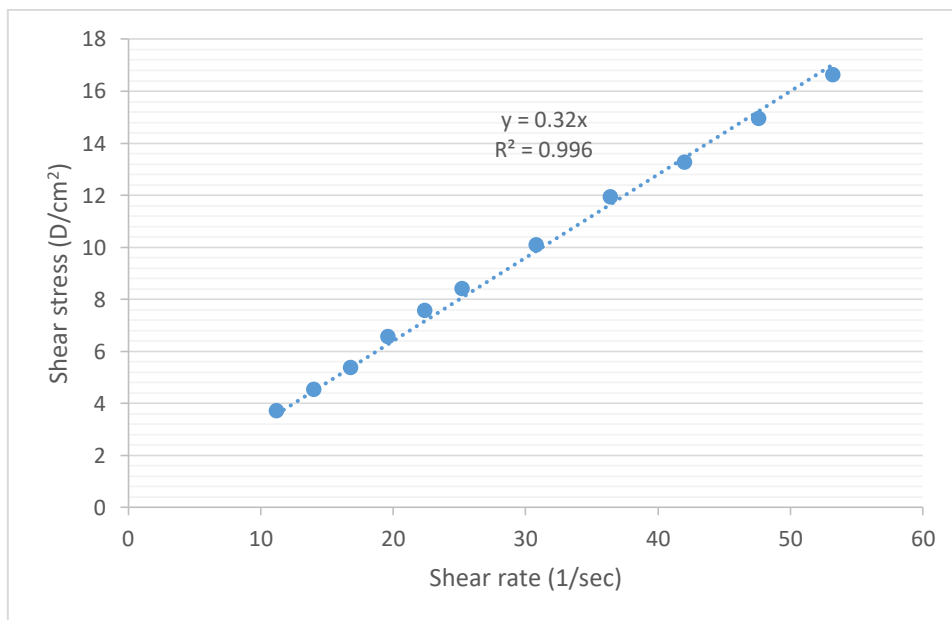
| 60 °C | | | | |
|----------------|-----|------------|-----------------------------------|--------------------|
| Viscosity (cP) | RPM | Torque (%) | Shear stress (D/cm ²) | Shear rate (1/sec) |
| 86.98 | 20 | 2.9 | 4.87 | 5.6 |
| 85.98 | 30 | 4.3 | 7.22 | 8.4 |
| 88.48 | 40 | 5.9 | 9.91 | 11.2 |
| 83.98 | 50 | 7 | 11.76 | 14 |
| 84.98 | 60 | 8.5 | 14.28 | 16.8 |
| 85.7 | 70 | 10 | 16.8 | 19.6 |
| 81.98 | 90 | 12.3 | 20.66 | 25.2 |
| 82.35 | 110 | 15.1 | 25.36 | 30.8 |
| 83.48 | 120 | 16.7 | 28.05 | 33.6 |
| 82.27 | 140 | 19.2 | 32.25 | 39.2 |
| 82.48 | 160 | 22 | 36.95 | 44.8 |



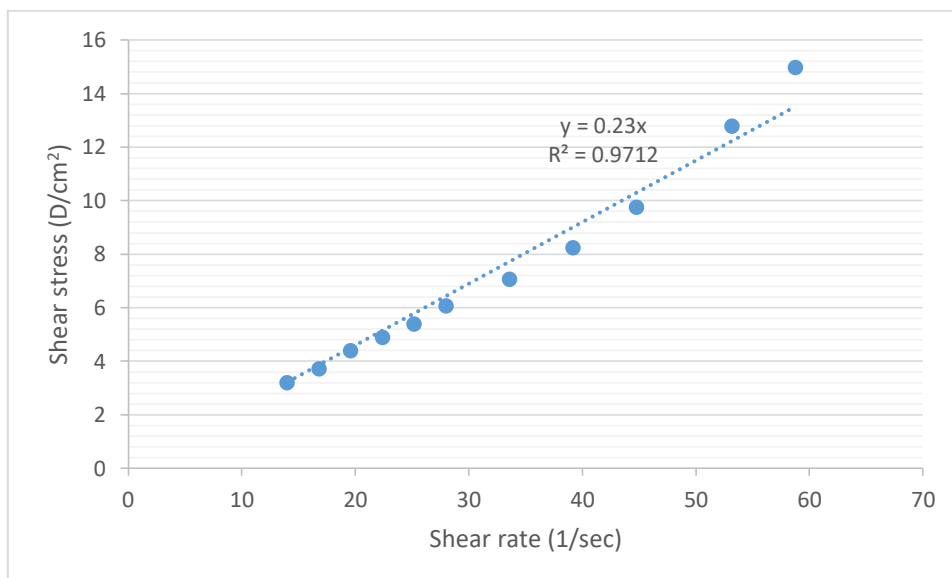
| 70 °C | | | | |
|----------------|-----|------------|-----------------------------------|--------------------|
| Viscosity (cP) | RPM | Torque (%) | Shear stress (D/cm ²) | Shear rate (1/sec) |
| 53.99 | 30 | 2.7 | 4.54 | 8.4 |
| 50.99 | 40 | 3.4 | 5.71 | 11.2 |
| 50.39 | 50 | 4.2 | 7.05 | 14 |
| 50.99 | 60 | 5.1 | 8.57 | 16.8 |
| 50.56 | 70 | 5.9 | 9.91 | 19.6 |
| 50.99 | 80 | 6.8 | 11.42 | 22.4 |
| 50.39 | 100 | 8.4 | 14.11 | 28 |
| 49.99 | 120 | 10 | 16.8 | 33.6 |
| 50.56 | 140 | 11.8 | 19.82 | 39.2 |
| 50.61 | 160 | 13.5 | 22.68 | 44.8 |
| 50.66 | 180 | 15.2 | 25.53 | 50.4 |



| 80 °C | | | | |
|----------------|-----|------------|-----------------------------------|--------------------|
| Viscosity (cP) | RPM | Torque (%) | Shear stress (D/cm ²) | Shear rate (1/sec) |
| 32.99 | 40 | 2.2 | 3.7 | 11.2 |
| 32.39 | 50 | 2.7 | 4.54 | 14 |
| 31.99 | 60 | 3.2 | 5.37 | 16.8 |
| 33.42 | 70 | 3.9 | 6.55 | 19.6 |
| 33.74 | 80 | 4.5 | 7.56 | 22.4 |
| 33.33 | 90 | 5 | 8.4 | 25.2 |
| 32.72 | 110 | 6 | 10.08 | 30.8 |
| 32.76 | 130 | 7.1 | 11.93 | 36.4 |
| 31.59 | 150 | 7.9 | 13.27 | 42 |
| 31.41 | 170 | 8.9 | 14.95 | 47.6 |
| 31.26 | 190 | 9.9 | 16.63 | 53.2 |

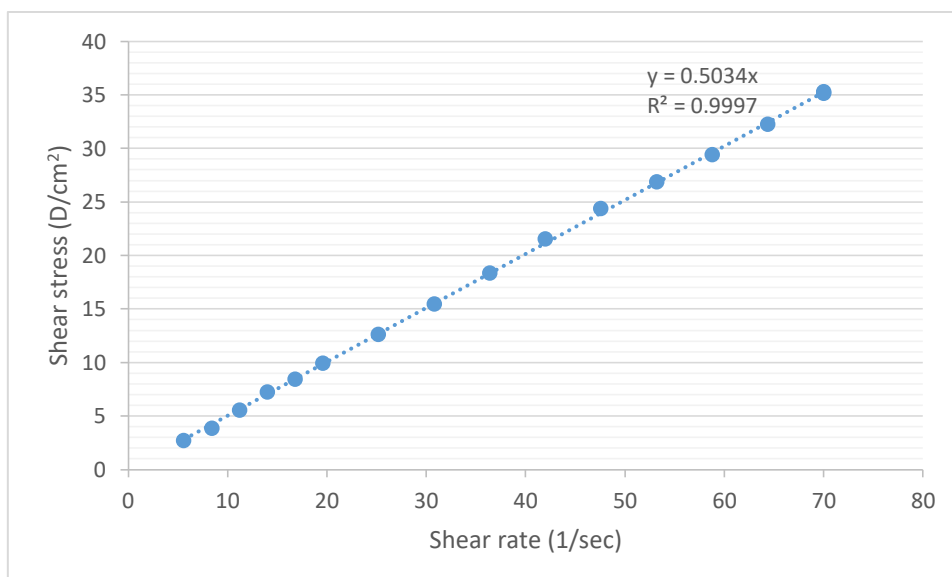


| 90 °C | | | | |
|----------------|-----|------------|-----------------------------------|--------------------|
| Viscosity (cP) | RPM | Torque (%) | Shear stress (D/cm ²) | Shear rate (1/sec) |
| 22.8 | 50 | 1.9 | 3.19 | 14 |
| 22 | 60 | 2.2 | 3.7 | 16.8 |
| 22.28 | 70 | 2.6 | 4.37 | 19.6 |
| 21.75 | 80 | 2.9 | 4.87 | 22.4 |
| 21.33 | 90 | 3.2 | 5.37 | 25.2 |
| 21.6 | 100 | 3.6 | 6.05 | 28 |
| 21 | 120 | 4.2 | 7.05 | 33.6 |
| 21 | 140 | 4.9 | 8.23 | 39.2 |
| 21.75 | 160 | 5.8 | 9.74 | 44.8 |
| 23.99 | 190 | 7.6 | 12.77 | 53.2 |
| 25.42 | 210 | 8.9 | 14.95 | 58.8 |

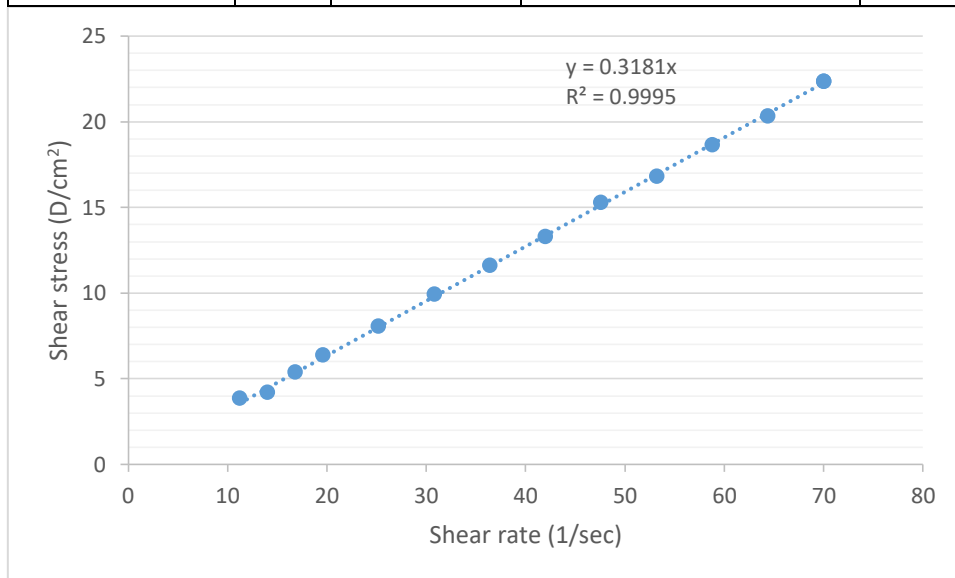


$$X_{IL}=0.1$$

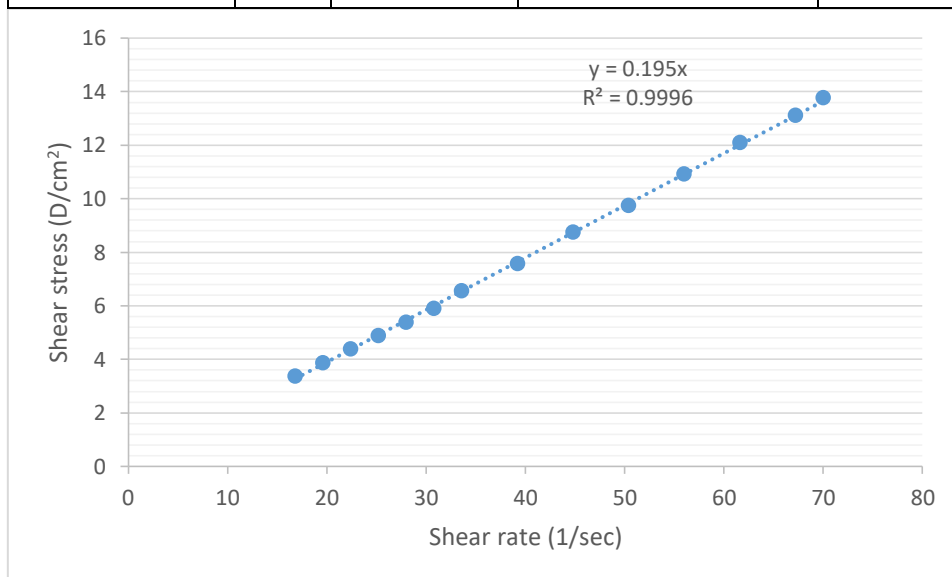
| 60 °C | | | | |
|----------------|-----|------------|-----------------------------------|--------------------|
| Viscosity (cP) | RPM | Torque (%) | Shear stress (D/cm ²) | Shear rate (1/sec) |
| 47.99 | 20 | 1.6 | 2.69 | 5.6 |
| 45.99 | 30 | 2.3 | 3.86 | 8.4 |
| 49.49 | 40 | 3.3 | 5.54 | 11.2 |
| 51.59 | 50 | 4.3 | 7.22 | 14 |
| 49.99 | 60 | 5 | 8.4 | 16.8 |
| 50.56 | 70 | 5.9 | 9.91 | 19.6 |
| 49.99 | 90 | 7.5 | 12.6 | 25.2 |
| 50.17 | 110 | 9.2 | 15.45 | 30.8 |
| 50.3 | 130 | 10.9 | 18.31 | 36.4 |
| 51.19 | 150 | 12.8 | 21.5 | 42 |
| 51.17 | 170 | 14.5 | 24.35 | 47.6 |
| 50.52 | 190 | 16 | 26.87 | 53.2 |
| 49.99 | 210 | 17.5 | 29.39 | 58.8 |
| 50.08 | 230 | 19.2 | 32.25 | 64.4 |
| 50.39 | 250 | 21 | 35.27 | 70 |
| 50.15 | 250 | 20.9 | 35.1 | 70 |



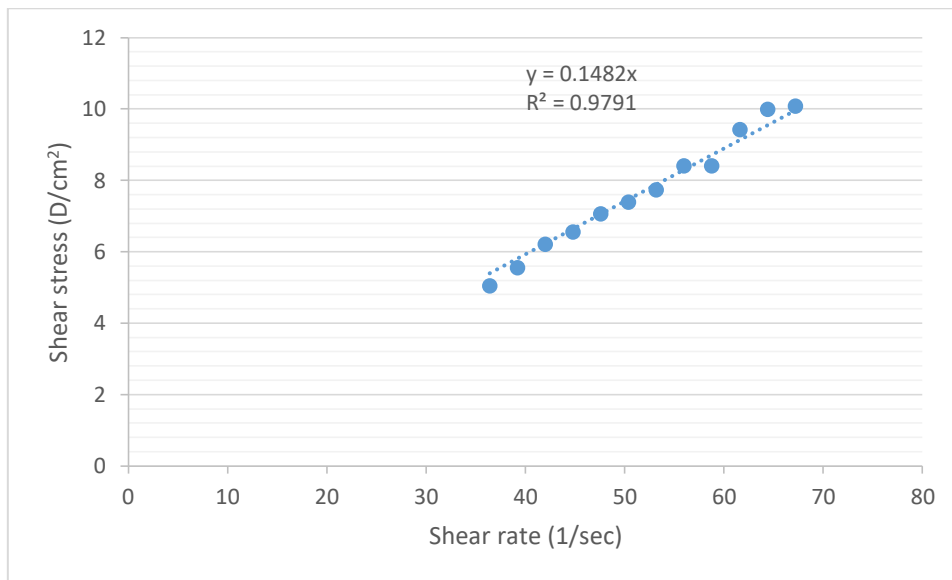
| 70 °C | | | | |
|----------------|-----|------------|-----------------------------------|--------------------|
| Viscosity (cP) | RPM | Torque (%) | Shear stress (D/cm ²) | Shear rate (1/sec) |
| 34.49 | 40 | 2.3 | 3.86 | 11.2 |
| 29.99 | 50 | 2.5 | 4.2 | 14 |
| 31.99 | 60 | 3.2 | 5.37 | 16.8 |
| 32.56 | 70 | 3.8 | 6.38 | 19.6 |
| 31.99 | 90 | 4.8 | 8.06 | 25.2 |
| 32.17 | 110 | 5.9 | 9.91 | 30.8 |
| 31.84 | 130 | 6.9 | 11.59 | 36.4 |
| 31.59 | 150 | 7.9 | 13.27 | 42 |
| 32.11 | 170 | 9.1 | 15.28 | 47.6 |
| 31.57 | 190 | 10 | 16.8 | 53.2 |
| 31.71 | 210 | 11.1 | 18.64 | 58.8 |
| 31.56 | 230 | 12.1 | 20.32 | 64.4 |
| 31.91 | 250 | 13.3 | 22.34 | 70 |
| 31.91 | 250 | 13.3 | 22.34 | 70 |



| 80 °C | | | | |
|----------------|-----|------------|-----------------------------------|--------------------|
| Viscosity (cP) | RPM | Torque (%) | Shear stress (D/cm ²) | Shear rate (1/sec) |
| 20 | 60 | 2 | 3.36 | 16.8 |
| 19.71 | 70 | 2.3 | 3.86 | 19.6 |
| 19.5 | 80 | 2.6 | 4.37 | 22.4 |
| 19.33 | 90 | 2.9 | 4.87 | 25.2 |
| 19.2 | 100 | 3.2 | 5.37 | 28 |
| 19.09 | 110 | 3.5 | 5.88 | 30.8 |
| 19.5 | 120 | 3.9 | 6.55 | 33.6 |
| 19.28 | 140 | 4.5 | 7.56 | 39.2 |
| 19.5 | 160 | 5.2 | 8.73 | 44.8 |
| 19.63 | 180 | 5.8 | 9.74 | 50.4 |
| 19.5 | 200 | 6.5 | 10.92 | 56 |
| 19.68 | 220 | 7.2 | 12.09 | 61.6 |
| 19.68 | 240 | 7.8 | 13.1 | 67.2 |
| 19.68 | 250 | 8.2 | 13.77 | 70 |

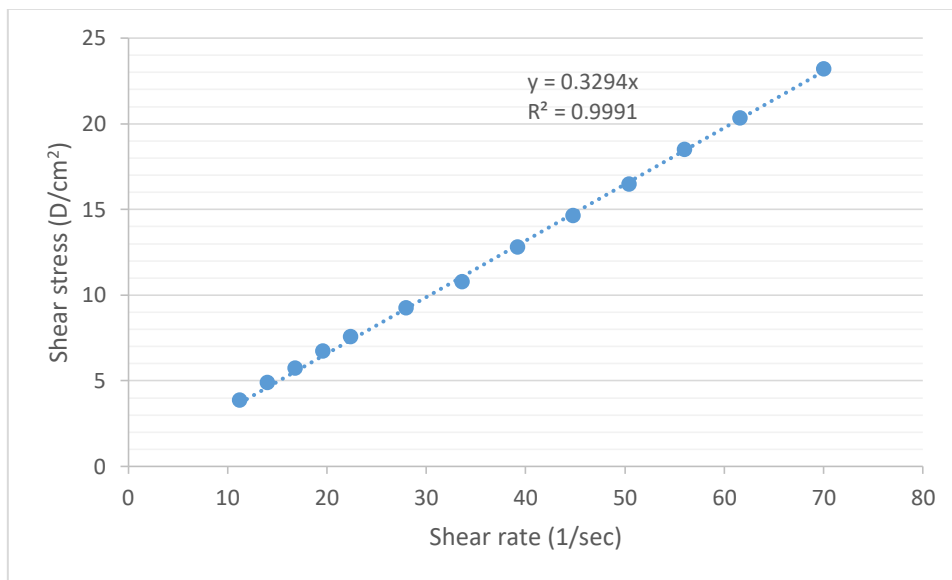


| 90 °C | | | | |
|----------------|------|------------|-----------------------------------|--------------------|
| Viscosity (cP) | RPM | Torque (%) | Shear stress (D/cm ²) | Shear rate (1/sec) |
| 13.84 | 130 | 30 | 5.04 | 36.4 |
| 14.14 | 140 | 3.3 | 5.54 | 39.2 |
| 14.8 | 150 | 3.7 | 6.21 | 42 |
| 14.62 | 160 | 3.9 | 6.55 | 44.8 |
| 14.82 | 170 | 4.2 | 7.05 | 47.6 |
| 14.66 | 180 | 4.4 | 7.39 | 50.4 |
| 14.52 | 190 | 4.6 | 7.73 | 53.2 |
| 15 | 2000 | 5 | 8.4 | 56 |
| 14.28 | 210 | 5 | 8.4 | 58.8 |
| 15.27 | 220 | 5.6 | 9.41 | 61.6 |
| 15.39 | 230 | 5.9 | 9.991 | 64.4 |
| 15 | 240 | 6 | 10.08 | 67.2 |

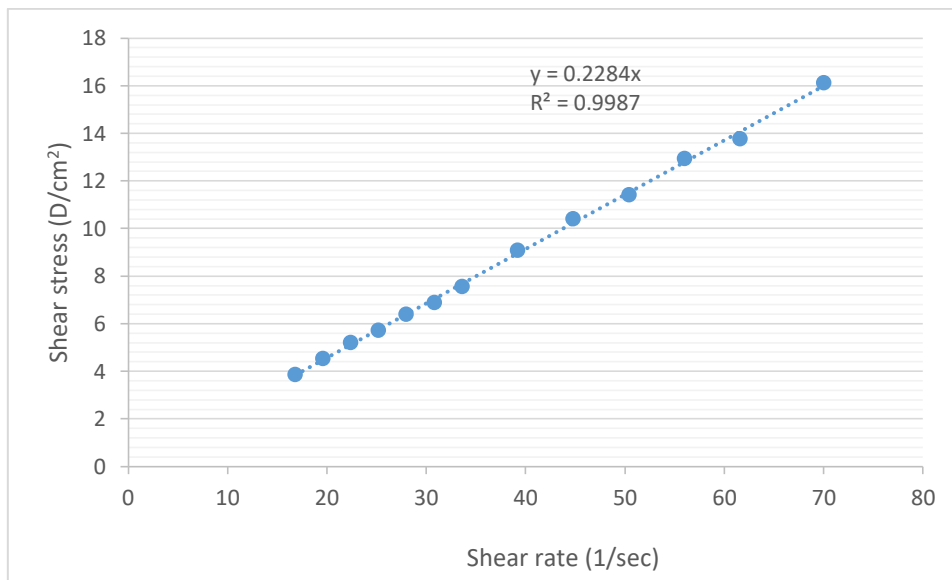


$$X_{IL}=0.2$$

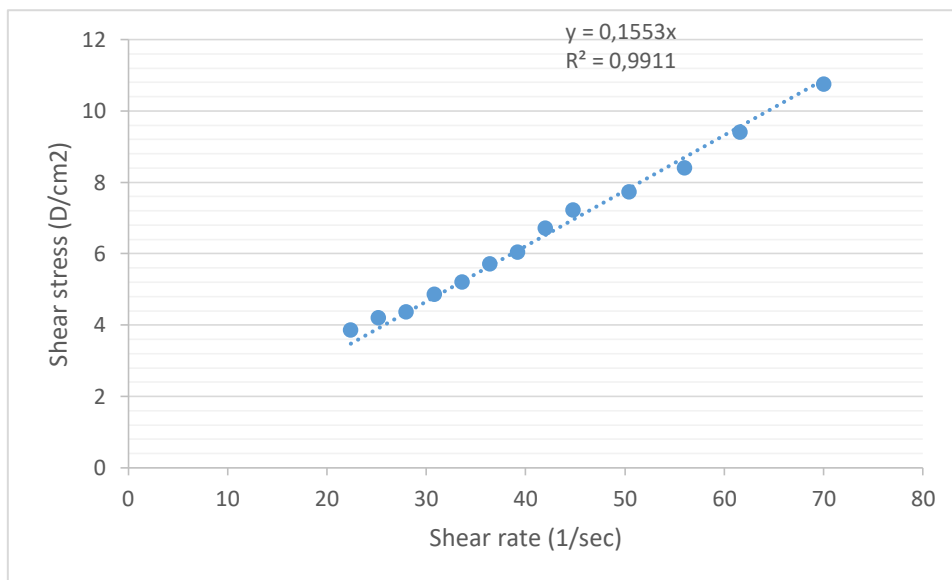
| 60 °C | | | | |
|----------------|-----|------------|-----------------------------------|--------------------|
| Viscosity (cP) | RPM | Torque (%) | Shear stress (D/cm ²) | Shear rate (1/sec) |
| 34.49 | 40 | 2.3 | 3.86 | 11.2 |
| 34.79 | 50 | 2.9 | 4.87 | 14 |
| 33.99 | 60 | 3.4 | 5.71 | 16.8 |
| 34.28 | 70 | 4 | 6.72 | 19.6 |
| 33.74 | 80 | 4.5 | 7.56 | 22.4 |
| 32.99 | 100 | 5.5 | 9.24 | 28 |
| 31.99 | 120 | 6.4 | 10.75 | 33.6 |
| 32.56 | 140 | 7.6 | 12.77 | 39.2 |
| 32.62 | 160 | 8.7 | 14.61 | 44.8 |
| 32.66 | 180 | 9.8 | 16.46 | 50.4 |
| 32.99 | 200 | 11 | 18.48 | 56 |
| 32.99 | 220 | 12.1 | 20.32 | 61.6 |
| 33.11 | 250 | 13.8 | 23.18 | 70 |



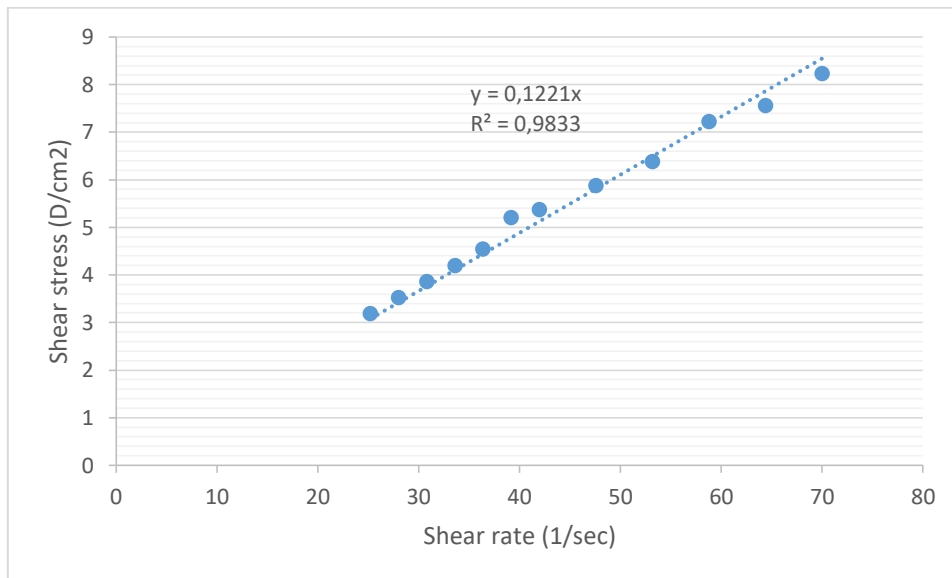
| 70 °C | | | | |
|----------------|-----|------------|-----------------------------------|--------------------|
| Viscosity (cP) | RPM | Torque (%) | Shear stress (D/cm ²) | Shear rate (1/sec) |
| 23 | 60 | 2.3 | 3.86 | 16.8 |
| 23.14 | 70 | 2.7 | 4.54 | 19.6 |
| 23.25 | 80 | 3.1 | 5.21 | 22.4 |
| 22.66 | 90 | 3.4 | 5.71 | 25.2 |
| 22.8 | 100 | 3.8 | 6.38 | 28 |
| 22.36 | 110 | 4.1 | 6.89 | 30.8 |
| 22.5 | 120 | 4.5 | 7.56 | 33.6 |
| 23.14 | 140 | 5.4 | 9.07 | 39.2 |
| 23.25 | 160 | 6.2 | 10.41 | 44.8 |
| 22.66 | 180 | 6.8 | 11.42 | 50.4 |
| 23.1 | 200 | 7.7 | 12.93 | 56 |
| 22.36 | 220 | 8.2 | 13.77 | 61.6 |
| 23.04 | 250 | 9.6 | 16.12 | 70 |



| 80 °C | | | | |
|----------------|-----|-----------|-----------------------------------|--------------------|
| Viscosity (cP) | RPM | Torque(%) | Shear stress (D/cm ²) | Shear rate (1/sec) |
| 17.25 | 80 | 2.3 | 3.86 | 22.4 |
| 16.66 | 90 | 2.5 | 4.2 | 25.2 |
| 15.6 | 100 | 2.6 | 4.37 | 28 |
| 15.81 | 110 | 2.9 | 4.87 | 30.8 |
| 15.5 | 120 | 3.1 | 5.21 | 33.6 |
| 15.69 | 130 | 3.4 | 5.71 | 36.4 |
| 15.43 | 140 | 3.6 | 6.05 | 39.2 |
| 16 | 150 | 4 | 6.72 | 42 |
| 17.25 | 160 | 4.6 | 7.22 | 44.8 |
| 15.33 | 180 | 4.6 | 7.73 | 50.4 |
| 15 | 200 | 5 | 8.4 | 56 |
| 15.27 | 220 | 5.6 | 9.41 | 61.6 |
| 15.36 | 250 | 6.4 | 10.75 | 70 |

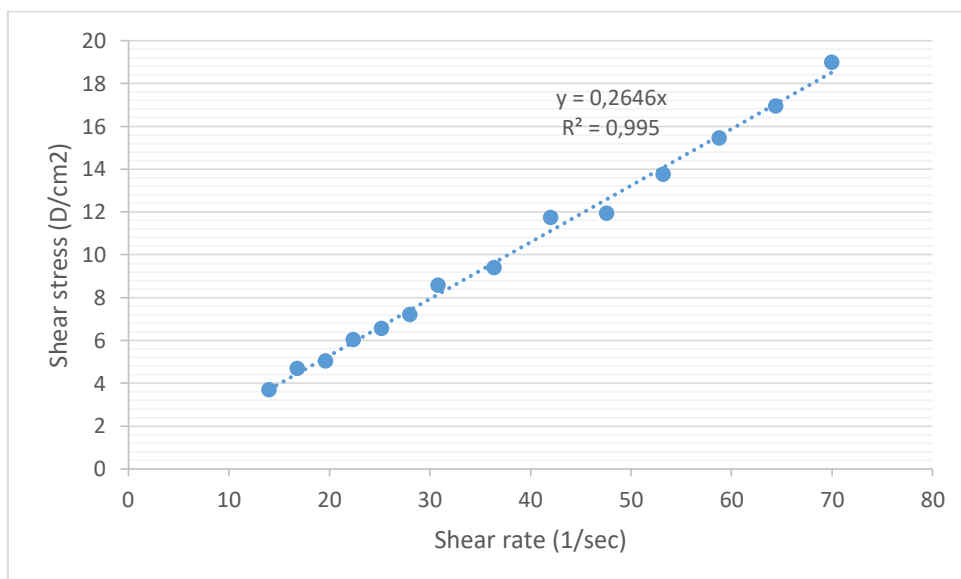


| 90 °C | | | | |
|----------------|-----|-----------|-----------------------------------|--------------------|
| Viscosity (cP) | RPM | Torque(%) | Shear stress (D/cm ²) | Shear rate (1/sec) |
| 12.66 | 90 | 1.9 | 3.19 | 25.2 |
| 12.6 | 100 | 2.1 | 3.53 | 28 |
| 12.54 | 110 | 2.3 | 3.86 | 30.8 |
| 12.5 | 120 | 2.5 | 4.2 | 33.6 |
| 12.46 | 130 | 2.7 | 4.54 | 36.4 |
| 13.28 | 140 | 3.1 | 5.21 | 39.2 |
| 12.8 | 150 | 3.2 | 5.37 | 42 |
| 12.35 | 170 | 3.5 | 5.88 | 47.6 |
| 12 | 190 | 3.8 | 6.38 | 53.2 |
| 12.28 | 210 | 4.3 | 7.22 | 58.8 |
| 11.74 | 230 | 4.5 | 7.56 | 64.4 |
| 11.76 | 250 | 4.9 | 8.23 | 70 |

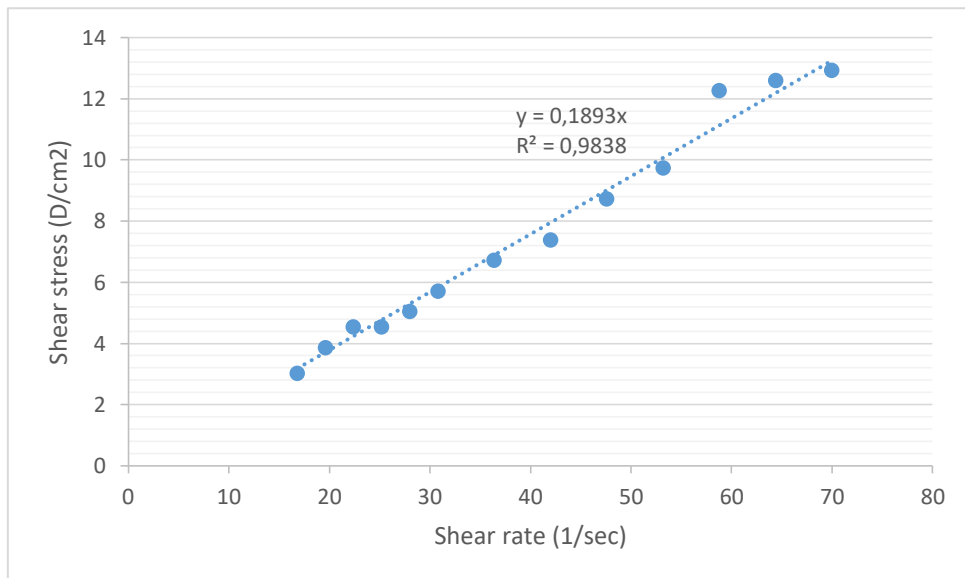


$$X_{IL}=0.3$$

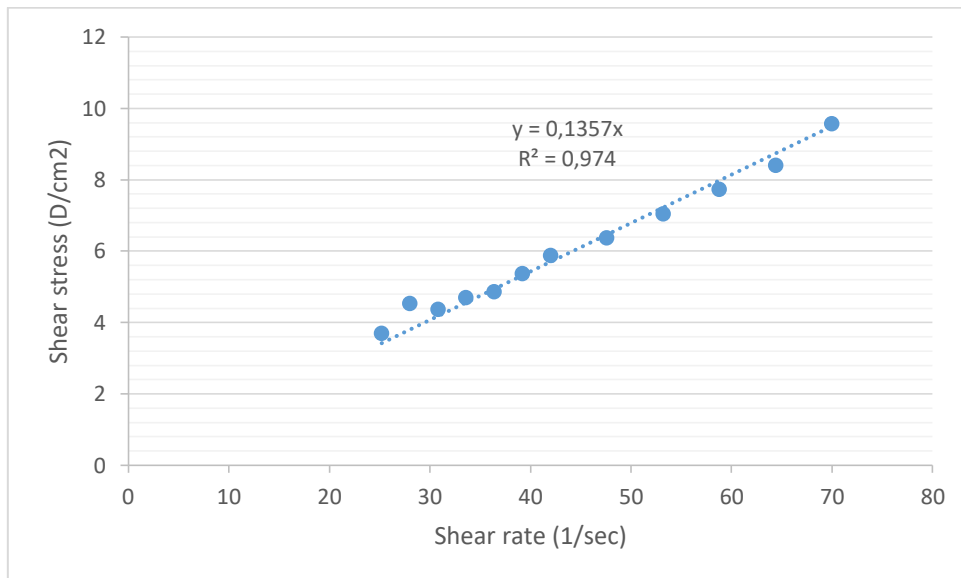
| 60 °C | | | | |
|----------------|-----|-----------|-----------------------------------|--------------------|
| Viscosity (cP) | RPM | Torque(%) | Shear stress (D/cm ²) | Shear rate (1/sec) |
| 26.39 | 50 | 2.2 | 3.7 | 14 |
| 27.99 | 60 | 2.8 | 4.7 | 16.8 |
| 25.71 | 70 | 3 | 5.04 | 19.6 |
| 26.99 | 80 | 3.6 | 6.05 | 22.4 |
| 25.99 | 90 | 3.9 | 6.55 | 25.2 |
| 25.79 | 100 | 4.3 | 7.22 | 28 |
| 27.81 | 110 | 5.1 | 8.57 | 30.8 |
| 25.84 | 130 | 5.6 | 9.41 | 36.4 |
| 25.59 | 150 | 6.4 | 11.75 | 42 |
| 25.05 | 170 | 7.1 | 11.93 | 47.6 |
| 25.89 | 190 | 8.2 | 13.77 | 53.2 |
| 26.28 | 210 | 9.2 | 15.45 | 58.8 |
| 26.34 | 230 | 10.1 | 16.96 | 64.4 |
| 27.11 | 250 | 11.3 | 18.98 | 70 |



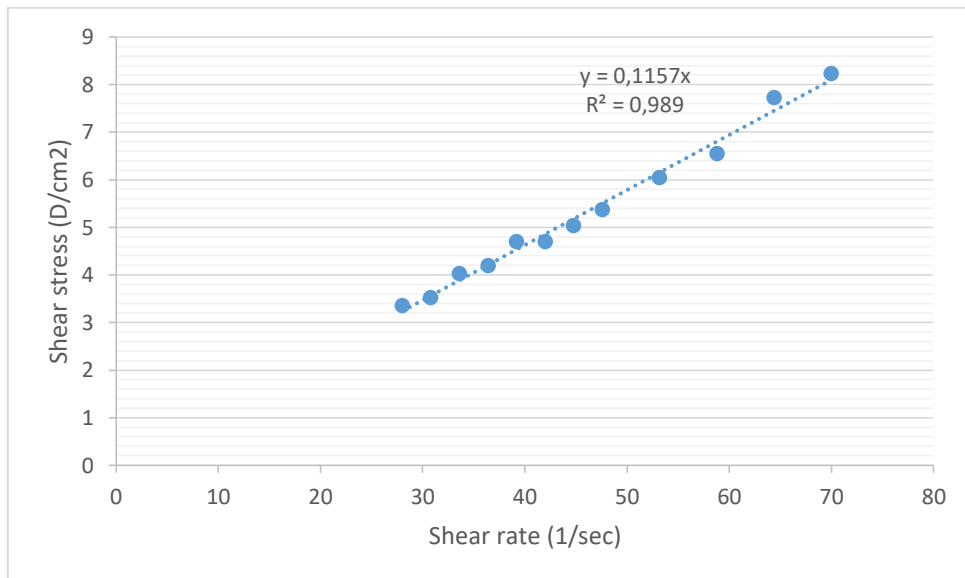
| 70 °C | | | | |
|----------------|-----|-----------|-----------------------------------|--------------------|
| Viscosity (cP) | RPM | Torque(%) | Shear stress (D/cm ²) | Shear rate (1/sec) |
| 18 | 60 | 1.8 | 3.02 | 16.8 |
| 19.71 | 70 | 2.3 | 3.86 | 19.6 |
| 20.25 | 80 | 2.7 | 4.54 | 22.4 |
| 18 | 90 | 2.7 | 4.54 | 25.2 |
| 18 | 100 | 3 | 5.04 | 28 |
| 18.54 | 110 | 3.4 | 5.71 | 30.8 |
| 18.46 | 130 | 4 | 6.72 | 36.4 |
| 17.6 | 150 | 4.4 | 7.39 | 42 |
| 18.35 | 170 | 5.2 | 8.73 | 47.6 |
| 18.31 | 190 | 5.8 | 9.74 | 53.2 |
| 20.85 | 210 | 7.3 | 12.26 | 58.8 |
| 19.56 | 230 | 7.5 | 12.6 | 64.4 |
| 18.48 | 250 | 7.7 | 12.93 | 70 |



| 80 °C | | | | |
|----------------|-----|-----------|-----------------------------------|--------------------|
| Viscosity (cP) | RPM | Torque(%) | Shear stress (D/cm ²) | Shear rate (1/sec) |
| 14.66 | 90 | 2.2 | 3.7 | 25.2 |
| 16.2 | 100 | 2.7 | 4.54 | 28 |
| 14.18 | 110 | 2.6 | 4.37 | 30.8 |
| 14 | 120 | 2.8 | 4.7 | 33.6 |
| 13.38 | 130 | 2.9 | 4.87 | 36.4 |
| 13.71 | 140 | 3.2 | 5.37 | 39.2 |
| 14 | 150 | 3.5 | 5.88 | 42 |
| 13.41 | 170 | 3.8 | 6.38 | 47.6 |
| 13.26 | 190 | 4.2 | 7.05 | 53.2 |
| 13.14 | 210 | 4.6 | 7.73 | 58.8 |
| 13.04 | 230 | 5 | 8.4 | 64.4 |
| 13.68 | 250 | 5.7 | 9.57 | 70 |

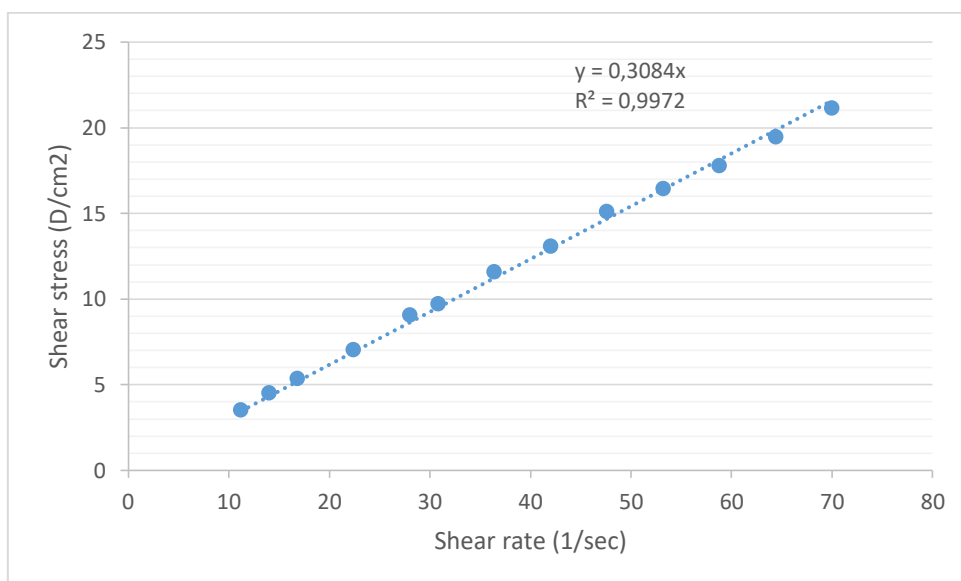


| 90 °C | | | | |
|----------------|-----|-----------|-----------------------------------|--------------------|
| Viscosity (cP) | RPM | Torque(%) | Shear stress (D/cm ²) | Shear rate (1/sec) |
| 12 | 100 | 2 | 3.36 | 28 |
| 11.45 | 110 | 2.1 | 3.53 | 30.8 |
| 12 | 120 | 2.4 | 4.03 | 33.6 |
| 11.54 | 130 | 2.5 | 4.2 | 36.4 |
| 12 | 140 | 2.8 | 4.7 | 39.2 |
| 11.2 | 150 | 2.,8 | 4.7 | 42 |
| 11.25 | 160 | 3 | 5.04 | 44.8 |
| 11.29 | 170 | 3.2 | 5.37 | 47.6 |
| 11.37 | 190 | 3.6 | 6.05 | 53.2 |
| 11.14 | 210 | 3.9 | 6.55 | 58.8 |
| 12 | 230 | 4.6 | 7.73 | 64.4 |
| 11.76 | 250 | 4.9 | 8.23 | 70 |

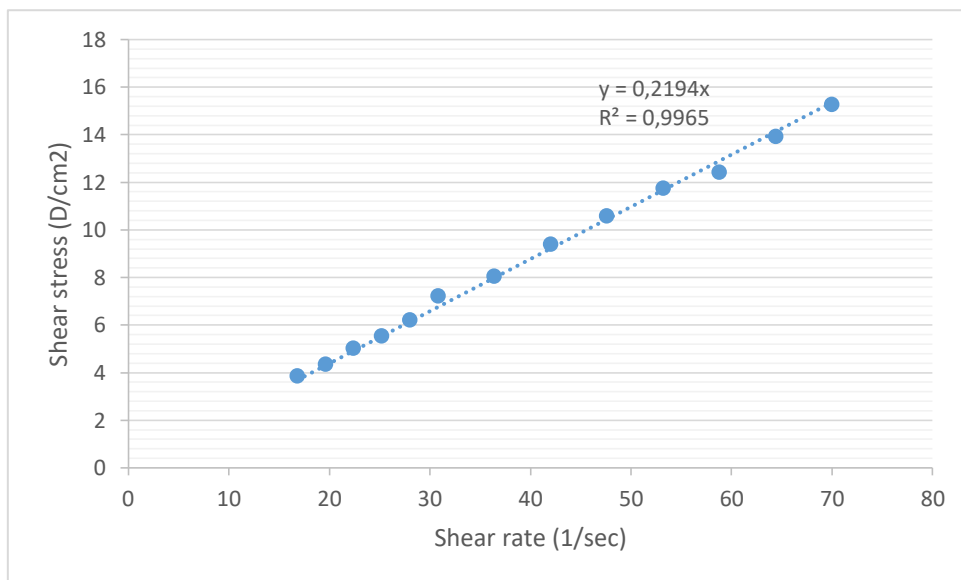


$$X_{IL}=0.4$$

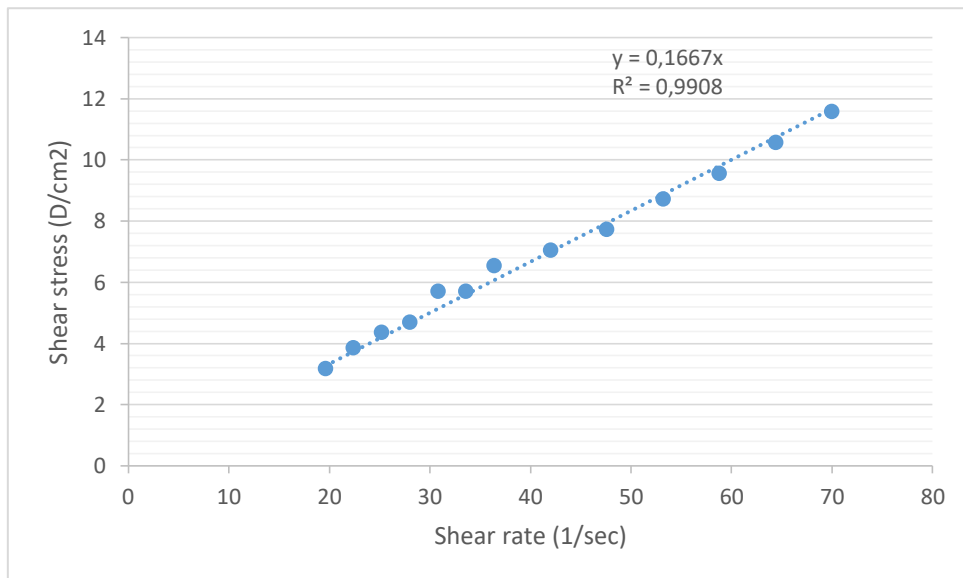
| 60 °C | | | | |
|----------------|-----|-----------|-----------------------------------|--------------------|
| Viscosity (cP) | RPM | Torque(%) | Shear stress (D/cm ²) | Shear rate (1/sec) |
| 31.49 | 40 | 2.1 | 3.53 | 11.2 |
| 32.39 | 50 | 2.7 | 4.54 | 14 |
| 31.99 | 60 | 3.2 | 5.37 | 16.8 |
| 31.49 | 80 | 4.2 | 7.05 | 22.4 |
| 32.39 | 100 | 5.4 | 9.07 | 28 |
| 31.63 | 110 | 5.8 | 9.74 | 30.8 |
| 31.84 | 130 | 6.9 | 11.59 | 36.4 |
| 31.19 | 150 | 7.8 | 13.1 | 42 |
| 31.76 | 170 | 9 | 15.12 | 47.6 |
| 30.94 | 190 | 9.8 | 16.46 | 53.2 |
| 30.28 | 210 | 10.6 | 17.8 | 58.8 |
| 30.25 | 230 | 11.6 | 19.48 | 64.4 |
| 30.23 | 250 | 12.6 | 21.16 | 70 |



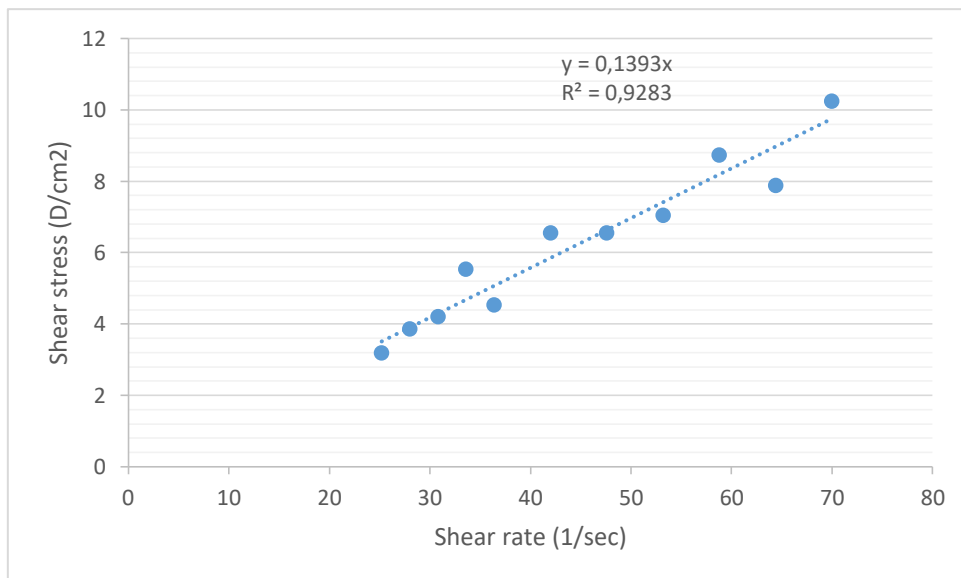
| 70 °C | | | | |
|----------------|-----|-----------|-----------------------------------|--------------------|
| Viscosity (cP) | RPM | Torque(%) | Shear stress (D/cm ²) | Shear rate (1/sec) |
| 23 | 60 | 2.3 | 3.86 | 16.8 |
| 22.28 | 70 | 2.6 | 4.37 | 19.6 |
| 22.5 | 80 | 3 | 5.04 | 22.4 |
| 22 | 90 | 3.3 | 5.54 | 25.2 |
| 22.2 | 100 | 3.7 | 6.21 | 28 |
| 23.45 | 110 | 4.3 | 7.22 | 30.8 |
| 22.15 | 130 | 4.8 | 8.06 | 36.4 |
| 22.4 | 150 | 5.6 | 9.41 | 42 |
| 22.23 | 170 | 6.3 | 10.58 | 47.6 |
| 22.1 | 190 | 7 | 11.76 | 53.2 |
| 21.14 | 210 | 7.4 | 12.43 | 58.8 |
| 21.65 | 230 | 8.3 | 13.94 | 64.4 |
| 21.84 | 250 | 9.1 | 15.28 | 70 |



| 80 °C | | | | |
|----------------|-----|-----------|-----------------------------------|--------------------|
| Viscosity (cP) | RPM | Torque(%) | Shear stress (D/cm ²) | Shear rate (1/sec) |
| 16.28 | 70 | 1.9 | 3.19 | 19.6 |
| 17.25 | 80 | 2.3 | 3.86 | 22.4 |
| 17.33 | 90 | 2.6 | 4.37 | 25.2 |
| 16.8 | 100 | 2.8 | 4.7 | 28 |
| 18.54 | 110 | 3.4 | 5.71 | 30.8 |
| 17 | 120 | 3.4 | 5.71 | 33.6 |
| 18 | 130 | 3.9 | 6.55 | 36.4 |
| 16.8 | 150 | 4.2 | 7.05 | 42 |
| 16.23 | 170 | 4.6 | 7.73 | 47.6 |
| 16.42 | 190 | 5.2 | 8.73 | 53.2 |
| 16.28 | 210 | 5.7 | 9.57 | 58.8 |
| 16.43 | 230 | 6.3 | 10.58 | 64.4 |
| 16.56 | 250 | 6.9 | 11.59 | 70 |

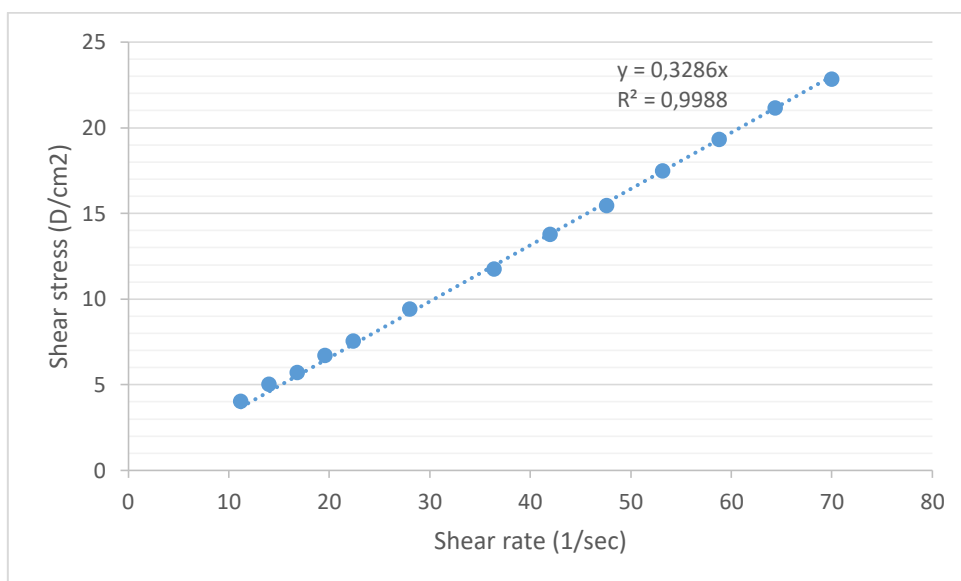


| 90 °C | | | | |
|----------------|-----|-----------|-----------------------------------|--------------------|
| Viscosity (cP) | RPM | Torque(%) | Shear stress (D/cm ²) | Shear rate (1/sec) |
| 12.66 | 90 | 1.9 | 3.19 | 25.2 |
| 13.8 | 100 | 2.3 | 3.86 | 28 |
| 13.63 | 110 | 2.5 | 4.2 | 30.8 |
| 16.5 | 120 | 3.3 | 5.54 | 33.6 |
| 12.46 | 130 | 2.7 | 4.54 | 36.4 |
| 15.6 | 150 | 3.9 | 6.55 | 42 |
| 13.76 | 170 | 3.9 | 6.55 | 47.6 |
| 13.26 | 190 | 4.2 | 7.05 | 53.2 |
| 14.85 | 210 | 5.2 | 8.73 | 58.8 |
| 12.26 | 230 | 4.7 | 7.89 | 64.4 |
| 14.64 | 250 | 6.1 | 10.25 | 70 |

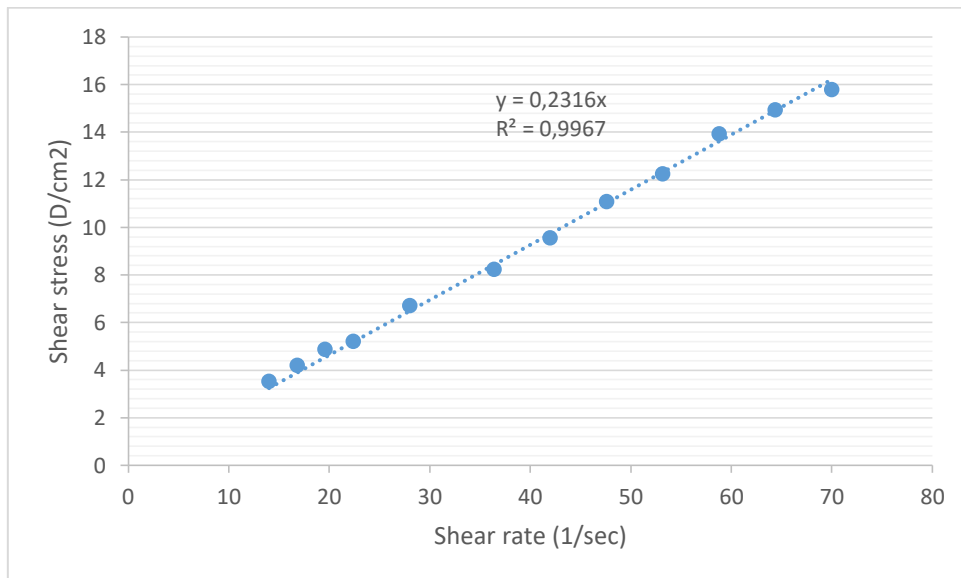


$$X_{IL}=0.5$$

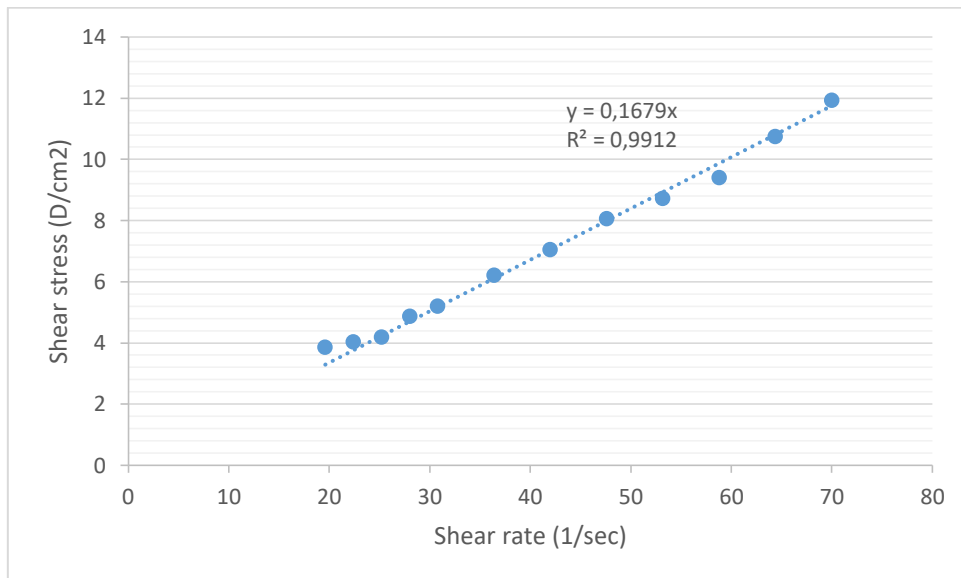
| 60 °C | | | | |
|----------------|-----|-----------|-----------------------------------|--------------------|
| Viscosity (cP) | RPM | Torque(%) | Shear stress (D/cm ²) | Shear rate (1/sec) |
| 35.99 | 40 | 2.4 | 4.03 | 11.2 |
| 35.99 | 50 | 3 | 5.04 | 14 |
| 33.99 | 60 | 3.4 | 5.71 | 16.8 |
| 34.28 | 70 | 4 | 6.72 | 19.6 |
| 33.74 | 80 | 4.5 | 7.56 | 22.4 |
| 33.59 | 100 | 5.6 | 9.41 | 28 |
| 32.3 | 130 | 7 | 11.76 | 36,4 |
| 32.79 | 150 | 8.2 | 13.77 | 42 |
| 32.46 | 170 | 9.2 | 15.45 | 47.6 |
| 32.84 | 190 | 10.4 | 17.47 | 53.2 |
| 32.85 | 210 | 11.5 | 19.32 | 58.8 |
| 32.86 | 230 | 12.6 | 21.16 | 64.4 |
| 32.63 | 250 | 13.6 | 22.84 | 70 |



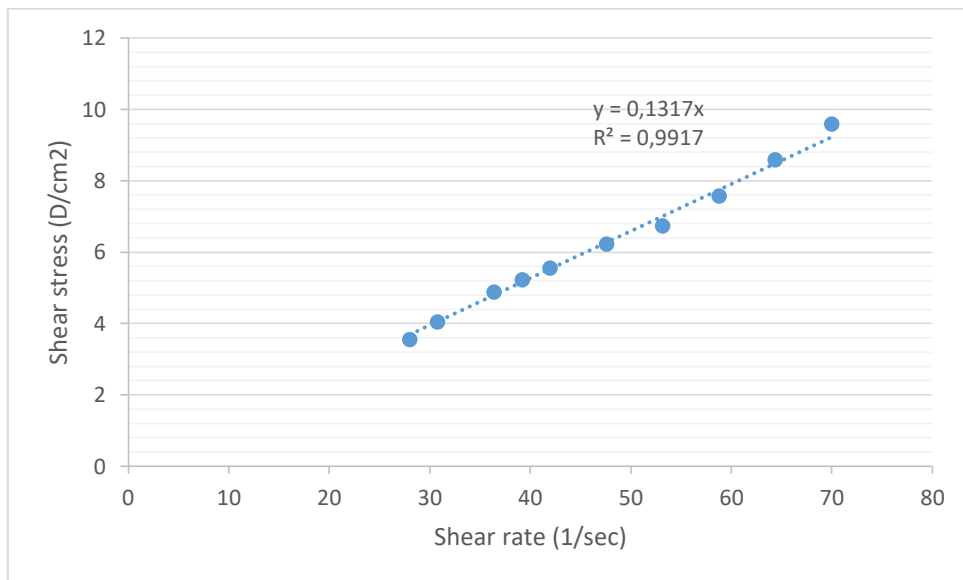
| 70 °C | | | | |
|----------------|-----|-----------|-----------------------------------|--------------------|
| Viscosity (cP) | RPM | Torque(%) | Shear stress (D/cm ²) | Shear rate (1/sec) |
| 25.19 | 50 | 2.1 | 3.53 | 14 |
| 24.99 | 60 | 2.5 | 4.2 | 16.8 |
| 24.85 | 70 | 2.9 | 4.87 | 19.6 |
| 23.25 | 80 | 3.1 | 5.21 | 22.4 |
| 23.9 | 100 | 4 | 6.72 | 28 |
| 22.61 | 130 | 4.9 | 8.23 | 36.4 |
| 22.8 | 150 | 5.7 | 9.57 | 42 |
| 23.29 | 170 | 6.6 | 11.09 | 47.6 |
| 23.05 | 190 | 7.3 | 12.26 | 53.2 |
| 23.71 | 210 | 8.3 | 13.94 | 58.8 |
| 23.21 | 230 | 8.9 | 14.95 | 64.4 |
| 22.56 | 250 | 9.4 | 15.79 | 70 |



| 80 °C | | | | |
|----------------|-----|-----------|-----------------------------------|--------------------|
| Viscosity (cP) | RPM | Torque(%) | Shear stress (D/cm ²) | Shear rate (1/sec) |
| 19.71 | 70 | 2.3 | 3.86 | 19.6 |
| 18 | 80 | 2.4 | 4.03 | 22.4 |
| 16.66 | 90 | 2.5 | 4.2 | 25.2 |
| 17.4 | 100 | 2.9 | 4.87 | 28 |
| 16.91 | 110 | 3.1 | 5.21 | 30.8 |
| 17.07 | 130 | 3.7 | 6.21 | 36.4 |
| 16.8 | 150 | 4.2 | 7.05 | 42 |
| 16.94 | 170 | 4.8 | 8.06 | 47.6 |
| 16.42 | 190 | 5.2 | 8.73 | 53.2 |
| 16 | 210 | 5.6 | 9.41 | 58.8 |
| 16.69 | 230 | 6.4 | 10.75 | 64.4 |
| 17.04 | 250 | 7.1 | 11.93 | 70 |

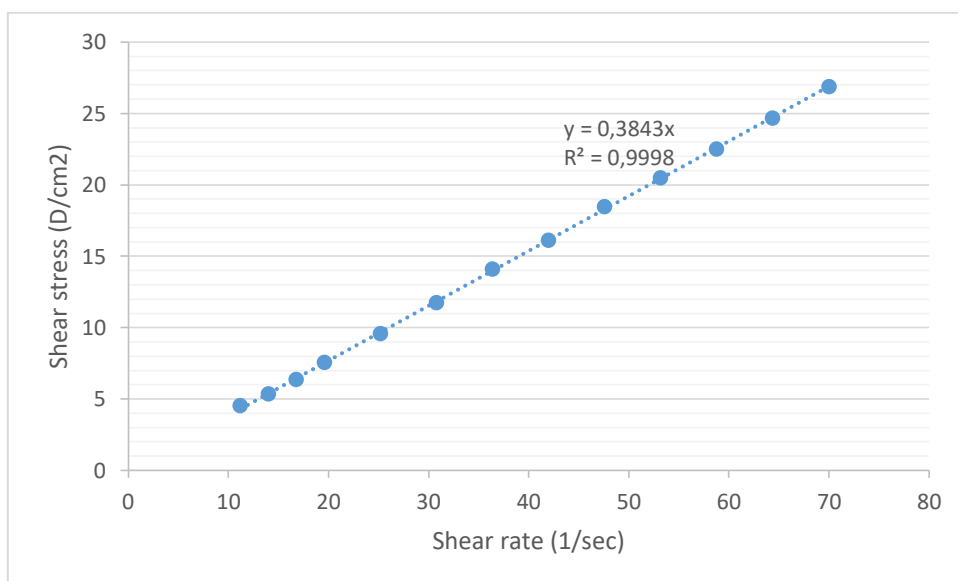


| 90 °C | | | | |
|----------------|-----|-----------|-----------------------------------|--------------------|
| Viscosity (cP) | RPM | Torque(%) | Shear stress (D/cm ²) | Shear rate (1/sec) |
| 12.6 | 100 | 2.1 | 3.53 | 28 |
| 13.09 | 110 | 2.4 | 4.03 | 30.8 |
| 13.38 | 130 | 2.9 | 4.87 | 36.4 |
| 13.28 | 140 | 3.1 | 5.21 | 39.2 |
| 13.2 | 150 | 3.3 | 5.54 | 42 |
| 13.06 | 170 | 3.7 | 6.21 | 47.6 |
| 12.63 | 190 | 4 | 6.72 | 53.2 |
| 12.85 | 210 | 4.5 | 7.56 | 58.8 |
| 13.3 | 230 | 5.1 | 8.57 | 64.4 |
| 13.6 | 250 | 5.7 | 9.57 | 70 |

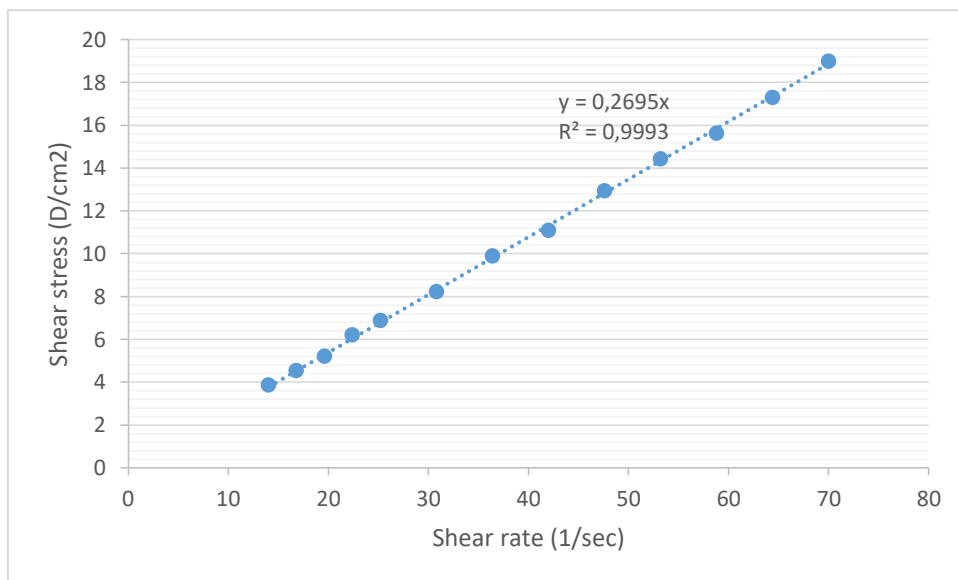


$$X_{IL}=0.6$$

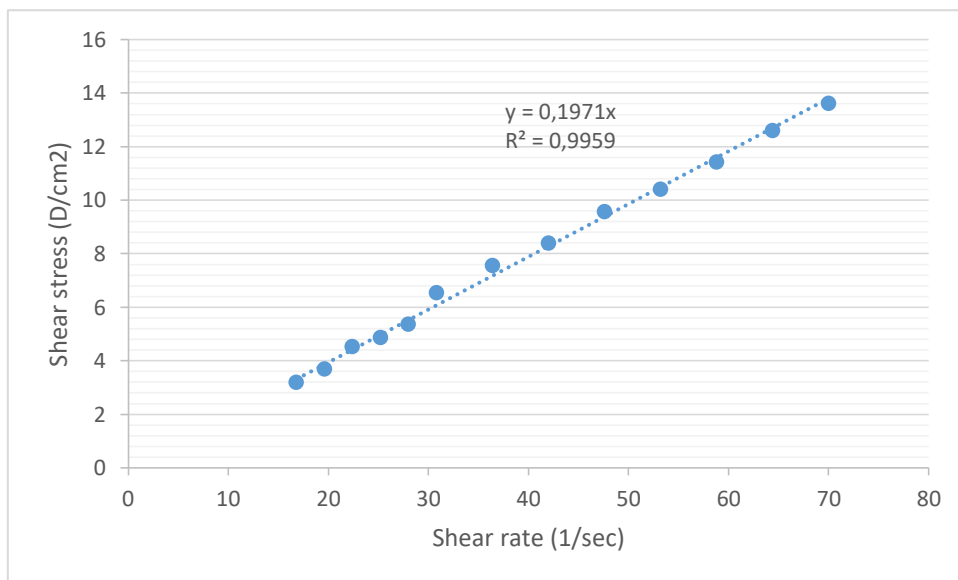
| 60 °C | | | | |
|----------------|-----|-----------|-----------------------------------|--------------------|
| Viscosity (cP) | RPM | Torque(%) | Shear stress (D/cm ²) | Shear rate (1/sec) |
| 40.49 | 40 | 2.7 | 4.54 | 11.2 |
| 38.39 | 50 | 3.2 | 5.37 | 14 |
| 37.99 | 60 | 3.8 | 6.38 | 16.8 |
| 38.56 | 70 | 4.5 | 7.56 | 19.6 |
| 37.99 | 90 | 5.7 | 9.57 | 25.2 |
| 38.17 | 110 | 7 | 11.76 | 30.8 |
| 38.76 | 130 | 8.4 | 14.11 | 36.4 |
| 38.39 | 150 | 9.6 | 16.12 | 42 |
| 38.82 | 170 | 11 | 18.48 | 47.6 |
| 38.52 | 190 | 12.2 | 20.49 | 53.2 |
| 38.28 | 210 | 13.4 | 22.51 | 58.8 |
| 38.34 | 230 | 14.7 | 24.69 | 64.4 |
| 38.39 | 250 | 16 | 26.87 | 70 |



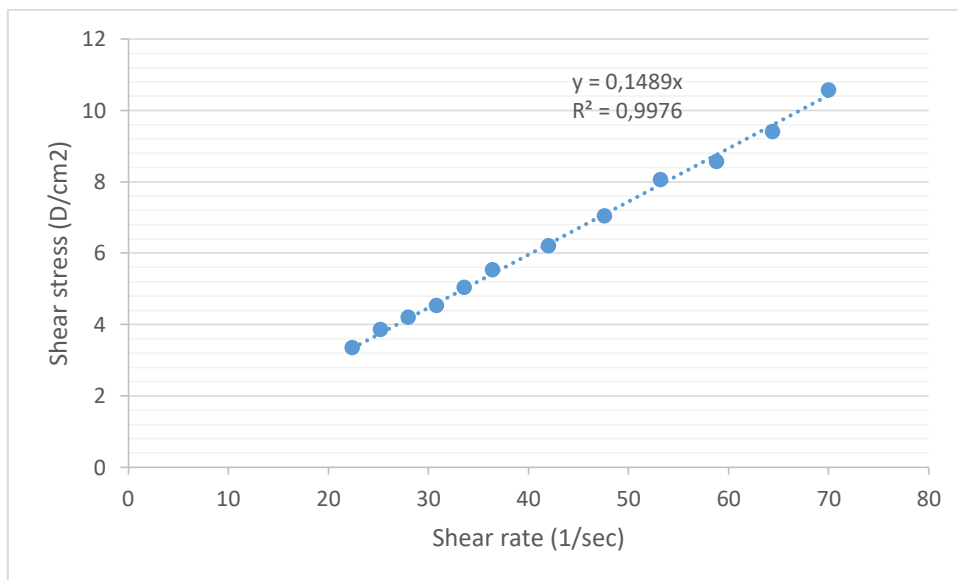
| 70 °C | | | | |
|----------------|-----|-----------|-----------------------------------|--------------------|
| Viscosity (cP) | RPM | Torque(%) | Shear stress (D/cm ²) | Shear rate (1/sec) |
| 27.59 | 50 | 2.3 | 3.86 | 14 |
| 26.99 | 60 | 2.7 | 4.54 | 16.8 |
| 26.57 | 70 | 3.1 | 5.21 | 19.6 |
| 27.74 | 80 | 3.7 | 6.21 | 22.4 |
| 27.33 | 90 | 4.1 | 6.89 | 25.2 |
| 26.72 | 110 | 4.9 | 8.23 | 30.8 |
| 27.22 | 130 | 5.9 | 9.91 | 36.4 |
| 26.39 | 150 | 6.6 | 11.09 | 42 |
| 27.17 | 170 | 7.7 | 12.93 | 47.6 |
| 27.15 | 190 | 8.6 | 14.44 | 53.2 |
| 26.57 | 210 | 9.3 | 15.62 | 58.8 |
| 26.86 | 230 | 10.3 | 17.3 | 64.4 |
| 27.11 | 250 | 11.3 | 18.98 | 70 |



| 80 °C | | | | |
|----------------|-----|-----------|-----------------------------------|--------------------|
| Viscosity (cP) | RPM | Torque(%) | Shear stress (D/cm ²) | Shear rate (1/sec) |
| 19 | 60 | 1.9 | 3.19 | 16.8 |
| 18.85 | 70 | 2.2 | 3.7 | 19.6 |
| 20.25 | 80 | 2.7 | 4.54 | 22.4 |
| 19.33 | 90 | 2.9 | 4.87 | 25.2 |
| 19.2 | 100 | 3.2 | 5.37 | 28 |
| 21.27 | 110 | 3.9 | 6.55 | 30.8 |
| 20.76 | 130 | 4.5 | 7.56 | 36.4 |
| 20 | 150 | 5 | 8.4 | 42 |
| 20.11 | 170 | 5.7 | 9.57 | 47.6 |
| 19.57 | 190 | 6.2 | 10.41 | 53.2 |
| 19.42 | 210 | 6.8 | 11.42 | 58.8 |
| 19.56 | 230 | 7.5 | 12.6 | 64.4 |
| 19.44 | 250 | 8.1 | 13.61 | 70 |

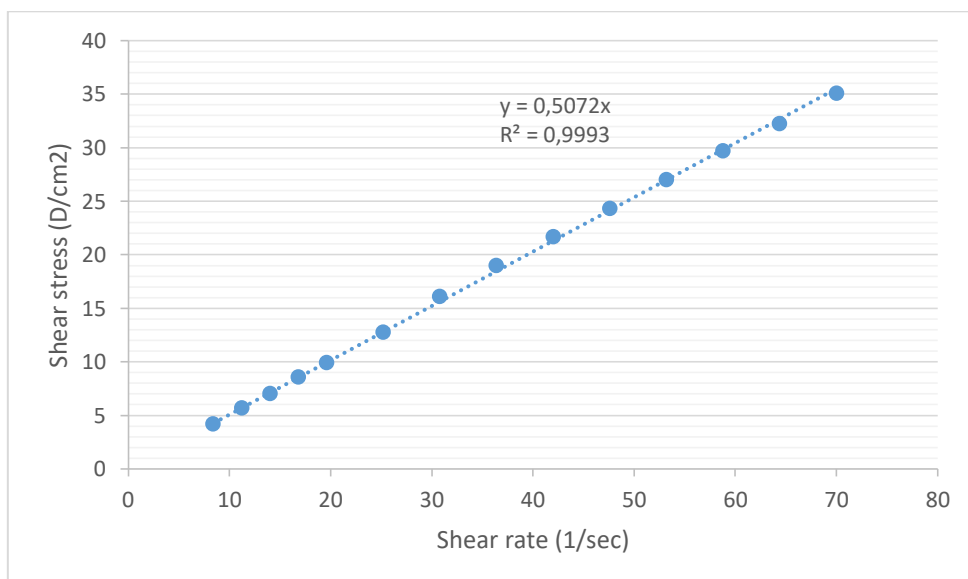


| 90 °C | | | | |
|----------------|-----|-----------|-----------------------------------|--------------------|
| Viscosity (cP) | RPM | Torque(%) | Shear stress (D/cm ²) | Shear rate (1/sec) |
| 15 | 80 | 2 | 3.36 | 22.4 |
| 15.33 | 90 | 2.3 | 3.86 | 25.2 |
| 15 | 100 | 2.5 | 4.2 | 28 |
| 14.72 | 110 | 2.7 | 4.54 | 30.8 |
| 15 | 120 | 3 | 5.04 | 33.6 |
| 15.23 | 130 | 3.3 | 5.54 | 36.4 |
| 14.8 | 150 | 3.7 | 6.21 | 42 |
| 14.82 | 170 | 4.2 | 7.05 | 47.6 |
| 15.15 | 190 | 4.8 | 8.06 | 53.2 |
| 14.57 | 210 | 5.1 | 8.57 | 58.8 |
| 14.61 | 230 | 5.6 | 9.41 | 64.4 |
| 15.12 | 250 | 6.3 | 10.58 | 70 |

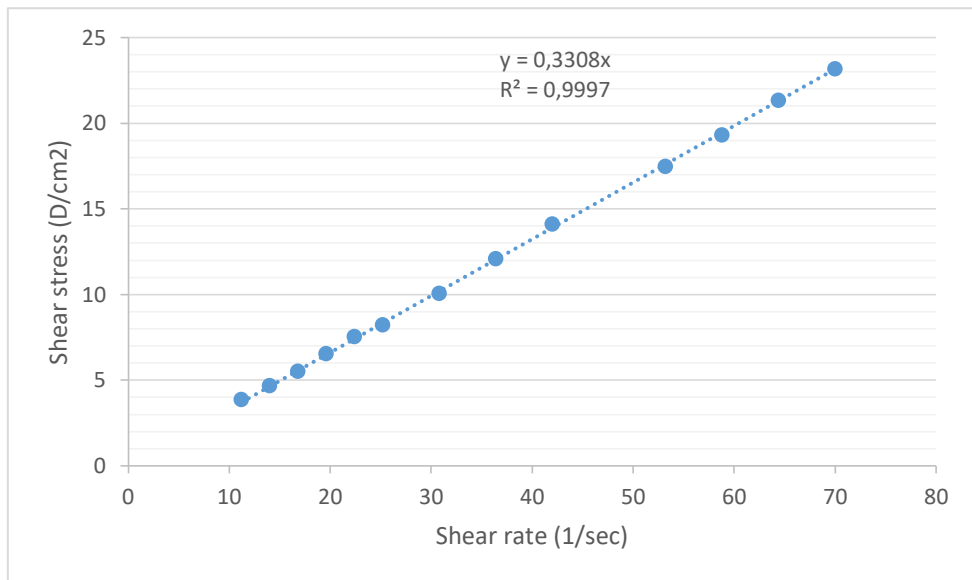


$$X_{IL}=0.7$$

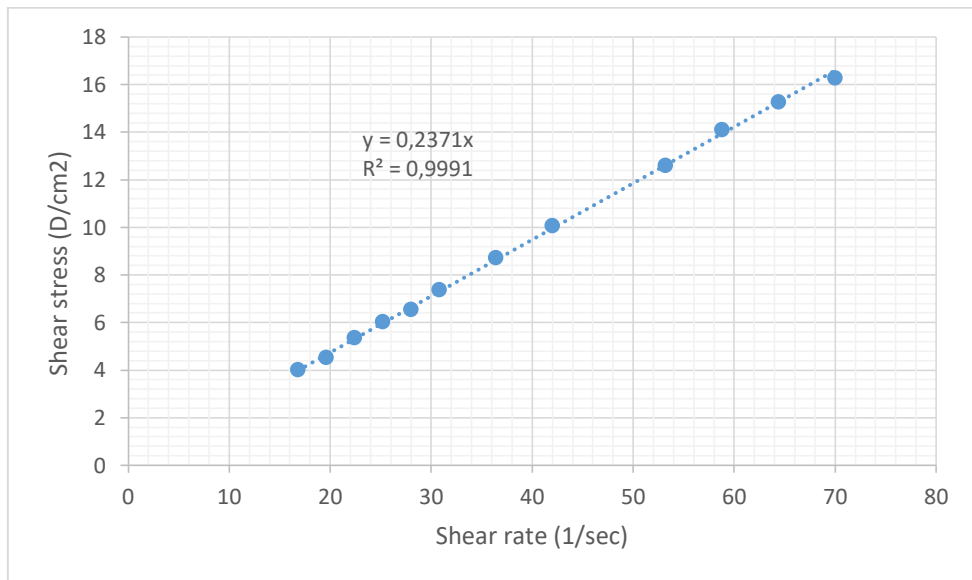
| 60 °C | | | | |
|----------------|-----|-----------|-----------------------------------|--------------------|
| Viscosity (cP) | RPM | Torque(%) | Shear stress (D/cm ²) | Shear rate (1/sec) |
| 49.99 | 30 | 2.5 | 4.2 | 8.4 |
| 50.99 | 40 | 3.4 | 5.71 | 11.2 |
| 50.3 | 50 | 4.2 | 7.05 | 14 |
| 50.99 | 60 | 5.1 | 8.57 | 16.8 |
| 50.56 | 70 | 5.9 | 9.91 | 19.6 |
| 50.66 | 90 | 7.6 | 12.77 | 25.2 |
| 52.35 | 110 | 9.6 | 16.12 | 30.8 |
| 52.14 | 130 | 11.3 | 18.98 | 36.4 |
| 51.59 | 150 | 12.9 | 21.67 | 42 |
| 51.17 | 170 | 14.5 | 24.35 | 47.6 |
| 50.83 | 190 | 16.1 | 27.04 | 53.2 |
| 50.56 | 210 | 17.7 | 29.73 | 58.8 |
| 50.08 | 230 | 19.2 | 32.25 | 64.4 |
| 50.15 | 250 | 20.9 | 35.1 | 70 |



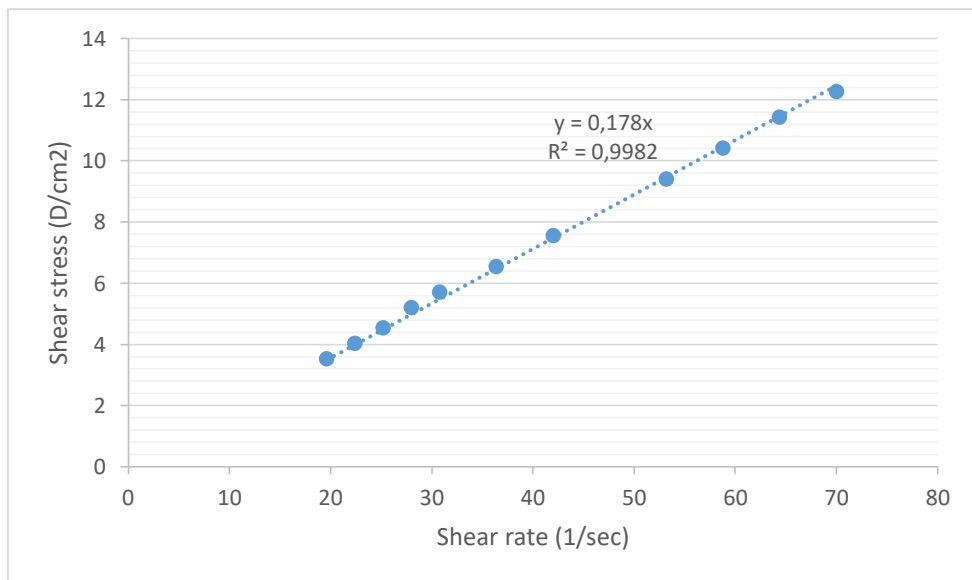
| 70 °C | | | | |
|----------------|-----|-----------|-----------------------------------|--------------------|
| Viscosity (cP) | RPM | Torque(%) | Shear stress (D/cm ²) | Shear rate (1/sec) |
| 34.49 | 40 | 2.3 | 3.86 | 11.2 |
| 33.59 | 50 | 2.8 | 4.7 | 14 |
| 32.99 | 60 | 3.3 | 5.54 | 16.8 |
| 33.42 | 70 | 3.9 | 6.55 | 19.6 |
| 33.74 | 80 | 4.5 | 7.56 | 22.4 |
| 32.66 | 90 | 4.9 | 8.23 | 25.2 |
| 32.72 | 110 | 6 | 10.08 | 30.8 |
| 33.22 | 130 | 7.2 | 12.09 | 36.4 |
| 33.59 | 150 | 8.4 | 14.11 | 42 |
| 32.84 | 190 | 10.4 | 17.47 | 53.2 |
| 32.85 | 210 | 11.5 | 19.32 | 58.8 |
| 33.12 | 230 | 12.7 | 21.33 | 64.4 |
| 33.11 | 250 | 13.8 | 23.18 | 70 |



| 80 °C | | | | |
|----------------|-----|-----------|-----------------------------------|--------------------|
| Viscosity (cP) | RPM | Torque(%) | Shear stress (D/cm ²) | Shear rate (1/sec) |
| 23.99 | 60 | 2.47 | 4.03 | 16.8 |
| 23.14 | 70 | 2.7 | 4.54 | 19.6 |
| 23.99 | 80 | 3.2 | 5.37 | 22.4 |
| 23.99 | 90 | 3.6 | 6.05 | 25.2 |
| 23.4 | 100 | 3.9 | 6.55 | 28 |
| 23.99 | 110 | 4.4 | 7.39 | 30.8 |
| 23.99 | 130 | 5.2 | 8.73 | 36.4 |
| 23.99 | 150 | 6 | 10.08 | 42 |
| 23.68 | 190 | 7.5 | 12.6 | 53.2 |
| 23.99 | 210 | 8.4 | 14.11 | 58.8 |
| 23.73 | 230 | 9.1 | 15.28 | 64.4 |
| 23.28 | 250 | 9.7 | 16.29 | 70 |

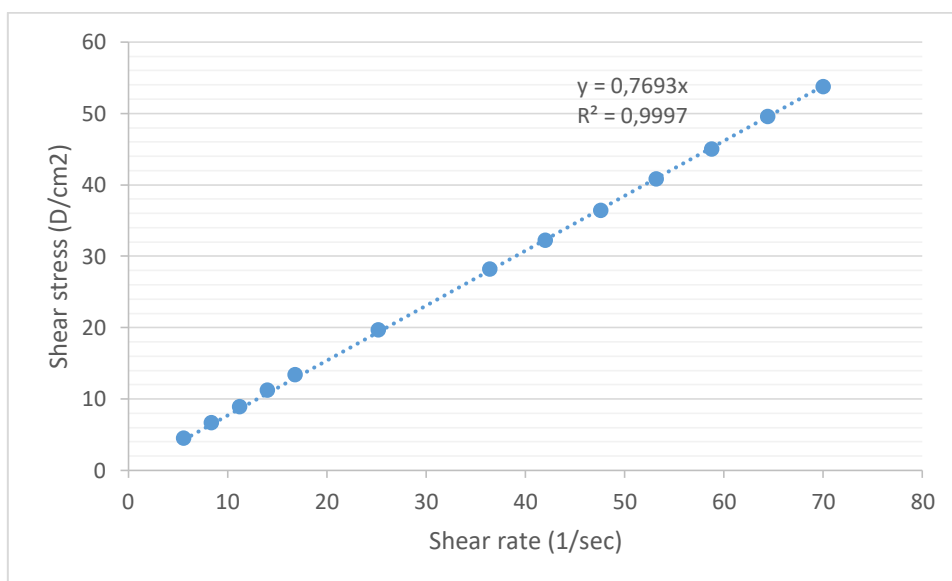


| 90 °C | | | | |
|----------------|-----|-----------|-----------------------------------|--------------------|
| Viscosity (cP) | RPM | Torque(%) | Shear stress (D/cm ²) | Shear rate (1/sec) |
| 18 | 70 | 2.1 | 3.53 | 19.6 |
| 18 | 80 | 2.4 | 4.03 | 22.4 |
| 18 | 90 | 2.7 | 4.54 | 25.2 |
| 18.6 | 100 | 3.1 | 5.21 | 28 |
| 18.54 | 110 | 3.4 | 5.71 | 30.8 |
| 18 | 130 | 3.9 | 6.55 | 36.4 |
| 18 | 150 | 4.5 | 7.56 | 42 |
| 17.68 | 190 | 5.6 | 9.41 | 53.2 |
| 17.71 | 210 | 6.2 | 10.41 | 58.8 |
| 17.74 | 230 | 6.8 | 11.42 | 64.4 |
| 17.52 | 250 | 7.3 | 12.26 | 70 |

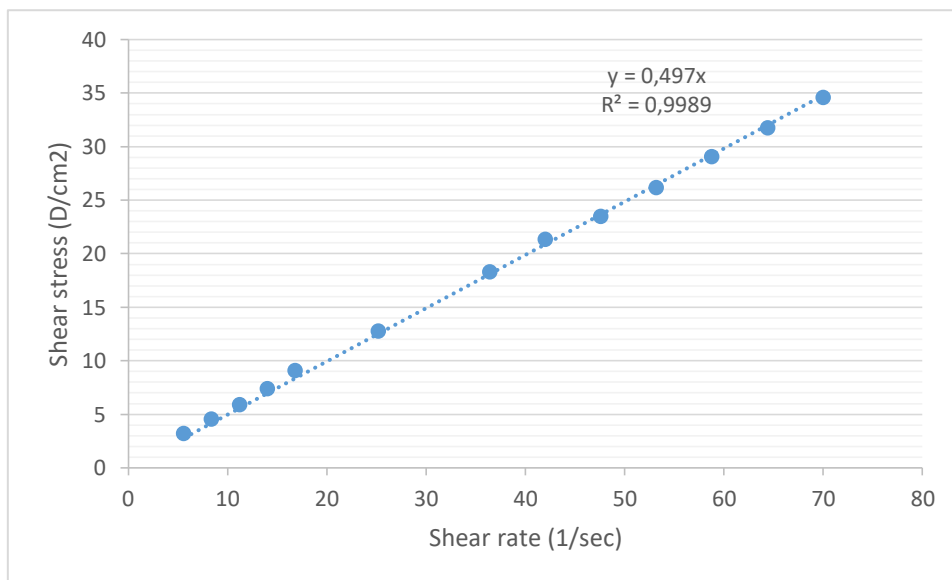


$$X_{IL}=0.85$$

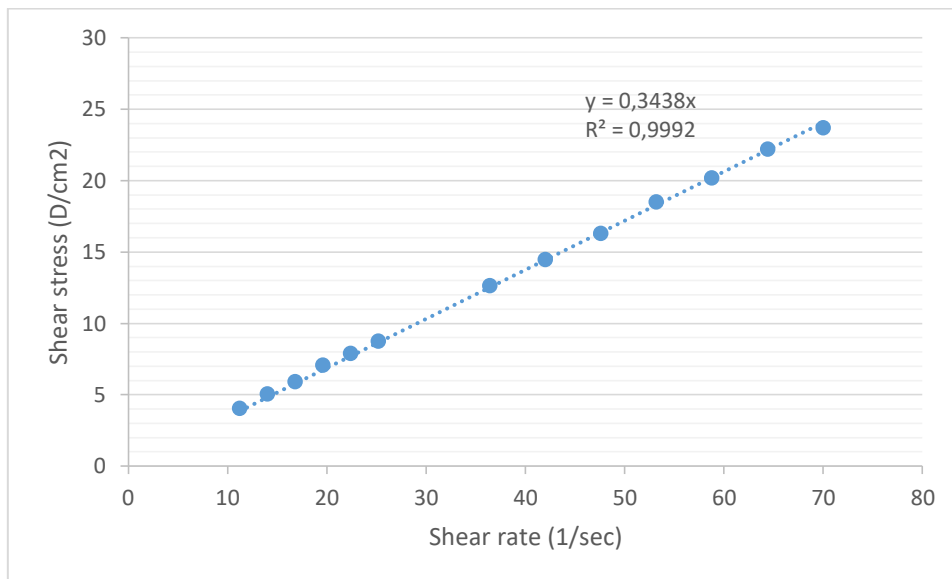
| 60 °C | | | | |
|----------------|-----|-----------|-----------------------------------|--------------------|
| Viscosity (cP) | RPM | Torque(%) | Shear stress (D/cm ²) | Shear rate (1/sec) |
| 80.98 | 20 | 2.7 | 4.54 | 5.6 |
| 79.98 | 30 | 4 | 6.72 | 8.4 |
| 79.48 | 40 | 5.3 | 8.9 | 11.2 |
| 80.38 | 50 | 6.7 | 11.25 | 14 |
| 79.98 | 60 | 8 | 13.44 | 16.8 |
| 77.98 | 90 | 11.7 | 19.65 | 25.2 |
| 77.52 | 130 | 16.8 | 28.22 | 36.4 |
| 76.78 | 150 | 19.2 | 32.25 | 42 |
| 76.57 | 170 | 21.7 | 36.45 | 47.6 |
| 76.72 | 190 | 24.3 | 40.82 | 53.2 |
| 76.56 | 210 | 26.8 | 45.01 | 58.8 |
| 76.94 | 230 | 29.5 | 49.55 | 64.4 |
| 76.78 | 250 | 32 | 53.75 | 70 |



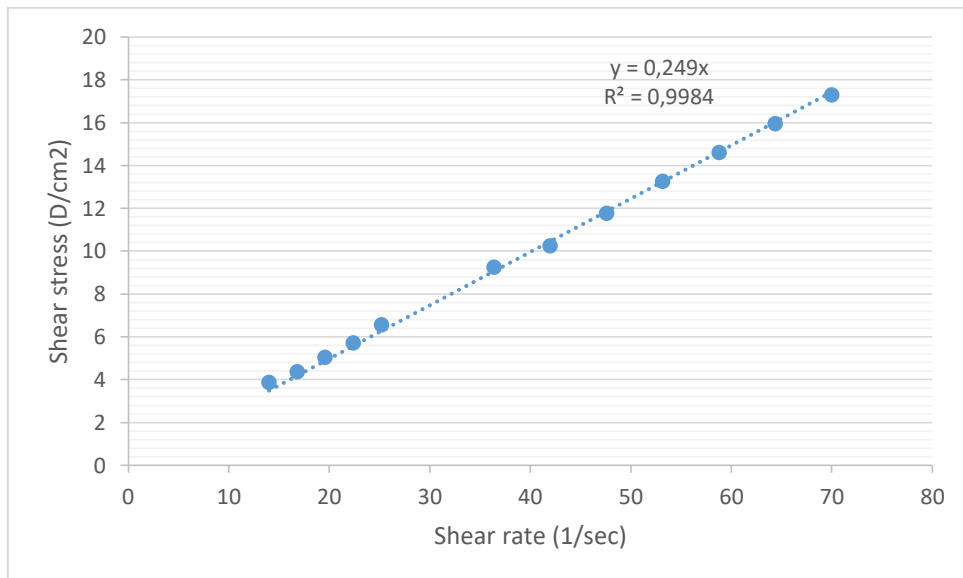
| 70 °C | | | | |
|----------------|-----|-----------|-----------------------------------|--------------------|
| Viscosity (cP) | RPM | Torque(%) | Shear stress (D/cm ²) | Shear rate (1/sec) |
| 56.99 | 20 | 1.9 | 3.19 | 5.6 |
| 53.99 | 30 | 2.7 | 4.54 | 8.4 |
| 52.49 | 40 | 3.5 | 5.88 | 11.2 |
| 52.79 | 50 | 4.4 | 7.39 | 14 |
| 53.99 | 60 | 5.4 | 9.07 | 16.8 |
| 50.66 | 90 | 7.6 | 12.77 | 25.2 |
| 50.3 | 130 | 10.9 | 18.31 | 36.4 |
| 50.79 | 150 | 12.7 | 21.33 | 42 |
| 49.4 | 170 | 14 | 23.51 | 47.6 |
| 49.25 | 190 | 15.6 | 26.2 | 53.2 |
| 49.42 | 210 | 17.3 | 29.06 | 58.8 |
| 49.29 | 230 | 18.9 | 31.75 | 64.4 |
| 49.43 | 250 | 20.6 | 34.6 | 70 |



| 80 °C | | | | |
|----------------|-----|-----------|-----------------------------------|--------------------|
| Viscosity (cP) | RPM | Torque(%) | Shear stress (D/cm ²) | Shear rate (1/sec) |
| 35.99 | 40 | 2.4 | 4.03 | 11.2 |
| 35.99 | 50 | 3 | 5.04 | 14 |
| 34.99 | 60 | 3.5 | 5.88 | 16.8 |
| 35.99 | 70 | 4.2 | 7.05 | 19.6 |
| 35.24 | 80 | 4.7 | 7.89 | 22.4 |
| 34.66 | 90 | 5.2 | 8.73 | 25.2 |
| 34.61 | 130 | 7.5 | 12.6 | 36.4 |
| 34.39 | 150 | 8.6 | 14.44 | 42 |
| 34.23 | 170 | 9.7 | 16.29 | 47.6 |
| 34.73 | 190 | 11 | 18.48 | 53.2 |
| 34.28 | 210 | 12 | 20.16 | 58.8 |
| 34.43 | 230 | 13.2 | 22.17 | 64.4 |
| 33.83 | 250 | 14.1 | 23.68 | 70 |

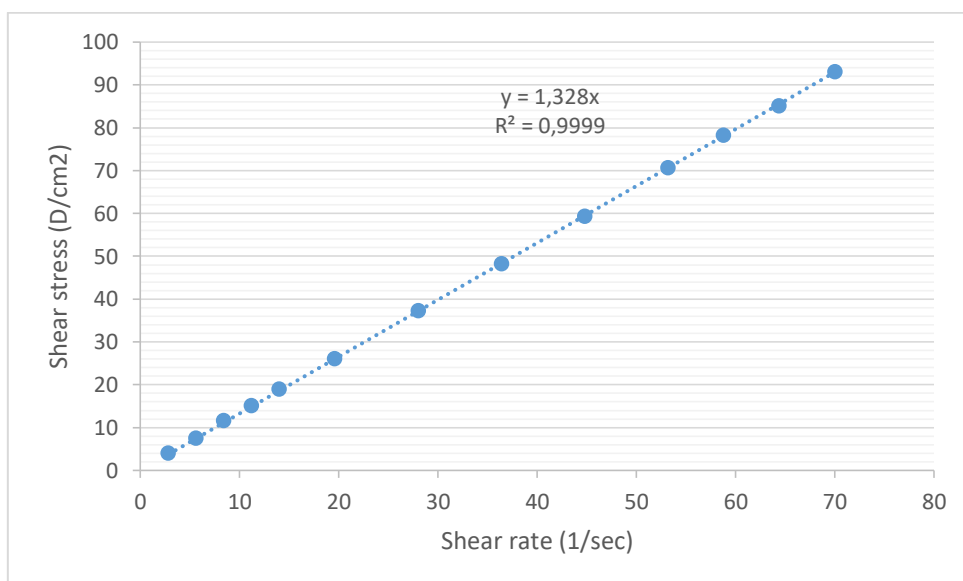


| 90 °C | | | | |
|----------------|-----|-----------|-----------------------------------|--------------------|
| Viscosity (cP) | RPM | Torque(%) | Shear stress (D/cm ²) | Shear rate (1/sec) |
| 27.59 | 50 | 2.3 | 3.86 | 14 |
| 25.99 | 60 | 2.6 | 4.37 | 16.8 |
| 25.71 | 70 | 3 | 5.04 | 19.6 |
| 25.49 | 80 | 3.4 | 5.71 | 22.4 |
| 25.99 | 90 | 3.9 | 6.55 | 25.2 |
| 25.38 | 130 | 5.5 | 9.24 | 36.4 |
| 24.39 | 150 | 6.1 | 10.25 | 42 |
| 24.7 | 170 | 7 | 11.76 | 47.6 |
| 24.94 | 190 | 7.9 | 13.27 | 53.2 |
| 24.85 | 210 | 8.7 | 14.61 | 58.8 |
| 24.78 | 230 | 9.5 | 15.96 | 64.4 |
| 24.71 | 250 | 10.3 | 17.3 | 70 |

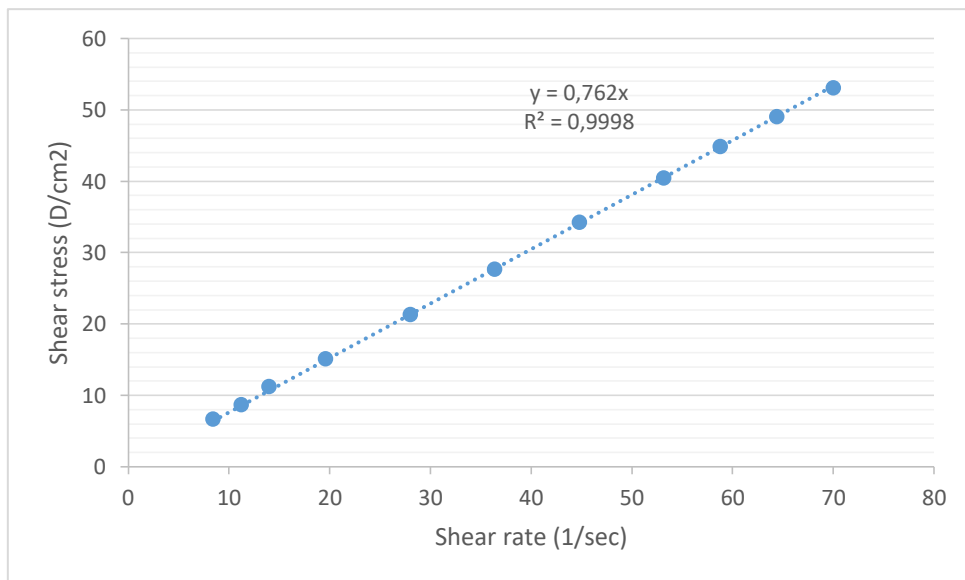


$$X_{IL}=0.95$$

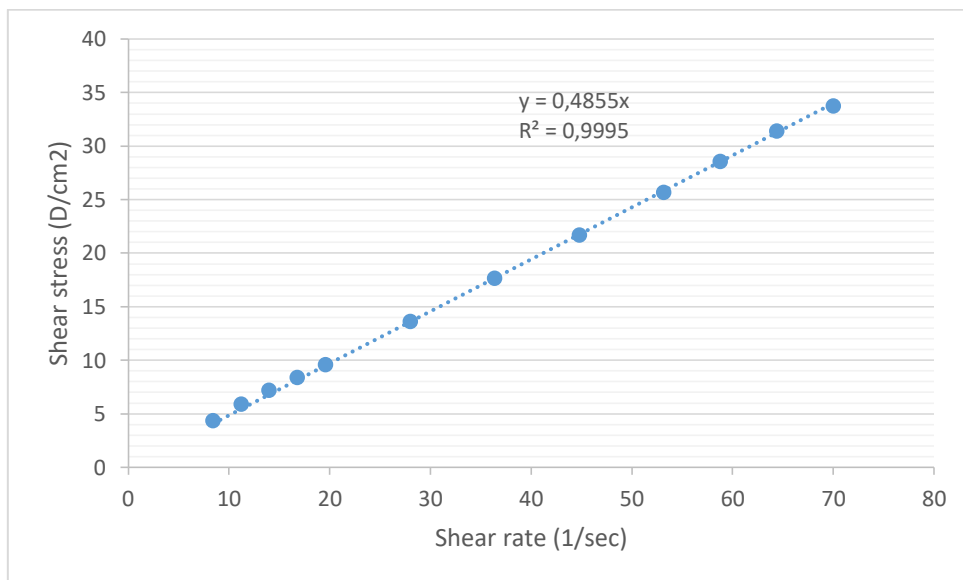
| 60 °C | | | | |
|----------------|-----|-----------|-----------------------------------|--------------------|
| Viscosity (cP) | RPM | Torque(%) | Shear stress (D/cm ²) | Shear rate (1/sec) |
| 143.97 | 10 | 2.4 | 4.03 | 2.8 |
| 134.97 | 20 | 4.5 | 7.56 | 5.6 |
| 137.97 | 30 | 6.9 | 11.59 | 8.4 |
| 134.97 | 40 | 9 | 15.12 | 11.2 |
| 135.57 | 50 | 11.3 | 18.98 | 14 |
| 132.83 | 70 | 15.5 | 26.03 | 19.6 |
| 133.17 | 100 | 22.2 | 37.29 | 28 |
| 132.43 | 130 | 28.7 | 48.21 | 36.4 |
| 132.35 | 160 | 35.3 | 59.29 | 44.8 |
| 132.92 | 190 | 42.1 | 70.71 | 53.2 |
| 133.11 | 210 | 46.6 | 78.27 | 58.8 |
| 132.23 | 230 | 50.7 | 85.16 | 64.4 |
| 132.93 | 250 | 55.4 | 93.05 | 70 |



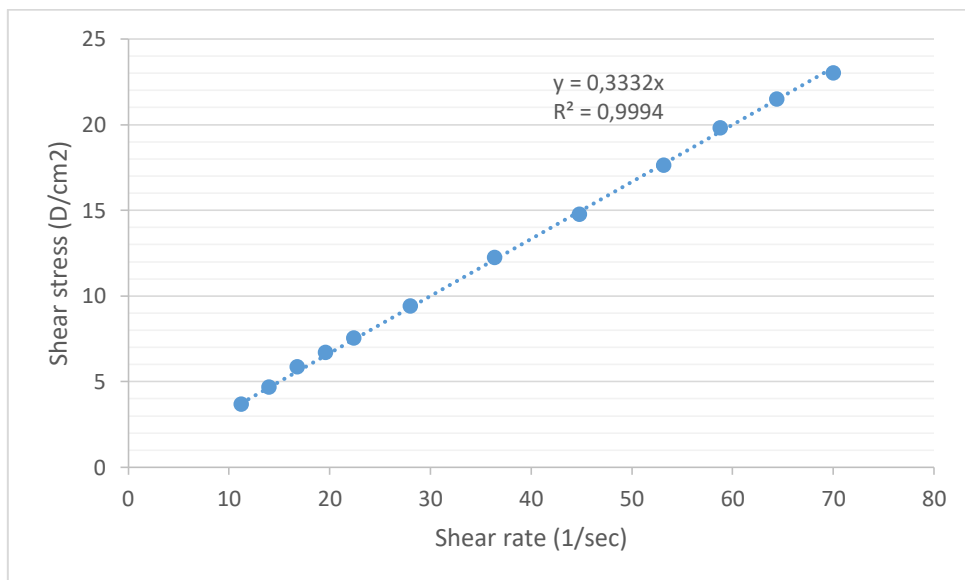
| 70 °C | | | | |
|----------------|-----|-----------|-----------------------------------|--------------------|
| Viscosity (cP) | RPM | Torque(%) | Shear stress (D/cm ²) | Shear rate (1/sec) |
| 79.98 | 30 | 4 | 6.72 | 8.4 |
| 77.98 | 40 | 5.2 | 8.73 | 11.2 |
| 80.38 | 50 | 6.7 | 11.25 | 14 |
| 77.13 | 70 | 9 | 15.12 | 19.6 |
| 76.18 | 100 | 12.7 | 21.33 | 28 |
| 76.14 | 130 | 16.5 | 27.71 | 36.4 |
| 76.48 | 160 | 20.4 | 34.26 | 44.8 |
| 76.09 | 190 | 24.1 | 40.48 | 53.2 |
| 76.27 | 210 | 26.7 | 44.85 | 58.8 |
| 76.16 | 230 | 29.2 | 49.05 | 64.4 |
| 75.82 | 250 | 31.6 | 53.08 | 70 |



| 80 °C | | | | |
|----------------|-----|-----------|-----------------------------------|--------------------|
| Viscosity (cP) | RPM | Torque(%) | Shear stress (D/cm ²) | Shear rate (1/sec) |
| 51.99 | 30 | 2.6 | 4.37 | 8.4 |
| 52.49 | 40 | 3.5 | 5.88 | 11.2 |
| 51.59 | 50 | 4.3 | 7.22 | 14 |
| 49.99 | 60 | 5 | 8.4 | 16.8 |
| 48.85 | 70 | 5.7 | 9.57 | 19.6 |
| 48.59 | 100 | 8.1 | 13.61 | 28 |
| 48.45 | 130 | 10.5 | 17.64 | 36.4 |
| 48.36 | 160 | 12.9 | 21.67 | 44.8 |
| 48.31 | 190 | 15.3 | 25.7 | 53.2 |
| 48.56 | 210 | 17 | 28.55 | 58.8 |
| 48.77 | 230 | 18.7 | 31.41 | 64.4 |
| 48.23 | 250 | 20.1 | 33.76 | 70 |

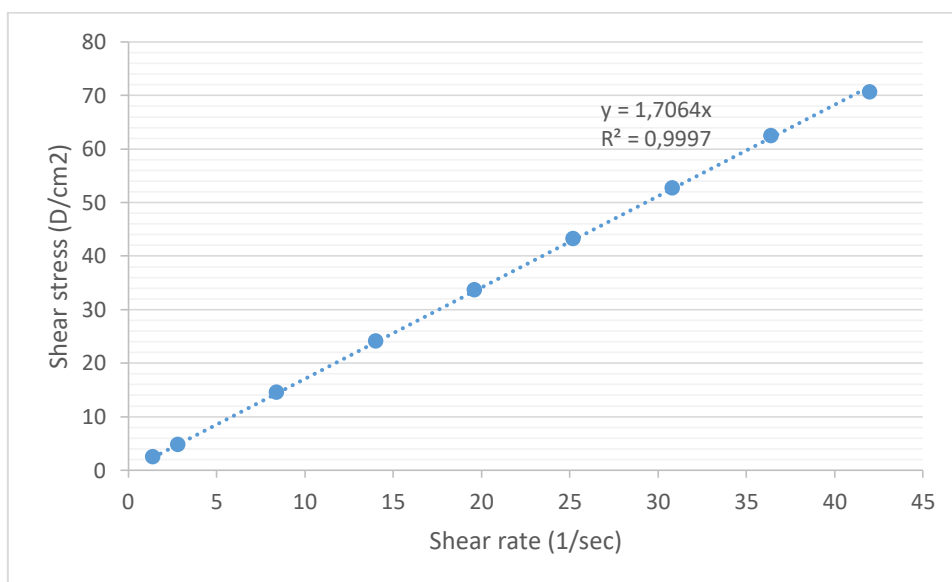


| 90 °C | | | | |
|----------------|-----|-----------|-----------------------------------|--------------------|
| Viscosity (cP) | RPM | Torque(%) | Shear stress (D/cm ²) | Shear rate (1/sec) |
| 32.99 | 40 | 2.2 | 3.7 | 11.2 |
| 33.59 | 50 | 2.8 | 4.7 | 14 |
| 34.99 | 60 | 3.5 | 5.88 | 16.8 |
| 34.28 | 70 | 4 | 6.72 | 19.6 |
| 33.74 | 80 | 4.5 | 7.56 | 22.4 |
| 33.59 | 100 | 5.6 | 9.41 | 28 |
| 33.69 | 130 | 7.3 | 12.26 | 36.4 |
| 32.99 | 160 | 8.8 | 14.78 | 44.8 |
| 33.15 | 190 | 10.5 | 17.64 | 53.2 |
| 33.71 | 210 | 11.8 | 19.82 | 58.8 |
| 33.38 | 230 | 12.8 | 21.5 | 64.4 |
| 32.87 | 250 | 13.7 | 23.01 | 70 |

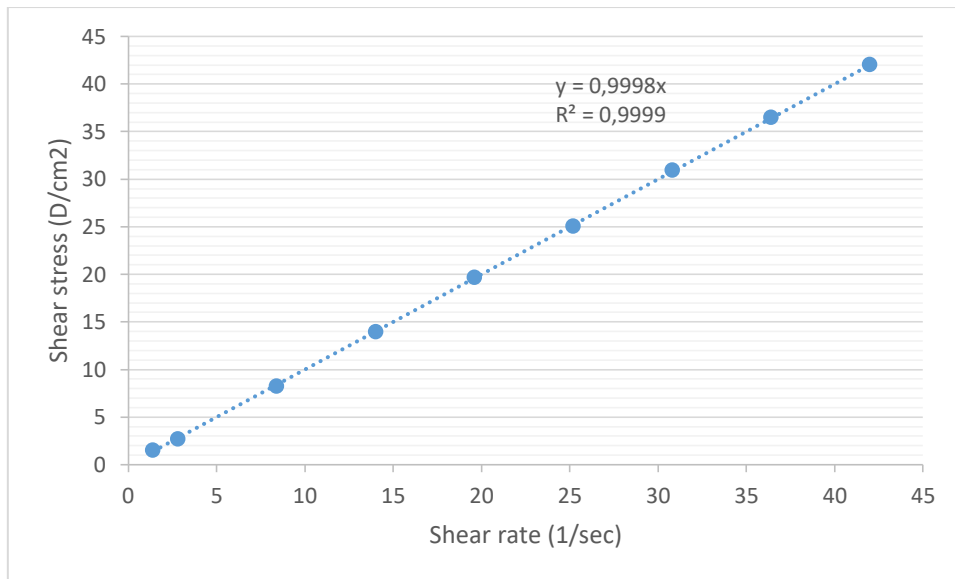


Pure [bmim][Cl]

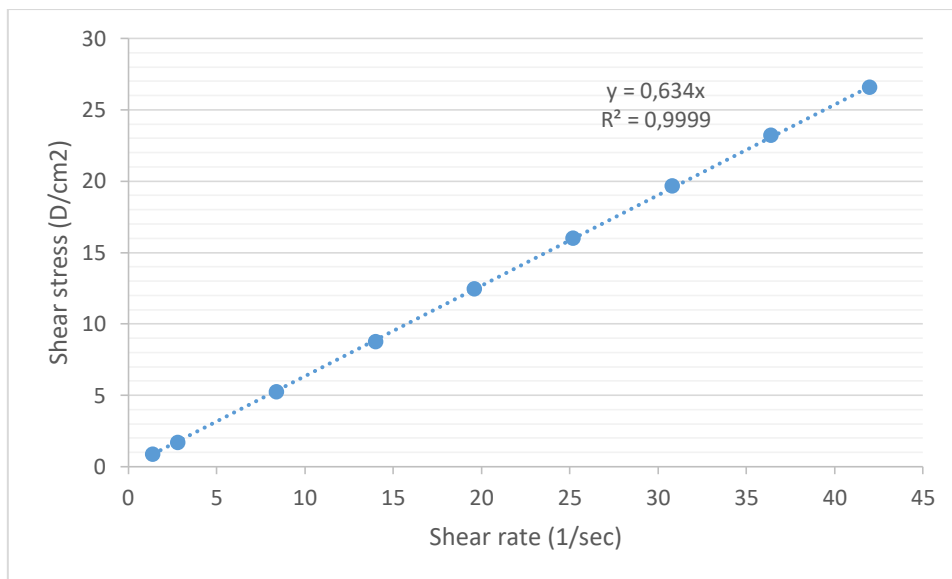
| 60 °C | | | | |
|----------------|-----|-----------|-----------------------------------|--------------------|
| Viscosity (cP) | RPM | Torque(%) | Shear stress (D/cm ²) | Shear rate (1/sec) |
| 179.96 | 5 | 1.5 | 2.52 | 1.4 |
| 173.96 | 10 | 2.9 | 4.87 | 2.8 |
| 173.96 | 30 | 8.7 | 14.61 | 8.4 |
| 172.76 | 50 | 14.4 | 24.19 | 14 |
| 172.25 | 70 | 20.1 | 33.76 | 19.6 |
| 171.96 | 90 | 25.8 | 43.33 | 25.2 |
| 171.24 | 110 | 31.4 | 52.74 | 30.8 |
| 171.66 | 130 | 37.2 | 62.48 | 36.4 |
| 168.36 | 150 | 42.1 | 70.71 | 42 |



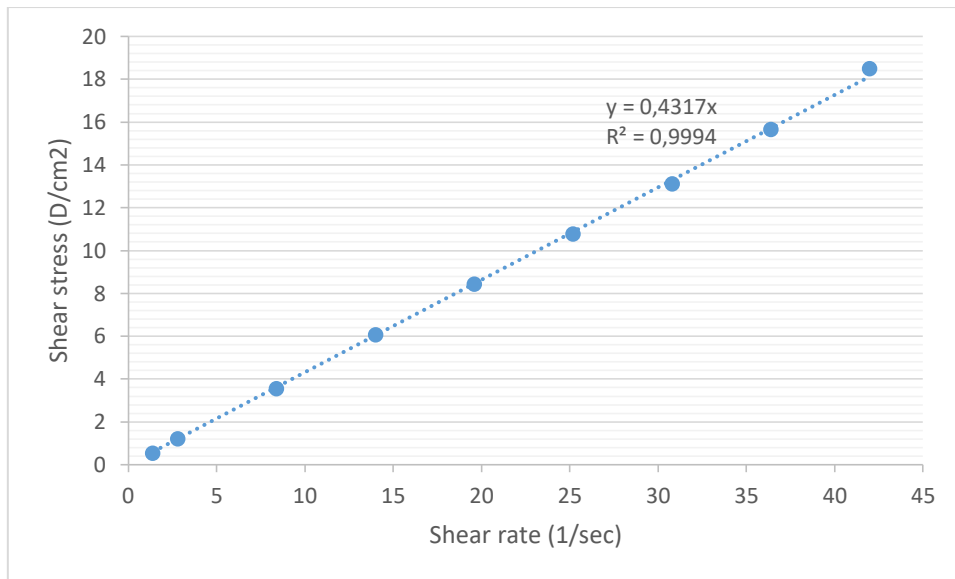
| 70 °C | | | | |
|----------------|-----|-----------|-----------------------------------|--------------------|
| Viscosity (cP) | RPM | Torque(%) | Shear stress (D/cm ²) | Shear rate (1/sec) |
| 107.98 | 5 | 0.9 | 1.51 | 1.4 |
| 95.98 | 10 | 1.6 | 2.69 | 2.8 |
| 97.98 | 30 | 4.9 | 8.23 | 8.4 |
| 99.58 | 50 | 8.3 | 13.94 | 14 |
| 100.26 | 70 | 11.7 | 19.65 | 19.6 |
| 99.31 | 90 | 14.9 | 25.03 | 25.2 |
| 100.34 | 110 | 18.4 | 30.91 | 30.8 |
| 100.13 | 130 | 21.7 | 36.45 | 36.4 |
| 99.98 | 150 | 25 | 41.99 | 42 |



| 80 °C | | | | |
|----------------|-----|-----------|-----------------------------------|--------------------|
| Viscosity (cP) | RPM | Torque(%) | Shear stress (D/cm ²) | Shear rate (1/sec) |
| 59.99 | 5 | 0.5 | 0.84 | 1.4 |
| 59.99 | 10 | 1 | 1.68 | 2.8 |
| 61.99 | 30 | 3.1 | 5.21 | 8.4 |
| 62.39 | 50 | 5.2 | 8.73 | 14 |
| 63.42 | 70 | 7.4 | 12.43 | 19.6 |
| 63.32 | 90 | 9.8 | 15.96 | 25.2 |
| 63.8 | 110 | 11.7 | 19.65 | 30.8 |
| 63.68 | 130 | 13.8 | 23.18 | 36.4 |
| 63.19 | 150 | 15.8 | 26.54 | 42 |



| 90 °C | | | | |
|----------------|-----|-----------|-----------------------------------|--------------------|
| Viscosity (cP) | RPM | Torque(%) | Shear stress (D/cm ²) | Shear rate (1/sec) |
| 35.99 | 5 | 0.3 | 0.5 | 1.4 |
| 41.99 | 10 | 0.7 | 1.18 | 2.8 |
| 41.99 | 30 | 2.1 | 3.53 | 8.4 |
| 43.19 | 50 | 3.6 | 6.05 | 14 |
| 42.85 | 70 | 5 | 8.4 | 19.6 |
| 42.66 | 90 | 6.4 | 10.75 | 25.2 |
| 42.54 | 110 | 7.8 | 13.1 | 30.8 |
| 42.91 | 130 | 9.3 | 15.62 | 36.4 |
| 43.99 | 150 | 11 | 18.48 | 42 |



References

- [1] J. Keith E., "What's an Ionic Liquid?," *Electrochem. Soc. Interface*, p. Spring 2007.
- [2] I. B. Theodore L., "Chemistry: The central science. 11th ed.," pp. 436–479.
- [3] T. Welton, "Room-Temperature Ionic Liquids. Solvents for Synthesis and Catalysis," *Chem Rev*, vol. 99, pp. 2071–2083, 1999.
- [4] I. Krossing and et al, "Why Are Ionic Liquids Liquid? A Simple Explanation Based on Lattice and Solvation Energies," *J AM CHEM SOC*, vol. 128, pp. 13427–13434, 2006.
- [5] Z. Lijuan, Z. Faqiong, and Z. Baizhao, "Preparation and application of sunset yellow imprinted ionic liquid polymer – ionic liquid functionalized graphene composite film coated glassy carbon electrodes," *Electrochimica Acta*, vol. 115, pp. 247–254, 2014.
- [6] L. A. J. D. Rocha, "USE OF IONIC LIQUIDS IN BIODIESEL PRODUCTION: A REVIEW," *Braz. J. Chem. Eng.*, vol. 29, no. 01, pp. 1–13, Mar. 2012.
- [7] A. A. S. R. Daik, "APPLICATIONS OF IONIC LIQUIDS AND THEIR MIXTURES FOR PREPARATION OF ADVANCED POLYMER BLENDS AND COMPOSITES: A SHORT REVIEW," *Adv. Study Cent. C Ltd*, vol. 40, pp. 45–59, 2015.
- [8] J. H. D. Fox Phillip A, "From curiosities to commodities: ionic liquids begin the transition," *Chemical Communications*, 2013.
- [9] S. Takahiro, "Use of task-specific ionic liquid for selective electrocatalytic fluorination.," *Organic letters*, pp. 644–646, 2010.
- [10] J. R. Nykaza, Y. Ye, and Y. A. Elabd, "Polymerized ionic liquid diblock copolymers with long alkylside-chain length," *Polymer*, vol. 55, pp. 3360–3369, 2014.
- [11] L. Yangyang and Y. Guoqiang, "Design and Synthesis of Thermoresponsive Ionic Liquid Polymer in Acetonitrile as a Reusable Extractant for Separation of Tocopherol Homologues," *Am. Chem. Soc.*, vol. 48, pp. 915–924.
- [12] D. Swapnil A. and V. Mahesh N., "Synthesis, Characterization and Application of 1-Butyl-3 Methylimidazolium Chloride as Green Material for Extractive Desulfurization of Liquid Fuel," *Sci. World J.*, vol. 2013, 2013.
- [13] S. Fendt, "Viscosities of Acetate or Chloride-Based Ionic Liquids and Some of Their Mixtures with Water or Other Common Solvents," *J Chem Eng Data*, vol. 56, 2011.
- [14] J. G. Huddleston and A. E. Visser, "Characterization and comparison of hydrophilic and hydrophobic room temperature ionic liquids incorporating the imidazolium cation," *Green Chem.*, vol. 3, pp. 156–164, 2001.
- [15] M. Hiroshi and T. Ryosuke, "Measurement and Correlation of High Pressure Densities of Ionic Liquids, 1-Ethyl-3-methylimidazolium 1-Lactate ([emim][Lactate]), 2-Hydroxyethyl-trimethylammonium 1-Lactate ([[(C2H4OH)(CH3)3N][Lactate]), and 1-Butyl-3-methylimidazolium Chloride ([bmim][Cl])," *J. Chem. Eng. Data*, vol. 56, no. 4, pp. 923–929, 2011.
- [16] S. Hina and Z. Xinjun Zhu, "Determination of physical properties for the mixtures of [BMIM]Cl with different organic solvents," *Chin. J. Chem. Eng.*, vol. 23, pp. 804–811, 2015.
- [17] I L Odinets and E V Matveeva, "The application of green chemistry methods in organophosphorus synthesis," *Russ. Chem. Rev.*, vol. 81, no. 3, pp. 221–238, 2012.

- [18] J. Ren, W. Zhang, and et al, “Characteristics of starch-based films produced using glycerol and 1-butyl-3-methylimidazolium chloride as combined plasticizers,” *Starch/Stärke*, vol. 69, no. 1600161, pp. 1–8, 2017.
- [19] S. A. Dharaskar, M. N. Varma, and et al, “Synthesis, Characterization and Application of 1-Butyl-3 Methylimidazolium Chloride as Green Material for Extractive Desulfurization of Liquid Fuel,” *Sci. World J.*, vol. 2013, no. ID 395274, p. 9, 2013.
- [20] Abiove, “ABIOVE, ASSOCIAÇÃO BRASILEIRA DAS INDÚSTRIAS DE ÓLEOS VEGETAIS. Disponível em: < <http://www.abiove.org.br/site/index.php>. >. Acessado em: Janeiro de 2017,” 2017.
- [21] USDA, “USDA, Foreign Agriculture Service Oilseeds: World Markets and Trade. Disponível em: <<https://apps.fas.usda.gov/psdonline/circulars/oilseeds.pdf>>. Acessado em: Abril de 2017,” 2017.
- [22] J. S. Vaz, “Biorrefinarias: Perspectivas e Cenários,” *Embrapa Agroenergia*, 2011.
- [23] J. A. Dutton, “<https://www.e-education.psu.edu/egee439/node/684>.” Penn State College of Earth and Mineral sciences, 14-Dec-2017.
- [24] A. P. Abbott and P. M. Cullis, “Extraction of glycerol from biodiesel into a eutectic based ionic liquid,” *Green Chem.*, vol. 9, pp. 868–872, 2007.
- [25] H. W. Tan and A. Abdul, “Glycerol production and its applications as a raw material: A review,” *Renew. Sustain. Energy Rev.*, vol. 27, pp. 118–127, 2013.
- [26] M. S. Ardi and M. K. Aroua, “Progress, prospect and challenges in glycerol purification process: A review,” *Renew. Sustain. Energy Rev.*, vol. 42, pp. 1164–1173, 2015.
- [27] C. L. Yaws, *Thermophysical Properties of Chemicals and Hydrocarbons*, 1st ed. William Andrew, 2008.
- [28] P. Nieves M.C.T., S. Thiago A, and et al, “Liquid glycerol: Experimental densities at pressures of up to 25 MPa, and some derived thermodynamic properties,” *J Chem Thermodyn.*, vol. 101, pp. 64–67, 2016.
- [29] J. B. SECUR and HELEN E. OBERSTAK, “Viscosity of glycerol and its aqueous solutions,” *Ind Eng Chem*, vol. 43, pp. 2117–2120, 1951.
- [30] K. Mirjana Lj and et al, “Experimental determination and modeling of excess molar volumes, viscosities and refractive indices of the binary systems (pyridine + 1-propanol, +1,2-propanediol, +1,3-propanediol, and +glycerol). New UNIFAC-VISCO parameters determination,” *J Chem Thermodyn.*, vol. 56, pp. 49–56, 2013.
- [31] K. Fardad, “Refractive Index and Its Applications,” vol. 2013, 4:2.
- [32] Borgnakke and Sonntag, *Fundamentals of Thermodynamics*, 7th ed. Wiley, 2009.
- [33] M. YAQUB, and et al, “SECOND-LAW-BASED THERMODYNAMIC ANALYSIS OF HOTGAS, BY-PASS, CAPACITY-CONTROL SCHEMES FOR REFRIGERATION AND AIR-CONDITIONING SYSTEMS,” *Energ*, vol. 20, no. 6, pp. 483–493, 1994.
- [34] D. F. YOUNG and et al, “A Brief Introduction to Fluid Mechanics,” 5th ed., Wiley, 2011.
- [35] B. E. Poling, J. Prausnitz, and J. P. O’Connell, *The Properties of Gases and Liquids*, 5th ed. McGraw-Hill Education, 2000.
- [36] R. B. Bird, *Fenomenos de Transporte*, 2da ed. Gen LTC.
- [37] Berkeley, “<https://nature.berkeley.edu/classes/eps2/wisc/L2c4.html>,” Dec. 2017.
- [38] F. Young and S. Sears, *Fisica universitaria con Fisica moderna*, 12th ed., vol. 2. Addison-Wesley, 2009.

- [39] K. ALEXANDER, C. GIUSEPPE, and et al, “High refractive index Fresnel lens on a fiber fabricated by nanoimprint lithography for immersion applications,” *Opt. Lett.*, vol. 41, no. 15, pp. 3423–3426, 2016.
- [40] R. Mohammad R. and R. Yousef A., “Use of the Refractive Index in the Estimation of Thermophysical Properties of Hydrocarbons and Petroleum Mixtures,” *Ind Eng Chem Res*, vol. 40, pp. 1975–1984, 2001.
- [41] Q. Zhang and S. Cai, “Density, viscosity, conductivity, refractive index and interaction study of binary mixtures of the ionic liquid 1-ethyl-3-methylimidazolium acetate with methyldiethanolamine,” *J. Mol. Liq.*, vol. 233, pp. 471–478, 2017.
- [42] J.M. Smith, H.C. Van Ness, and M.M. Abbott, *Introduction to Chemical Engineering Thermodynamics*, 7th ed. Mc Graww Hill.
- [43] D. DAS, “Viscosity Arrhenius Activation Energy and Derived Partial Molar Properties in Isobutyric Acid + Water Binary Mixtures Near and Far Away from the Critical Temperature, 302.15 to 313.15 K,” *J Solut. Chem*, vol. 44:54, no. 66, 2015.
- [44] H. D. Chandler, “Activation energy and entropy for viscosity of wormlike micelle solutions,” *J. Colloid Interface Sci.*, vol. 409, pp. 98–103, 2013.
- [45] Rosana J., “Excess Gibbs Free Energy Model for Calculating the Viscosity of Binary Liquid Mixtures,” *Ind Eng Chem Res*, vol. 39, pp. 849–854.
- [46] J. D. PANDEY and S. VINAY, “Theoretical estimations of thermodynamic properties of liquid mixtures by Flory’s statistical theory,” *Phys. Chem. Liq.*, vol. 46, no. 4, pp. 417–432.
- [47] Houger and Watson, “Enthalpy-Concentration diagram for aqueous sulfuric acid at 1 atm.,” *Chem. Process Princ. Part 1* Wiley N. Y. 1943.
- [48] Perry, *Chemical engineering—Handbooks, manuals, etc. I.*, 7th ed., vol. 1. USA: Mc Graw Hill, 1997.
- [49] K. V. Kumar, “Isotherms and thermodynamics by linear and non-linear regression analysis for the sorption of methylene blue onto activated carbon: Comparison of various error functions,” *J. Hazard. Mater.*, vol. 151, pp. 794–804, 2008.
- [50] C. Carcasci and et al, “A new modular procedure for industrial plant simulations and its reliable implementation,” *Energy*, vol. 94, pp. 380–390, 2016.
- [51] H. M. Machlab, “Thermal diffusivity measurements by photothermal laser beam deflection (PTD): data analysis using the Levenberg-Marquardt algorithm,” *Thin Solid Films*, vol. 215, pp. 103–107, 1992.
- [52] The Mathwork INC, “MATLAB HELP.” 2017.
- [53] A.-M. Bonsa and J. K. Lehmann, “Partial molar enthalpies of organic solutes in the ionic liquid [EMIM][EtSO₄],” *J. Mol. Liq.*, vol. 226, pp. 96–99, 2017.
- [54] M. I. C. H. A. E. L. J. . MORAN, *FUNDAMENTALS OF ENGINEERING THERMODYNAMICS*, 7th ed. John Wiley & Sons, Inc., 2011.
- [55] D. Soldatovic and J. Vuksanovic’, “Excess molar volumes and viscosity behaviour of binary mixtures of aniline/or N,N-dimethylaniline with imidazolium ionic liquids having triflate or bistriflamide anion,” *J Chem Thermodyn.*, vol. 109, pp. 137–154, 2017.
- [56] M. Moosavi and A. Daneshvar, “Rheological properties of {[bmim]PF₆ + methanol} mixtures at different temperatures, shear rates and compositions,” *J. Mol. Liq.*, vol. 209, pp. 693–705, 2015.
- [57] Brookfield Engineering Labs., Inc., *MORE SOLUTIONS TO STICKY PROBLEMS*, vol. 1. MA, USA, 2014.
- [58] J. A. Smith and G. B. Webber, “Rheology of Protic Ionic Liquids and Their Mixtures,” *J Phys Chem B*, vol. 113, pp. 13930–13935, 2013.

- [59] A. Faraone and et al, "Glycerol Hydrogen-Bonding Network Dominates Structure and Collective Dynamics in a Deep Eutectic Solvent," *J Phys Chem B*, 2018.
- [60] A. S. L. Gouveia and L. C. Tome, "Density, Viscosity, and Refractive Index of Ionic Liquid Mixtures Containing Cyano and Amino Acid-Based Anions," *J Chem Eng Data*, vol. 61, pp. 83–93, 2016.
- [61] E. Vercher and F. J. Llopis, "Volumetric properties, viscosities and refractive indices of binary liquid mixtures of tetrafluoroborate-based ionic liquids with methanol at several temperatures," *J Chem Thermodyn.*, vol. 90, pp. 174–184, 2015.
- [62] V. Govinda and et al, "Thermophysical properties of dimethylsulfoxide with ionic liquids at various temperatures," *Fluid Phase Equilibria*, vol. 304, pp. 35–43, 2011.
- [63] P. Attri and et al, "Measurements and Molecular Interactions for N,N-Dimethylformamide with Ionic Liquid Mixed Solvents," *J Phys Chem B*, vol. 114, pp. 6126–6133.
- [64] L. Chen and et al, "Densities, viscosities, and excess properties of binary mixtures of two imidazolide anion functionalized ionic liquids with water at T = (293.15 to 313.15) K," *J Chem Thermodyn.*, vol. 91, pp. 292–300, 2015.
- [65] Kavitha T., T. Vasantha, and et al, "Thermophysical properties for the mixed solvents of N-methyl-2-pyrrolidone with some of the imidazolium-based ionic liquids," *J. Mol. Liq.*, vol. 198, pp. 11–20, 2014.
- [66] R. Salinas and et al, "Density, Speed of Sound, Viscosity, and Excess Properties of Binary Mixtures Formed by Ethanol and Bis(trifluorosulfonyl)imide-Based Ionic Liquids," *J Chem Eng Data*, vol. 60, pp. 525–540, 2015.
- [67] G. R. Chaudhary, "Structural and interactional behaviour of aqueous mixture of room temperature ionic liquid; 2-hydroxyethyl-trimethylammonium L-lactate," *J Chem Thermodyn.*, vol. 76, pp. 134–144, 2014.
- [68] X. Yang and et al, "Temperature and composition dependence of the density, viscosity and refractive index of binary mixtures of a novel gemini ionic liquid with acetonitrile," *RSC Adv*, vol. 6, pp. 29172–29181, 2016.
- [69] Z. R. Master, "Molecular interaction study through experimental and theoretical volumetric, transport and refractive properties of N-ethylaniline with aryl and alkyl ethers at several temperatures," *Phys. Chem. Liq.*, vol. 54, no. 2, pp. 223–244, 2016.
- [70] M. Teodorescu, "Isothermal (vapour + liquid) equilibrium and thermophysical properties for (1-butyl-3-methylimidazolium iodide + 1-butanol) binary system," *J Chem Thermodyn.*, vol. 87, pp. 58–64, 2015.
- [71] F. Ye and et al, "Physicochemical properties of binary mixtures of 1,1,3,3-tetramethylguanidine imidazolide ionic liquid with water and alcohols," *J Chem Thermodyn.*, vol. 97, pp. 39–47.
- [72] Y. Litaïem and M. Dhahbi, "Measurements and correlations of viscosity, conductivity and density of an hydrophobic ionic liquid (Aliquat 336) mixtures with a non-associated dipolar aprotic solvent (DMC)," *J. Mol. Liq.*, vol. 169, pp. 54–62, 2012.
- [73] F. Bandarkar and et al, "Viscosity and surface tension of glycerol + N-methyl-2-pyrrolidone mixtures from 293 to 323 K," *Phys. Chem. Liq.*, vol. 53, no. 1, 2015.
- [74] N. Ouerfelli and et al, "The reduced Redlich–Kister excess molar Gibbs energy of activation of viscous flow and derived properties in 1,4-dioxane Ywater binary mixtures from 293.15 to 309.15 K," *Phys. Chem. Liq.*, vol. 49, no. 6, pp. 777–800.
- [75] S. M. Islam and M. A. Saleh, "Thermodynamic activation parameters for viscous flow of dilute aqueous solutions of ethylenediamine, trimethylenediamine and N,N-dimethyltrimethylenediamine," *Phys. Chem. Liq.*, vol. 48, no. 2, pp. 156–170.

- [76] D. M. Bajic and et al, "Experimental measurement and modelling of viscosity of the binary systems pyridine or nicotine with polyethylene glycols at $T = (288.15\text{--}333.15)$ K. New UNIFAC–VISCO and ASOG–VISCO interaction parameters," *Fluid Phase Equilibria*, vol. 338, pp. 282–293.
- [77] D. Camargo and et al, "Investigation of the rheological properties of protic ionic liquids," *J Phys Org Chem*, vol. 29, pp. 604–612, 2016.
- [78] C. E. Ferreira and et al, "Measurements of pVT, viscosity, and surface tension of trihexyltetradecylphosphonium tris(pentafluoroethyl)trifluorophosphate ionic liquid and modelling with equations of state," *J Chem Thermodyn.*, vol. 47, pp. 183–196, 2012.
- [79] C.T. Pinheiro, R.F. Pais, and et al, "Measurement and correlation of thermophysical properties of waste lubricant oil," *J Chem Thermodyn.*, vol. 116, pp. 137–146, 2018.
- [80] M. H. Ghatee, "Temperature-Dependent Density and Viscosity of the Ionic Liquids 1-Alkyl-3-methylimidazolium Iodides: Experiment and Molecular Dynamics Simulation," *J Chem Eng Data*, vol. 55, pp. 3084–3088, 2010.
- [81] J. D. Gomes de Oliveira and J. C. R. Reis, "The two faces of the Redlich–Kister equation and the limiting partial molar volume of water in 1-aminopropan-2-ol," *Thermochim. Acta*, vol. 468, pp. 119–123, 2008.
- [82] C. W. Yea and J. Lib, "Density, Viscosity, and Surface Tension of nOctanol–Phosphoric Acid Solutions in a Temperature Range 293.15–333.15 K1," *Russ. J. Phys. Chem. A*, vol. 86, no. 10, pp. 1515–1521, 2012.
- [83] F. Kermanpour and et al, "Measurement and Calculation the Excess Molar Properties of Binary Mixtures Containing Isobutanol, 1-Amino-2-Propanol, and 1-Propanol at Temperatures of (293.15 to 333.15) K," *J Solut. Chem*, vol. 46, pp. 446–460, 2017.